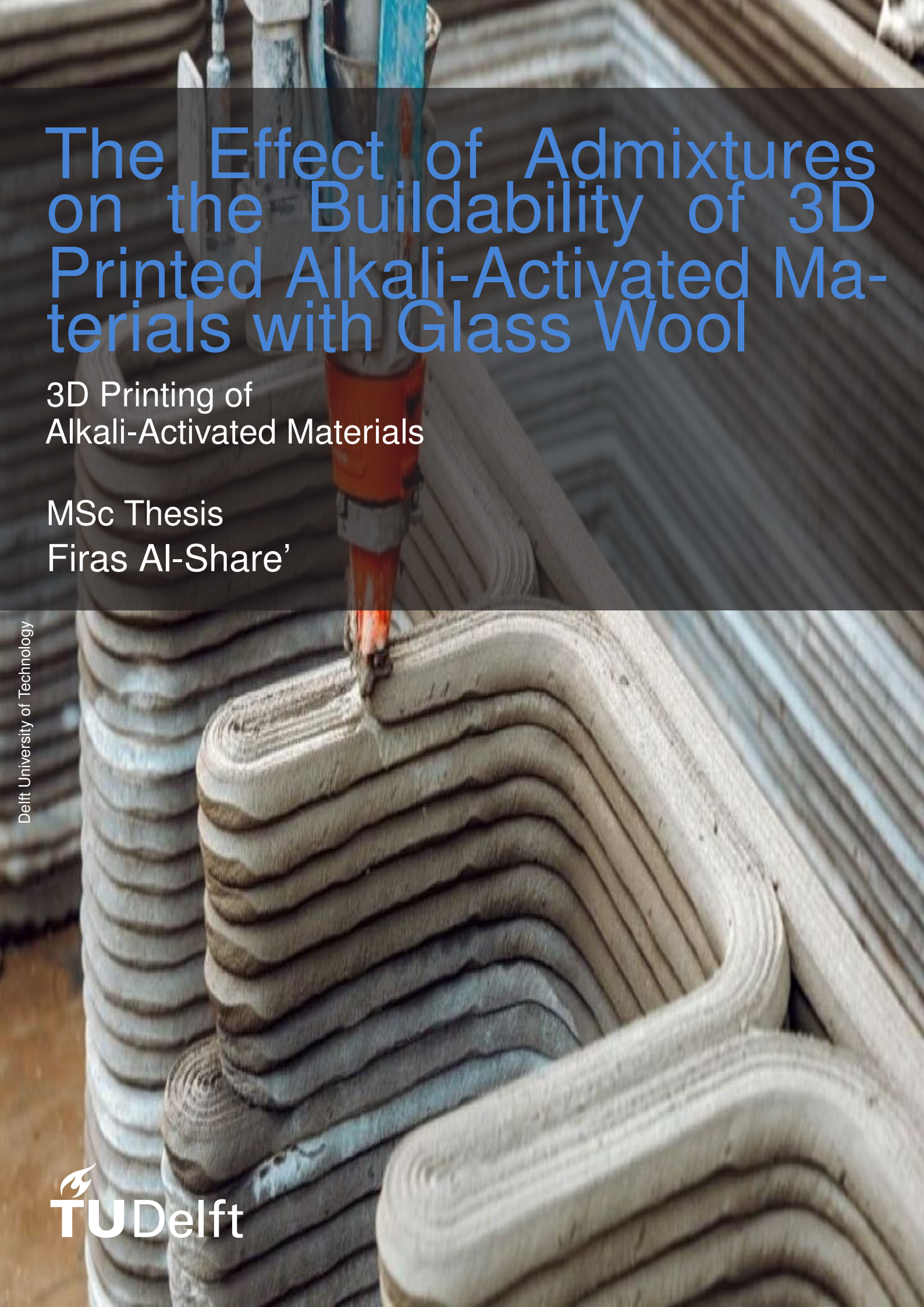

The Effect of Admixtures on the Buildability of 3D Printed Alkali-Activated Materials with Glass Wool

3D Printing of Alkali-Activated Materials

MSc Thesis

Firas Al-Share'

Delft University of Technology

TU Delft

The Effect of Admixtures on the Buildability of 3D Printed Alkali-Activated Materials with Glass Wool

3D Printing of Alkali-Activated Materials

by

Firas Al-Share'

Student Name	Student Number
Firas Al-Share'	5202078

Thesis submitted to Delft University of Technology for the degree of
Master of Science
in Civil Engineering
to be publicly defended on 30/November/2022

Chair: Dr. Guang Ye
Committee Members: Dr. Branko Šavija
Dr. Mladena Lukovic

Institution:	Delft University of Technology
Place:	Faculty of Civil Engineering, Delft
Project Duration:	December, 2021 - November, 2022

An electronic version of this thesis is available at http://repository.tudelft.nl.

TU Delft

Acknowledgements

I would like to sincerely thank my graduation committee for all their help during my thesis as this wouldn't have been possible without them. First of all, I would like to thank Dr. Guang Ye for his guidance and valuable advice through out the thesis and his understanding regarding the difficult situations that occurred during the thesis. I would like to extend my heartfelt gratitude for Dr. Branko Šavija for all the help he provided me with through out the entire duration of my thesis, for his patience, and for always directing me into the right path. I would also like to thank Dr. Mladena Lukovic for her valuable insights and it was an honour working with her as a student assistant. Moreover, I would like to thank my daily supervisor PhD candidate Irving Flores for all his valuable input, the tips and advice he gave me, and helping me with the experimental procedures. Additionally, I would like to express my gratitude to Luiz Miranda for his support and valuable advice during my research. Lastly, huge thanks to Dr. Yu Chen for all his advice regarding the tests and helping with 3D printing.

Furthermore, I would like thank Maiko van Leeuwen, Ton Blom, and Amir Hussein for their technical support and their help with the experimental procedures I conducted. Moreover, I would like to thank all the members of the CMMB research group for their help. It was a pleasure being a part of this group and I would like to specifically thank Guilherme Munhoz, Hu Shi, and Dr. Zhenming Li.

I would also like to thank all my friends for their support during my thesis. They supported and motivated me throughout my entire journey at TU Delft and for that I'm thankful. Lastly, my deepest and greatest gratitude for my family for all their support whether it was mentally or financially as this wouldn't have been possible without them.

Abstract

Research about alkali-activated materials or geopolymers has increased in the past decade as they are regarded as a potential replacement to cement-based materials. This is due to the fact that alkali-activated materials possess several advantages over cement-based materials, and the most important one is that they are more sustainable to the environment, as they have less CO_2 emissions, less energy consumption during the production process, and the use of byproducts as a binder.

The main aim of this work is to develop a mixture that has superior buildability properties with an open time of two hours or more. In order to achieve this, the effect of admixtures, specifically retarders and viscosity modifying admixtures had to be studied. The use of admixtures in geopolymer has been regarded as a complex subject because multiple factors influence their effect on the mixture, like: binders used and their percentages, alkaline activator used, and liquid to binder ratio.

In this work, the effect of 3 retarders: sucrose, sodium chloride, and sodium borate on the setting time, flowability, and yield stress development was studied. Moreover, the effect of those retarders was studied with the addition of viscosity modifying admixtures: nano-clay (attapulgite), xanthan gum, sodium carboxymethyl starch, and sodium carboxymethyl cellulose on the same properties.

The binders and the alkaline activator used were fixed through out the entire work. the binder composed of 60% fly ash, 20% blast furnace slag, and 20% glass wool. The alkaline activator consists of sodium hydroxide and sodium silicate with a SiO_2/Na_2O ratio of 1.5.

The addition of sucrose didn't lead to any delay in the setting time. While both sodium chloride and sodium borate delayed the setting time, increased the flowability, and improved the extrudability of the mixtures. Out of the viscosity modifying admixtures, attapulgite had the most positive effect as it improved the thixotropic behaviour of all the mixes and improved the yield stress. Sodium carboxymethyl starch and cellulose almost had the same effect on the all the mixtures as they both improved extrudability and the yield stress in a similar trend. Xanthan gum was considered a poor admixture to be added to this mixture as it led to significant dryness which led to loss in fluidity which affected both flowability and extrudability.

The most suitable design was the B3lbA0.5 mixture which has 3% borax and 0.5% attapulgite and a liquid to binder ratio of 0.45. It had an initial setting time of more than 8 hours, flowability was maintained for 2.5 hours and it remained extrudable for 2 hours. Its yield stress ranged from 1360.87 Pa to 1977.78 Pa. After 28 days, it had a flexural and compressive strength of 5.72 MPa and 30.42 MPa respectively. Moreover, the flexural and compressive strength of 3D printed prisms was tested in the vertical and horizontal direction on the 7^{th} day. The results showed that the flexural strength of the 3D printed prism tested in the vertical direction was the highest compared to the cast prism and 3D printed prism tested in the horizontal direction by 0.29% and 0.43% respectively. While the compressive strength of 3D printed cube tested in the horizontal direction was higher than both the cast cube and the 3D printed cube tested in the vertical direction by 0.24% and 0.32% respectively. The strength results indicate that the mixture could be used in structural applications. The tensile bond strength was 0.69 MPa and the failure occurred near the glue, meaning that the interface is stronger than the material. In 3D printed concrete, usually the interface between the layers is the weakest point, however due to the addition of attapulgite the interface was strengthened. This explains why the compressive strength in the horizontal direction was higher than the vertical one as the interface was no longer the weak link in the specimen. The mixture's buildability wasn't optimal as the bottom layer had a slight big deformation and it had only ten layers of printed material, but that is reasonable since the open time is 2 hours. This means that for big spans this mixture can be useful as it can be printed for a long period of time and its yield stress will develop.

In order for the mixture to be printable, it had to have an initial setting time higher than three hours, a spread diameter between 150-200mm and a yield stress above 1400 Pa. The above mentioned results fall within the range of values that were needed to have a printable mixture. However, after printing the mixture it was concluded that a spread diameter of 150-180mm and a yield stress above 1600 Pa would be more suitable for both printability and buildability, because when the spread diameter was above 180mm and the yield stress was lower than 1600 Pa, the mixture's viscosity impacted the buildability.

Contents

List of Figures

List of Tables

1

Introduction

Currently, concrete is the second most used material on the planet with the first item being water [1]. Its production volume has exceeded 10 billion tonnes per year globally [2]. According to recent publications, production of cement is responsible for approximately 5% of the total anthropogenic CO_2 emissions and 12-15% of the industrial sector's global energy use [3]. According to the Emission Database for Global Atmospheric Research (EDGAR) and CO_2 Emissions from Fuel Combustion (IEA), in 2016 the fossil fuel emissions in the Netherlands were 163,419,285 tons [4]. These emissions were divided into percentage of emissions per sector. Figure 1.1 shows these percentages:

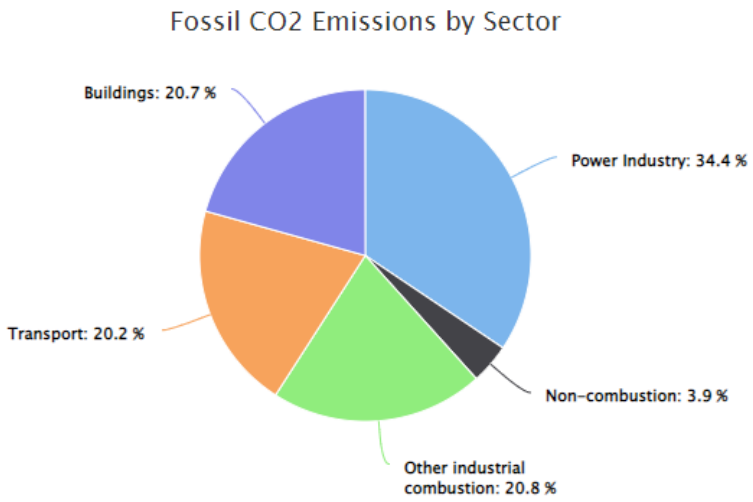

Figure 1.1: Fossil CO_2 Emissions by Sector [4]

According to figure 1.1, the buildings sector is responsible for 20.7% of CO_2 emissions. This includes the whole life cycle of a building which includes raw material supply, manufacturing of materials, construction and use stage, demolition, and recycling of waste [5]. In accordance with the Paris Agreement, the Dutch government aims to reduce its greenhouse gas emissions by 49% by 2030 and 95% by 2050 compared to the levels in 1990 [6].

Another important environmental factor that plays a hand is the management of construction and demolition waste (CDW). Based on the Waste Framework Directive of the EU council, the EU aims to manage waste in an environmentally sound way [7]. The objectives of the Waste Framework Directive are:

- The preparing and re-use, recycling, and other material recovery of non-hazardous CDW should be increased to a minimum of 70% by weight by 2020
- Promotion of selective demolition
- The reduction of waste generation

CDW takes up more than one-third of the total waste generated in the EU. This waste includes a lot of materials like concrete, wood, metals, and plastic. The recycling of CDW is essential for several reasons but maybe two of the most important reasons are [7]:

- Some components of the CDW have a high resource value, and they can be easily recycled into new products and materials.
- If kept non-recycled, some of the waste material can be hazardous to the environment.

Therefore, due to these goals and the environmental impact of the production of OPC, the search for a more sustainable concrete began. The aim was to find a concrete with similar or superior mechanical properties to cement-based concrete. One example of these types of concrete is geopolymer concrete. Geopolymer is a reasonable substitution for Ordinary Portland cement (OPC) because it has similar mechanical properties and lower CO_2 emissions. Another advantage of geopolymers is that waste material is included in its production which is beneficial to the environment and the economy.

Currently, there is a growing interest in the usage of a CDW which is a mineral wool waste. One of the uses of CDW is as a binder in geopolymer concrete. In Europe alone, the amount of mineral wool waste generated is over 2.3Mt annually. Mineral wool waste can consist of two types: glass wool (GW) and rock wool (RW) [8].

As an initiative from the EU for a more circular economy, the Wool2Loop-project was proposed. The main objective of this project is to decrease the amount of mineral wool waste in landfills and put it to good use while providing the construction industry with sustainable material [9]. The outline of the Wool2Loop project is shown in figure 1.2 below:

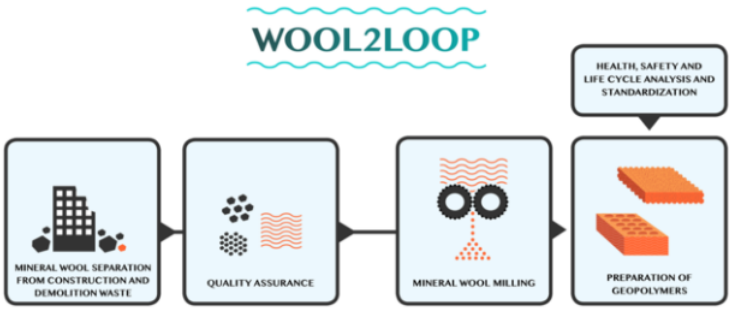

Figure 1.2: Wool2Loop project outline [9]

In the Wool2Loop project, the goal for mineral wool waste is to be separated from CDW, milled, used as a binder in geopolymer concrete, and then recycled again. This requires appropriate demolition approaches, quality control, and solving the low-density problem.

The Wool2Loop project involves research about cast alkali-activated materials and 3D printed alkali-activated materials. The 3D printing platform focuses on the printability of alkali-activated materials with binders containing demolition waste.

3D printing of materials has been used effectively in many industries. More specifically it has been used effectively in the construction industry. Techniques of 3D printing in this industry can be divided into 2 forms [10]:

1. Extrusion printing.
   It is similar to the Fused Deposition Modelling (FDM) method by extruding cementitious material

from a nozzle to print layer by layer. Examples of extrusion printing are Contour Crafting (CC) invented by Khoshnevis [11] and Concrete Printing (CP) by Lim et al [12].

2. Powder printing.
   It is a process that creates structures with complex geometries by depositing binder liquid into a powder bed [13]. One of the examples of powder printing is the D-shape technique created by Cesaretti et al [14].

The reasons 3D printing is becoming more popular in the construction industry are:

1. Reducing labour requirements hence lower construction costs and a higher level of safety on site.
2. Less on-site construction time
3. Reducing the possibility of errors by accurate material deposition
4. More architectural freedom

There have been several successful large-scale 3D printed structures recently. On April 30, 2021, the first 3D printed concrete house was available for its tenants. This project was carried out by the Eindhoven University of Technology with other institutions. The house fully complies with the building requirements in The Netherlands [15]. Another major project is the world's first 3D-printed apartment complex in China. The structure was built using recycled building materials and fast-hardening cement [16].

(a) 3D Printed House [15]

(b) Multistory Apartment Complex [16]

Figure 1.3: Large scale 3D printed structures

3D printed concrete is a type of concrete that can be used in construction using a 3D printer without the use of frameworks or vibrating the mix [17]. The 3D printing process starts with designing a building path using 3D printing software. The shape of the object is then sliced into flat thin layers with a certain thickness. The main idea behind this process is that a nozzle moves according to the predetermined path and then the fresh concrete is extruded [17].

As mentioned above, the printability of alkali-activated materials (or geopolymer) are studied. Hence, the following paragraphs will explain what geopolymers are. Geopolymer is an alkali aluminosilicate material made from the reaction of an aluminosilicate source with highly concentrated aqueous alkaline solutions like alkali hydroxides and concentrated metal alkali metal silicates [18]. The most obvious difference between alkali-activated binders and Portland cement is the alkaline activation process needs an aqueous alkaline component to be added while the hardening of cement requires the addition of water. Geopolymers have good properties including high early strength, low shrinkage, good sulphate, and corrosion resistance [19]. The aluminosilicate source is the alkali-activated binder (precursor).

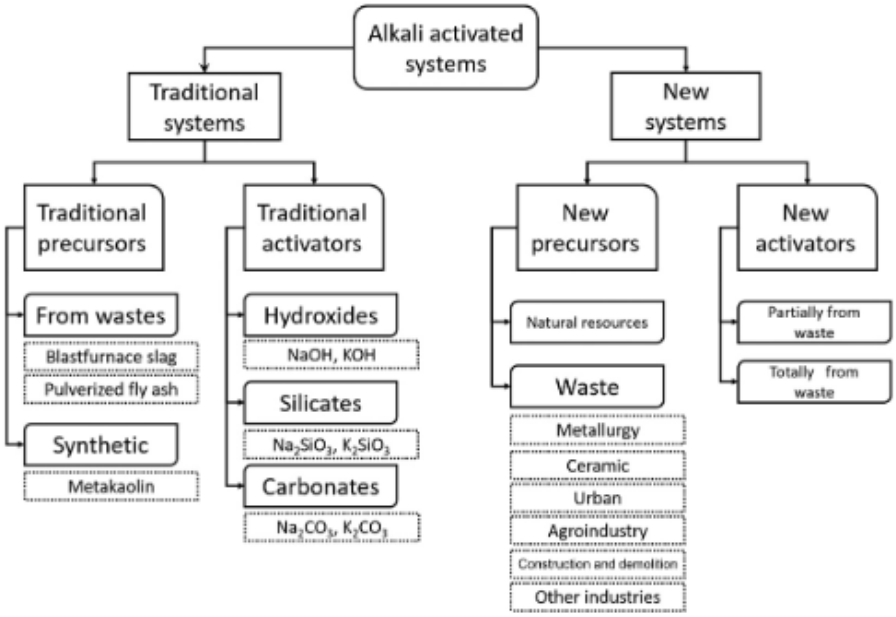

Figure 1.4: Traditional and New Alkali Activated Systems [20]

There are certain aspects of the aluminosilicate sources that affect the properties of the geopolymer [21]:

1. Particle size distribution / specific surface area
2. Reactivity of precursor, which can be influenced by:
   (a) Thermal activation
   (b) Mechanical activation
   (c) Chemical activation
3. Chemical composition
   (a) influence of Si and Al ions
   (b) influence of Na and K ions
   (c) influence of Ca ions

There are two types of Alkali activated binders [2, 22]:

- Low-calcium alkali-activated binders, like fly ash, metakaolin, and glass wool
- High-calcium alkali-activated binders, like blast furnace slag.

The distinction between these two types is based on the type of gel found in the structure. As shown in figure 1.5 the primary reaction product can be a calcium aluminosilicate hydrate (C-A-S-H) type gel or an alkali-aluminosilicate type gel (N-A-S-(H)). [2]

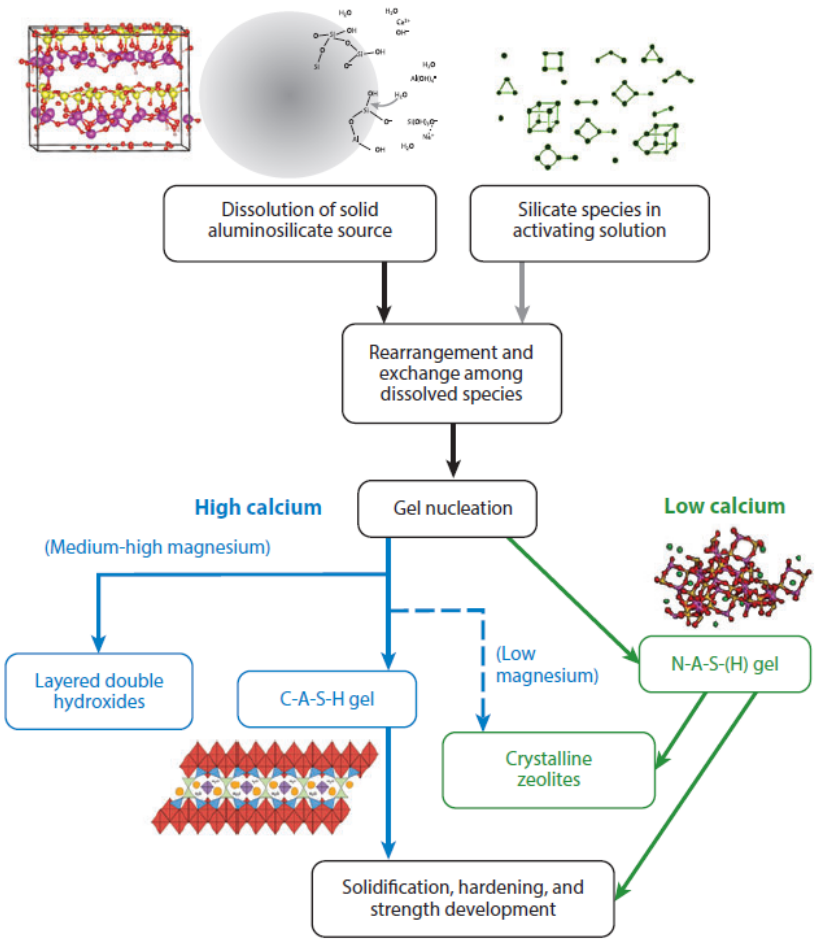

Figure 1.5: Reaction products of alkaline activation of a solid aluminosilicate-precursor [2]

1.1 High-calcium alkali-activated binders

For a system to be classified as a high calcium binder system, it should have a Ca/(Si+Al) ratio of 1. These systems are usually produced by the alkaline activation of blast furnace slag [2]. According to Provis et al. [23], calcium can improve many aspects of geopolymer concrete's durability because of its effect in reducing permeability which helps in having a longer service life.

1.1.1 Blast Furnace Slag (BFS)

Blast furnace slag is one of the by-products of iron production inside blast furnaces. It is produced when iron-ore, coke, and limestone are melted in the blast furnace. The cooling method influences the type of the BFS, it can be air-cooled, granulated, pelletized, and expanded [24]. Rapid cooling of BFS creates a glassy structure which is essential to have a reactive material while on the other hand slow-cooled BFS crystallize and have low reactivity [2]. BFS is made up of silica, alumina, and lime combined with sulfur, magnesia, and some oxides [25]. The physical and chemical properties of the BFS depend on the furnace. Usually, BFS that is produced in a certain furnace has similar physical and chemical properties [26].

Based on the work of Fernández-Jiménez, 2000; Shi et al., 2006; Provis and van Deventer, 2009 [27, 28, 26], it was concluded that the requirements for slag to be used as a binder are [29]:

- It has to be granulated or pelletized and have a vitreous phase of 85-95%.

- It must have a highly disorganized structure because the higher its glass polymerisation, the lower its hydraulicity will be.
- In terms of pH, it must be basic. For example, it should have a $CaO+MgO/SiO_2$ ratio of > 1. Basic slag has a higher hydraulic potential due to the fact that its activation is controlled by its lime content.
- It must have a specific surface within the range of 400-600 m^2/Kg.

Figure 1.6: Blast Furnace Slag [30]

The pH of the activator used has an important effect on the activation of BFS. This is due to the fact that calcium solubility is affected by pH; the higher the pH the lower its solubility. Hence, hydroxide-activated binders tend to have a lower reaction extent and lower mechanical strength than silicate-activated binders, as hydroxides have a higher pH than silicates [31, 32]. According to Wang et al., (2005) [33], one of the aspects that affect the slag's reactivity is its particle size. When the size of the slag particles is over 20 microns it has very low reactivity, while when the sizes were below 2 microns the slag fully reacted within 24 hours of activation.

The outcome of all studies related to the reaction products of the alkaline activation of BFS is that the primary product is a C-A-S-H gel [34]. While the second reaction product is usually hydrotalcite (Mg6Al2CO3(OH)16·4HO) [29].

1.2 Low-calcium alkali-activated binders

The most used binders in low-calcium systems are Fly Ash (FA) and Metakaolin. The main reaction product of the alkaline activation of these silica- and alumina-rich materials is an amorphous alkaline aluminosilicate hydrate (N-A-S-(H)) [35]. The H is in parentheses to show that water is not a vital structural component in this gel [36]. The secondary reaction product of such systems are zeolites [37].

The general mechanism for the activation reactions of low-calcium materials proposed by Glukhovsky (1994) [38] is defined by 3 stages:

- Destruction-coagulation
- Coagulation-condensation
- Condensation-crystallisation

1.2.1 Fly Ash (FA)

Fly ash is an industrial by-product of coal combustion. Fly ash is the solid waste collected using electrostatic precipitation or mechanical capture of the particles in the combustion gas. Before combustion, coal is milled to a powder. Then it is blown into a furnace at high speed. This suspension is heated to a temperature of 1500 $\pm$ 200 °C. This temperature is above the melting point of most of the minerals present. Ash is then released due to this process. [29].

There are mainly two types of waste produced from coal-fired steam power plants: fly ash and bottom ash or slag. The difference between them is their particle size. Fly ash which are the finer particles are collected by electrostatic precipitation or mechanical capture, while the coarser particles (bottom ash or slag) falls to the bottom of the furnace and is removed to provisional storage silos with wet discharge [29].

Figure 1.7: Fly Ash [39]

The chemical composition of fly ash depends on coal composition. The main components of fly ash are silica (SiO_2), alumina (Al_2O_3), iron oxides (Fe_2O_3), lime (CaO) and unburnt coal. It has smaller amounts of magnesia (MgO), sulfur oxide (SO_3), alkalis (Na_2O and K_2O). Fly ash is classified into two types based on its lime content [29]:

- Type F fly ash: it has a CaO content below 10%. It is the result of anthracite or bituminous coal calcination. It mainly consists of these oxides: SiO_2, Al_2O_3 and iron oxides. It is the the most abundant and frequently re-used.
- Type C fly ash: it has a high CaO content (higher than 10%), usually from 15% to 30%. It is produced during the calcination of sub-bituminous coal or lignite. It exhibits pozzolanic and cementitious properties.

The quality of fly ash varies with the coal type and the combustion furnace. According to Fernández-Jiménez and Palomo (2003) [40], there are certain requirements that have to be met by fly ash to be considered a good binder, mainly:

- Less than 5% unburnt material
- Fe_2O_3 content under 10%
- Low CaO content
- 40-50% reactive silica content

- 80-90% particles with a size under 45 μm
- High vitreous content

The alkaline activation of type F fly ash induces the precipitation of an amorphous alkaline aluminosilicate hydrate knows as N-A-S-H gel [41]. The secondary reaction products are zeolites such as hydroxysodalite, zeolite P, Na-Chabazite, zeolite Y and faujasite [29].

1.2.2 Glass Wool (GW)

Glass wool is one of the most common insulation materials used in buildings. Glass wool is considered unrecyclable due to its fibrous nature and low density [42]. GW is produced by melting sand, and soda ash with a high proportion of recycled glass at around 1400-1500 °C. Then after melting they are spun into fibres and mixed with organic resins before curing. During the spinning process, an aqueous binder is sprayed onto the fibres then the fibres are allowed to cool down and stiffen like glass. GW gains its structural stability when it is hardened inside a tunnel stove at approximately 250 °C [43]. Glass wool has a large percentage of Si and x-ray amorphous mineralogy and a high specific area hence it has the capability of being an AAM precursor [42].

Figure 1.8: Glass Wool [44]

The chemical composition of GW could be different depending on where it came from. Nonetheless, the main components are approximately: 60-65% SiO_2, 16% Na_2O and 7% CaO. Upon Alkaline activation, the binder gels formed are C-(N)-A-S-H, N-A-S-H, and layered double hydroxides (LDHs) [45]. Due to the low amounts of CaO that GW has, the formation of C-(N)-A-S-H is minimal. The main reaction product was an X-ray amorphous sodium silicate gel. Moreover, an additional reaction product was formed which is a partially Ca- and Al- substituted sodium silicate gel (N-(C)-(A)-S-H) [46].

Nevertheless, it has been denoted that the use of GW as the only precursor is not optimal as it has low reactivity, and it yields a mixture with low compressive strength [47, 48]. According to the work [48], even when GW is mixed with BFS, if the percentage of GW exceeds 50% of the binder, a very limited reaction degree occurred which can also be an indication of limited strength later on. Therefore, both BFS and GW will be used together as precursors to try to obtain optimum properties. This is also encouraged by the work of [48], as the results indicated that using waste glass wool with slag is feasible and can yield a mixturewith improved early-age properties like a prolonged setting time and reduced shrinkage.

1.3 Alkaline Activators

Alkali activators are the second most important component of geopolymer concrete. Alkali activators are capable of freeing silicate and the aluminate monomers in the precursor, which dissolves and forms an aluminosilicate gel [49]. There are many alkaline solutions that are used like: alkalis (hydroxides),

concentrated alkali metal silicates, Weak acid salts (alkali metal carbonates), strong acid salts(alkali metal sulfates), Aluminates, and aluminosilicates [2, 38]. Although, the most used activators are alkaline hydroxides, alkaline silicates, or a mix of both of them. The initial mechanism of the geopolymerization reaction is driven by the alkaline solution and its ability to dissolve the pozzolanic material and release reactive silicon and aluminum into the solution [50]. The cations and anions play two different roles in the alkaline activation process. The cation form the structural element and balance the negative framework of the tetrahedral aluminum. While the anions are an essential factor of the reactions happening in the systems and mineralogical and microstructural characteristics of the materials created [29].

1.3.1 Sodium Hydroxide (NaOH)

NaOH is a white ionic compound that is made up of Na^+ cations and OH^- anions. In water, sodium hydroxide breaks into one sodium ion and one hydroxide ion releasing heat. According to Glukhovsky (1967), the OH^- ions catalyze the dissolution of Si^4+ and Al^3+ by inducing the hydrolysis of Si-O-Si and Si-O-Al bonds. OH^- ions catalyze the hydrolytic reactions involved in many stages of the alkaline activation and it also raises the pH to the required value to start the initial dissolution of the precursor and the following condensation reactions.

However, when slag is used as the binder, it is not recommended to have very high OH^- concentrations. This is due to the fact again that Ca is less soluble in higher pH. As a result, a lower concentration of the alkaline solution is needed to activate slag [29]. NaOH was proven to be effective as a BFS activator as it can from calcium compounds less soluble than $Ca(OH)_2$ due to their reaction with the Ca^+2 ions from the slag [27]. Thus, a concentration of 2-4 M is needed to prepare a slag-based geopolymer [29].

It is also advised to keep the Na_2 concentration at 5% or lower in the activation of slag, as a higher percentage than that hinders the raise of strength. Moreover, such a high dose could prove to be more harmful, increase efflorescence and make the material more brittle, plus a higher cost [29]. On the other hand, a N_2O concentration below 4% of the binder affects the activation negatively resulting in lower strength of the paste [51, 48]

1.3.2 Sodium Silicate (Na_2SiO_3) / Waterglass

Sodium silicate is the second most common used agent in the alkaline activation of slag. it consists of Sodium oxide (Na_2O) and silica (SiO_2). It forms a glassy solid and is soluble in water. Soluble silica affects workability, setting, and mechanical strength development. It also modifies the gel composition and the microstructure of the material formed. There are two factors that have to be kept in mind when adding soluble silica: the silica concentration and the SiO_2/Me_2O molar ratio. Sodium silicate has a twofold contribution to strength development; one as an alkaline activator and it prompts the formation of a high silica primary gel [29].

When slag is activated using sodium silicate, the reaction products usually have high strength and short setting times due to the fact that sodium silicate leads to the formation of a high-silica primary gel [29].

According to Smolcyk, 1980; Wang and Scrivener,1995, Wang et al., 1995 [52, 53, 34], the optimal Na_2O content is approximately 4% of the slag weight and the most favourable SiO_2/Na_2O ratio for basic slag is between 1-1.5. It is believed that the soluble silica content in the waterglass can affect the reactivity in the raw material. This occurs because a higher silica percentage lowers the pH and increases the solutions' viscosity.

The use of both alkaline activators was studied in literature and it proved to be beneficial as it accelerates the dissolution of Si and Al components in the raw materials and also encourages the formation of Si-O-Al and Si-O-Si-O-Al and other prepolymer formation [54].

1.4 Problem Statement

One of the biggest gaps in the research relating to alkali-activated material is the effect of admixtures. This has to do with the fact that the their effect depends on many factors that change from one author to the other. To be more specific, when it comes to the 3D printing of alkali-activated materials, the gap in research becomes even bigger. This is because 3D printing of concrete is relatively a very recent innovation and not many research has been done on it using alkali-activated materials. This will be discussed further in the next chapter. The reason the effect of admixtures is important in this work is because alkali-activated materials are known for having very fast setting which is not suitable for 3D printing. Hence, admixtures need to be used to prolong the setting time and ensure that the viscosity of the mixture is adequate for good buildability. Thus, to reach the research aim of developing a mixture with good buildability properties, the effect of admixtures has to be studied to see which admixtures are mores suitable for the chosen binder.

1.5 Research aim and Objectives

1.5.1 Research Aim

The general aim of this thesis is to create a mixture enhanced by admixtures that has high quality 3D printing buildability properties. The admixtures used are retarders and viscosity modifying admixtures mainly used to increase the open time and improve the viscosity and yield strength of the mix. This project is part of the Wool2Loop project as glass wool is part of the binder that will be used.

1.5.2 Objectives

In order to reach the research goal, several objectives have been set to help reach this goal:

- Study the effects of various retarders (sucrose, sodium chloride, and sodium borate) and viscosity modifying admixtures (nano-clay, xanthan gum, and sodium carboxymethyl starch) on the early-age and rheological properties of a composite geopolymer binder.
- Create a mixture with an open time of 2 hours or more.
- Create a mixture with adequate early age and rheological properties; an initial setting time higher than 180 minutes, a spread diameter between 150-200mm and a yield stress around 1400 Pa.

1.6 Methodology

In order to study the effects of the admixtures to check if the mixtures reach the required early-age and rheological properties, several tests were conducted. First, the setting time, flowability, and yield stress development of the mixture with retarders was tested in order to choose the optimum percentage of each retarder. Second, the viscosity modifying admixtures were added to the mixtures with different retarders. The setting time, flowability, and yield stress development were tested for each mixture to first find the optimum percentage of the viscosity modifying admixtures and to find which mixture exhibits the best early-age and rheological properties. Then in the last stage, this mixture will be 3D printed. Furthermore, to further study this mixture, a flexural, compressive, and tensile bond strength tests were carried out to study its applicability in the industry. The methodolgy will be further discussed in chapter 3.

2

Literature review

2.1 3D Printing

3D printing of geopolymer concrete is relatively a new topic, hence there is a brief amount of studies regarding this topic. The reason behind this is the different material behaviour of geopolymer compared to cementitious concrete. The most important difference between geopolymer and cementitious concrete is the binders used as geopolymer does not have Portland cement. Moreover, they have a big difference when it comes to their rheological behaviour which is considered of immense importance when it comes to 3D printing [55].

Moreover, there are several factors affecting the printing process of geopolymer concrete, like the geometry and size of the components, material parameters, and machine parameters. Each category has essential parameters: open time, properties that influence buildability, and pumping are the most essential material parameters. Machine parameters include layer height, pressure, and speed [56].

A crucial aspect in 3D printing of concrete is the rheology of the concrete. Concrete should be pumped without needing too much pressure to mitigate the risk of segregation while retaining the shape under the self-weight of the layers after extrusion[57]. The extruded material must have plastic behaviour and deform irreversibly while preserving its shape after extrusion and handling its own self-weight. Thus, the required paste viscosity is higher than pastes used for cast concrete [58].

One of the most important rheological variables is the dynamic viscosity (η) [58]. It's a measure of the resistance when a material deforms irreversibly when an external load is applied. This occurs due to the internal friction in the material which are generated during the deformation. As the viscosity of a certain material increases, it will be less susceptible to deformation per time unit under an equal applied force. When it comes to viscosity there are 2 types of fluids: Newtonian and non-Newtonian. Non-Newtonian fluids are fluids that have a change in viscosity because of a change in the shear rate only while Newtonian fluids' viscosity stays constant. Two of the Non-Newtonian fluids categories are:

- Shear-thinning: their viscosity decreases as the shear rate increases.
- Shear thickening: their viscosity increases as the shear rate increases

Due to the fact that the viscosity of non-Newtonian materials is not constant, it is defined as apparent viscosity. However, the behaviour of geopolymers is generally described as time-dependent. Time-dependent behaviour is almost the same as non-Newtonian except that in time-dependent behaviour the change in viscosity happens at a constant shear rate or shear stress. Time-dependent behaviour consists of two opposite phenomena: anti-thixotropy (rheopexy) and thixotropy [58].

Thixotropy is defined as a time-dependent shear thinning property where gels flow under shear stress, but they are thick under static conditions [59], hence thixotropic materials are suitable for 3D printing. To further explain this, thixotropic materials are described by static and dynamic yield stress.

When the static yield stress is exceeded the material starts to flow. The minimum shear stress that maintains the flow is dynamic yield stress. Therefore, a low dynamic yield stress is ideal for pumping and a high static yield stress is required after extrusion to have better buildability [57, 60].

To define the rheological properties of materials, different tools can be used to measure these properties. A slug test setup was used to measure the yield stress development of the mixtures. The yield stress measurement is based on the length of the slug when it falls under the effect of its own weight and gravity.

According to the work of S. Muthukrishnan et al. [61], fresh concrete has to have a dynamic yield strength/initial static yield strength at time t=0 of 0.5-1.3 kPa to have uniform extrusion. They used a Viskomat XL (Schleibinger, Germany), which is a rotational rheometer with vane-in cup geometry. A 6-blade vane with blade dimensions of 69mm height and 43.5 mm radius was immersed in a cup with a radius of 82.5 mm filled with the sample. Furthermore, it should have a viscosity higher than 10^5 Pa.s after extrusion to maintain its shape. Nevertheless, the values of the yield strength development and stiffness to achieve good buildability can be different depending on the process parameters which include the printing rate, nozzle orientation, shape and size of the filament, and the structure to be built. According to Biranchi Panda et al. [62], a yield strength of 180-1000 Pa is required for the stability of a single layer with a height of 15mm. While the bottom layer requires a yield strength of -12 kPa to support a 1m structure. Using an Anton Par MCR 301 rotational rheometer, Chenchen Sun et al. [63] reported that a sample with a yield stress and a plastic viscosity of 72.25 Pa and 35.09 Pa.s respectively was too difficult to extrude.

According to the results of [54], rheology is important for the extrudability and buildability of 3D printed geopolymers. To be more specific, the workability and interlayer forces of printing pastes can influence these properties. The paper also investigated the effect of the Si/Na ratio on the extrudability and buildability of a BFS-based paste. Firstly, as the Si/Na ratio decreases the yield stress increases significantly. This is explained by the fact that Na ions can accelerate the dissolution of raw materials. Secondly, the speed of yield stress development of fresh pastes decreases when the Si/Na ratio increases. Hence, a lower Si/Na ratio leads to the rapid development of the yield stress which can help stabilize the layer-layer buildup thus better buildability. Lastly, sodium hydroxide increased the rebuilding potential of the pastes due to the fact that sodium hydroxide accelerates the rate of geopolymerization. This acceleration leads to an increase in the coagulation of the system enhancing its rebuilding potential.

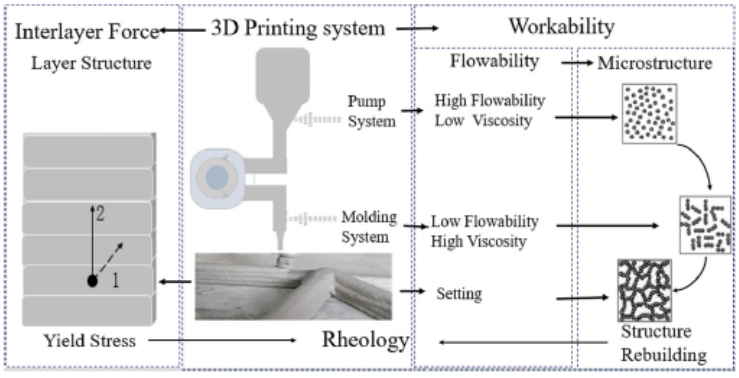

Figure 2.1: Workability of 3D printing concrete [54]

Moving on from rheology, an important element when it comes to 3D printed structures is the interlayer bond between the printed layers. One factor that affects this tensile bond strength between the printed layers is the rest time. This bond strength is important because it can notably affect the hardened properties of 3D-printed concrete. Rest time can be defined as the time interval during which the mixed concrete loses its fresh properties in the printer before printing [17]. Increasing the rest time enhances the stability of the layers [64]. When the rest time was increased by 20 minutes per layer,

they managed to avert destructive deformation but the total needed construction time increased. They also found out that heat application to the nozzle while printing can enhance the stability of the layers.

To further emphasize the significance of the rest time as a parameter of 3D printing, it does not only affect the bond strength but also the workability and the mechanical properties [17]. Ma et al. [65] managed to find a relation between workability and mechanical properties to find the optimum rest time: in general, extrudability decreases when the rest time is increased, while buildability increases. Workability was characterized by extrudability coefficients while the mechanical properties were characterized by the coefficients of buildability.

Based on the work done in the laboratory, the initial setting time for a 3D printable paste was between 1-1.5 hours. While the required spread using a mini-slump test with dimensions of D_1 = 100 mm, D_2 = 60 mm, H = 70 mm is between 150-200mm for good flowability. Initial setting time is an important early-age property because it is often regarded as open time when it comes to 3D printing. Open time is a time interval in which the freshly mixed materials maintain their consistency for smooth transportation and extrusion. A lengthy open time can be advantageous to extrusion and good interlayer bonding. However, it negatively affects the shape stability of printed objects [66].

To obtain the above mentioned properties and further enhance them, two types of admixtures will be used: retarders and viscosity modifying admixtures. They will be further discussed in the next section.

2.2 Admixtures

Admixtures are artificial or natural materials added to the concrete mix besides cement, water and aggregate immediately before or during mixing [67]. They can be inorganic like minerals or organic in solid or liquid form [68]. Most of them come in a ready-to-use liquid form. They are primarily used to reduce the cost of concrete construction, to alter the properties of hardened concrete, guarantee a good quality of concrete during mixing, transporting, placing, and curing. The successful use of these admixtures relies on the use of proper methods of batching and mixing [69].

Admixtures work by interacting with the cementitious system by physical, chemical, or physicochemical action, adjusting one or more properties of the concrete, mortar, or paste at different states whether it is the fresh, setting, hardening, or hardened state [68]. Admixtures are classified based on their function. There are five main classes of admixtures:

1. Air-entraining admixtures
2. Water-reducing admixtures
3. Retarding admixtures
4. Accelerating admixtures
5. Plasticizers (superplasticizers)

Furthermore, all the other types of admixtures fall into the specialty category. They can be used for corrosion inhibition, shrinkage reduction, alkali-silica reactivity reduction, workability enhancement, bonding, damp proofing, and coloring [69].

When it comes to alkali-activated systems there is confusion about what's considered an admixture. This is because sometimes FA and BFS are added to OPC as an admixture. However, in the case of alkali-activated systems, neither the alkaline activator nor the solid aluminosilicates should be considered as admixtures because they are binder components [70].

Unfortunately, there is a lack in literature regarding the effects of admixtures on alkali-activated systems. This is because it is hard to find an admixture that has an effect on these systems unlike in OPC where there is a wide variety of admixtures. One other reason is that even for the admixtures that do have an effect on alkali-activated systems, the results reported by different authors are sometimes contradictory. The difference in the results is because the admixtures' effect depends on the precursor

used, the type and concentration of the alkali activator, and the dosage of the admixture [70].

There are two things that should be taken into consideration when dealing with admixtures and alkali-activated materials [70]:

- When a liquid admixture is added to the mix, the water content of the admixture should be considered in the mix design because these mixes are highly sensitive to different water/binder ratios.
- The effects of the admixture should be analyzed in the context of what the admixture is supposed to do. For instance, the more hydrophobic a polymer is, the more air-entraining it is, which could be either a positive attribute or a negative one depending on the desired outcome. On one hand, hydrophobicity helps in making the surface water-resistant and facilitates controlled air entrainment which is necessary for freeze-thaw resistance, however too much air can severely affect the durability and permeability. Moreover, some plasticizers can increase the slump but this is not necessarily an advantage if this outcome was because of the air entrainment and not caused by a plasticizing action.

As mentioned in section 2.1, We are looking for admixtures that can prolong the setting time and improve workability. Thus, retarders and viscosity modifying admixtures will be used to achieve these properties.

2.2.1 Retarders

Retarders in concrete are used to slow down the setting of concrete. Retarders are usually used in hot weather or transportation to delay the setting. They maintain the workability of concrete during placement and postpone the initial set [71]. Unfortunately, most of the retarders available in the market are not fit for geopolymer concrete. Some of the retarders that have proven to be effective are sucrose, sodium chloride, and sodium borate.

2.2.1.1 Sucrose

Sucrose has been studied by some authors [72, 73, 74, 61]. It was concluded that sucrose had the same effect of prolonging the setting time. According to [73], sucrose combined with Ca, Al, and Fe forming insoluble metal-organic complexes that covered fly ash particles and delayed the geopolymerization process causing the retarding effect. While according to [74], the reason for the retardation effect was the increase of viscosity by the addition of sucrose which postponed the initiation of the geopolymerization process.

Based on [61], the increase in sucrose concentration led to a slower yield strength development of concrete which was expected, it had no effect on the dynamic viscosity even under different shear rates. Compared to the reference sample without sucrose, the sample with 1% sucrose could only recover 70% of its viscosity after a shearing rate of $13s^{-1}$. The change in yield strength development rate between the sample with and without sucrose was due to the delay in formation of C-S-H bridges.

Based on the above mentioned papers [72, 73, 74, 61], the optimum sucrose dosage could be between 0.5-3% depending on the type of precursor used and the alkaline activator. These percentages lead to a sufficient retardation effect without a drastic effect on the compressive and flexural strength.

According to the results of Andri Kusbiantoro et al. [73], an addition of 1.5% and 2.5% of sucrose led to a delay in the initial setting time of 10 minutes and 15 minutes, respectively. While Bong et al.[72] results indicated a delay in initial setting time of 188 minutes when 1% sucrose was added and it increased the spread diameter by 27% thus improving its workability. Furthermore, based on [74], 3% sucrose improved the initial setting time by 100%.

2.2.1.2 Sodium Chloride (NaCl)

Sodium chloride can act as either an accelerator or a retarder depending on its dosage [75]. At low dosages, it acts as an accelerator but at high dosages, it acts as a retarder. Based on the work of Brough et al. [75], when sodium chloride's mass percentage compared to the mass of the binder is 4% or below it acts as an accelerator but when it is 8% or above it acts as a retarder.

NaCl was added to the activator solution before mixing. The addition of 8% significantly retarded the strength development that it was too weak to demould at on day 1 but instead it was demoulded on day 3. The initial setting time of the control sample without any NaCl was 4 hours. 3 different mass percentages of NaCl were added: 1%, 4%, and 8%, and the initial setting times for these samples were: 2 hours, 3hours, and 10 hours, respectively.

Moreover, according to the calorimetry test, the addition of NaCl caused a delay in the two main heat evolution peaks which were observed in the control sample. However, even though the heat evolution and the time at which it evolved were affected by the addition of NaCl, the total heat evolved in each stage was the same. This along with the fact that the nature of the hydration products were similar and no new phases were observed by XRD, means that NaCl did not affect the mechanism of hydration. It was concluded that the retarding effect was caused by that fact the NaCl lowered the pH of the system, hence slowing down the reaction.

Based on A.R. Sakulich et al. results [76], 4 mass percentages of NaCl of 5%, 10%, 15%, and 20% were added. NaCl was added to the powder reactants rather than to the activation solution. It was concluded that 20% was the minimum percentage needed to effectively delay the setting time without affecting the compressive strength. Figure 2.2 shows the effect of NaCl concentration on the 7^{th} day compressive strength and setting time.

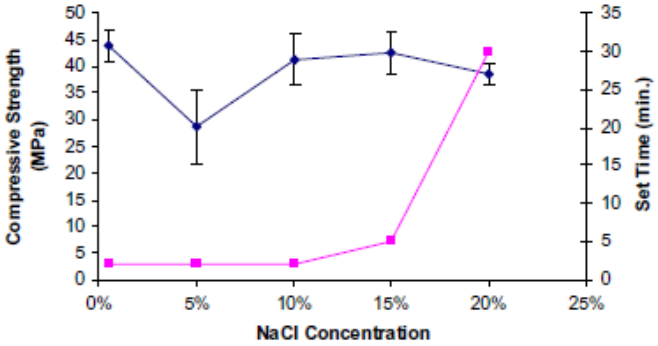

Figure 2.2: Effect of NaCl concentration on 7 days compressive strength and setting time [76]

After 1 day, the compressive strength of the sample was 50% of the strength achieved by the control sample, but after one month, the sample recovered all of its compressive strength.

2.2.1.3 Sodium Borate (borax)

Borax has been used as a retarder in OPC. It was concluded that it is capable of delaying the setting time while speeding up the hardening process in OPC [77]. Several authors investigated the effect of borax on alkali-activated materials [72, 78, 79, 80].

Sinha [78] concluded that the setting time and workability were changed by different dosages of borax. It was observed that as the dosage of borax increased the delay in setting time and flowability increased. However, according to the results, there is a minimum borate dosage that needs to be added to have an effective improvement on the initial setting time. This percentage was 4% according to the results obtained. The mixes with 4% and 6% retained fluidity for more than 30 minutes. Borate also has

water-retaining nature which also contributes to the better flowability of the mixes. The compressive strength was not affected when 4% and 6% were added but there was a slight improvement in flexural strength.

The retarding mechanism observed was the same for all authors [78, 79, 80]. When the borate is added to the alkaline solution, it reacts with the silicate group forming a B-O-Si bond. In this bond, boron has a four-coordinated bond with weak bond energy. When it is mixed with the binder, the aluminate ions that are released in the solution by the aluminosilicate material break the B-O-Si bond and then link with it by forming a B-O-Al-O-Si bond which is a more stable structure of boron having a three coordinated bond. This transformation occurs due to the fact that in a B-O-Si bond, boron has a tetrahedral geometry which is unstable with weak bonding energy and has a tendency to break and rearrange into a trigonal planner coordination. This coordination is more stable and has higher bonding energy. Consequently, this change of bond from B-O-Si to B-O-Al-O-Si retards the formation of the Si-O-Al bond. Hence, this delay in the formation of geopolymer products led to the prolongation of setting time.

The results of Jixiang Wang at al. work [79] also showed a retarding effect of sodium borate. The optimum dosage observed was 5%. Borate did not only prolong the setting time but it also changed its early rheological behaviour. It was observed that there was an increase in viscosity with shear rate. The compressive strength slightly decreased with $\leq$ 5% borax but it was severely affected when the concentration was 8%. There was also a decrease in the free drying shrinkage due to the moisture-retaining capabilities of borate.

One important conclusion from Huajie Liu et al's results [80], is that the retarding effect of borax is affected by the concentration of the alkali and temperature. Bong et al. [72] also observed a delay in setting time and a 27% increase in the spread diameter when borax was used.

2.2.2 Viscosity Modifying Admixtures (VMA's)

VMA's are water-soluble materials which increase the viscosity of mixing water and they improve cement paste's ability to retain its components in suspension. They are mainly added to self-compacting concrete, underwater concrete or shotcrete to improve their stability [81]. This increase in stability is due to a combination of different physio-chemical processes which depend on the nature and concentration of the VMA [82].

Pastes with VMA's display shear-thinning behaviour by which the apparent viscosity decreases with the increase in shear rate [81]. These mixtures are often thixotropic in which the viscosity buildup is accelerated due to the association and entanglement of polymer chains of the VMA at a low shear rate which can inhibit flow and increase viscosity [81].

VMA's can also retard the initial setting time, delay hydration and increase the porosity content [83, 84]. Furthermore, VMA's proved to be useful for 3D printing applications. According to the results of Chaves Figueiredo et al. [83], mixtures with higher concentrations of VMA can help in achieving better shape stability of extruded mortar filaments. However, they showed higher extrusion pressure, bulk and shear yield stress which might have affected extrudability.

In the following sections, 3 VMA's that were used in alkali-activated materials and will be used in this thesis are going to be discussed and how they affected the paste's properties. These VMA's are nano-clay (attapulgite), sodium carboxymethyl starch (CMS), and xanthan gum (XG).

2.2.2.1 Nano-clay (attapulgite)

Attapulgite is a form of purified magnesium aluminosilicate. It's a thixotropic additive used to enhance workability. Its particles are positively charged at the ends and negatively charged along the axis. This helps MAS to agglomerate and increase the flocculation rate of the geopolymer by dipole-dipole interactions. With enough shear, the geopolymer regains its workability because the dipole-dipole

interactions are weak [85].

Muthukrishnan et al. [61] also studied the effect of adding MAS and sucrose to a BFS and FA geopolymer mix. 0.75% of MAS was added to the sample with 1% sucrose. The sample was able to recover 200% higher viscosity than the sample with sucrose only. Moreover, the sample was able to recover 303% higher elastic modulus but with a shorter open time for printing. Thus the sucrose dosage was increased to 1.5% which increased the open time but lowered buildability with a reduction in viscosity recovery and elastic modulus by 15.6% and 30.8% respectively. It was also reported that the addition of MAS led to an increase in the dynamic viscosity which could affect pumpability. Nevertheless, due to the high thixotropic properties of MAS, there was a notable reduction in the viscosity when the shear rate was increased. In addition, due to the formation of a lubrication layer due the shear-induced particle migration, the difference in bulk viscosity between the samples with and without MAS would not affect the pumpability a lot.

After printing, it was concluded that the mixturewith 0.75% MAS and 1.5% sucrose was the most successful printable one. There were able to print more than 120 layers which had a height of > 1.4m from the print bed. The reason behind the increase of open time was the formation of water molecules as a by-product of the condensation reaction. This may have happened when the entrapped water molecules were released during shearing. The water molecules acted as a lubricant to the concrete layers to regain its initial rheology [61].

According to the results of Panda et al. [86], when 1.2% of clay was added, the sample had better viscosity recovery and higher yield stress (when the material was at rest) than the original sample. Furthermore, during extrusion, viscosity went down which led to a well extrudable mix without any discontinuity and clogging issues even though it has high static yield stress. Interestingly enough, even though the addition of clay caused an increase in the yield stress to a value beyond the defined limit of extrusion by the author, it did not cause any clogging of the pump or discontinuities while printing. However, this is expected because this yield stress was caused by the thixotropy effect that easily breaks down during extrusion because of the pressure of the pump.

In the work of Panda et al. [62], nano-clay was added to improve the thixotropy of the mixes. This was done by spreading the clay in water and it was added to the geopolymer mortar at the end of the mixing procedure. 0.5% of nano-clay was added to the mix. This small amount resulted in a significant improvement of the yield stress of the sample. During the flow of the material, the positive and negative charged nano-clay particles are on opposite ends. They aligned themselves in the direction of the flow because of the repulsion between similar charges. However, when the material was at rest, the oppositely charged ends attracted each other and flocculated. The addition of nano-clay leads to an increase in the apparent viscosity due to the improved flocculation. This process can be improved if there was extra free water present [87].

When the activator to binder ratio was 0.4, there was no significant effect due to clay. This can be due to the higher pH of the solution under higher activator concentration. At higher pH, the negatively charged clay particles were not aggregated enough due to the electrostatic repulsive forces [88]. It was reported also that clay enhanced the recoverability within 60s of extrusion. This was an indication of the material viscosity after it went through shearing. It was also concluded that clay improved the shear-thinning behaviour. This improvement occurred due to the stiffening mechanism of nano-clay that increases the bonding strength between different phases hence leading to a higher equilibrium stress. The fact that the mixture with clay needed a shorter time to reach this equilibrium, the mixture could be easily broken down during extrusion thus less extrusion pressure is required. Nano-clay had no effect on the initial setting time nor in accelerating the rate of strength development. It also had no influence on the heat flow and cumulative heat of the mixes, which means that the addition of clay did not change the reaction mechanisms. A slight decrease in compressive strength was observed in the samples that had nano-clay [62].

2.2.2.2 Xanthan Gum (XG)

Xanthan gum is a naturally obtained polysaccharide. It has rheological properties of high quality which helps to improve other materials' rheological properties. Xanthan gum is an excellent rheological admixture because its solutions have similar properties as non-Newtonian fluids, and they show high pseudoplastic behaviour under shear. Furthermore, XG is considered thermally stable and is not affected by a wide range of pH which makes it a suitable admixture for alkali-activated material [89].

Aboulayt et al. [90] concluded that the addition of xanthan gum improved the stability of a metakaolin-fly ash mix without affecting the geopolymerization reaction. They also observed that the marsh cone flow time increased as the xanthan gum percentage increased. After studying the rheological behaviour they found out that as the concentration of XG increases the yield stress and the consistency of the activation solution increases while the shear thinning index decreases. When the fly ash content was kept constant, the increase of XG concentrations led to an increase in both the yield stress and the plastic viscosity. It was also observed that XG's influence on viscosity was higher at lower shear rates.

In a different study, Aboulayt et al. [91] again observed that the marsh flow time of a BFS and FA mix increased as the XG's concentration increased. This increase was explained by the fact that XG increases the viscosity of the activation solution. They also concluded that XG's content had no effect on the calorimetric responses.

2.2.2.3 Sodium Carboxymethyl Starch (CMS)

CMS is a uniform homogeneous paste of enough consistency that can be effectively used as a VMA. It allows the deposition of the extrusion line layer by layer while avoiding deformation or collapsing due to self-weight. It is a white or yellowish powder which is a kind of an anionic natural polymer polyelectrolyte ether with starch as a raw material [63].

Five samples were tested in Sun et al. work [63], with CMS dosages of 0%, 2%, 4%, 6%, and 8% to investigate the effect of changing the amount of VMA to adjust the paste. Under ambient temperature of $23 \pm 2\ ^{\circ}C$, as the CMS content increases, the setting time increases. The initial setting time of the control group is 58 minutes while the initial setting time of the sample with 8% CMS was 252 minutes. This retarding effect was due to the fact that when CMS was dissolved in water and added to the binder, it covered the surfaces of the slag particles hindering the reaction between the alkaline activator and slag.

It was also concluded that CMS increased the viscosity of the solution while also decreasing ion binding rate and migration rate of water and active particles thus retarding the process of depolymerization-polycondensation. Since CMS has good water-retaining properties, enough water remained in the paste slowing down the evaporation process leading to a prolonged setting time [63].

Moreover, CMS altered the fluidity of the mix. Fluidity decreased as the CMS content increased. It was also reported that the shear stress increased with the increase in CMS content. At a shear rate of $100\ s^{-1}$, the shear stresses for each CMS percentage were 547 Pa, 636 Pa, 1050 Pa, 1080 Pa, and 3220 Pa. The paste with CMS showed shear-thinning properties and acted like a pseudoplastic fluid which can prove to be beneficial during extrusion [63].

The molecular chain of CMS had high viscosity when the shear rate was low, however, when at higher shear rates the molecules moved in a way parallel to the direction of the shear force causing a reduction in viscosity and easing the sliding of the molecules. As the CMS content increased, the plastic viscosity and yield stress increased. This is advantageous because the risk of segregation in the extrusion process is lowered when plastic viscosity increases. While when the yield stress is higher, it prevents the printing layer from collapsing due to the weight of the subsequent layer [63].

As a result of the aeration effect of CMS, as the CMS content increased, a larger number of pores appeared in the interior of the mortar. This was caused by the higher concentration which lowered the surface tension of the aqueous phase of the paste resulting in more air in the paste. This led to a

decrease in the compressive and flexural strength of the paste [63].

It was concluded that CMS had no hand in the chemical reaction during the synthesis of geopolymer. This was due to the fact that CMS did not affect the crystal shape of the material while the diffraction peak was still the same as the control sample. Lastly, drying shrinkage decreased with the increase of CMS content [63].

Samples with 2% and 8% of CMS were not printable. However, the samples with 4% and 6% were extruded continuously at a speed of 30 mm/s without any fracture or discontinuity and also without any collapsion of printing layers [63].

2.2.2.4 Sodium Carboxymethyl Cellulose (CMC)

Ma [92] studied the effect of 4 kinds of CMC's on the properties of alkali activated cement materials. The difference between the CMC's was the pH and their molecular weight. They concluded that the molecular weight and viscosity of CMC were positively correlated. They also concluded that the addition of CMC increased the fluidity while increasing the viscosity of the fly ash and slag based composite binder. It was also noticed that CMC decreased the fluid loss of the sample minimizing the decline in strength.

Furthermore, Bong [93] concluded that the addition of CMC also improved the workability of alkali-activated concrete. The purpose of his study was to optimise sustainable geopolymers for 3D printing construction applications. Hence among the tests they performed was an extrudability test, and a shape retention ability test. Both tests showed positive results regarding the addition of CMC. With the addition of CMC none of the samples had a blockage, segregation, tearing, or bleeding problem during extrusion. They also concluded that as the CMC content increases, the shape retention ability is better.

2.3 Concluding Remarks

Based on this literature review, 3 types of retarders and viscosity modifying admixtures will be used to enhance both the early-age and rheological properties of the geopolymer mix that will be used. The retarders used will be sucrose, sodium chloride, and sodium borate. While, the viscosity modifying admixtures will be nano-clay (attapulgite), xanthan gum, sodium carboxymethyl starch, and sodium carboxymethyl cellulose.

Furthermore, the combination of these retarders with the viscosity modifying admixtures will be tested to check if they will be compatible with each other. The reason behind this is because the retarders are used to slow down the reaction to increase the open time of the mix but on the same hand the mix should not be to flowable because otherwise the printed layers will not be able to handle the self weight. Thus, the use of viscosity modifying admixtures to improve the viscosity and the yield strength of the mix.

3

Materials and Methods

3.1 Overview

This section includes the materials used and their chemical composition. The experimental methods, test program and parameters used to obtain the results required are also presented in this section. As mentioned earlier, the effect of admixtures on the early-age and rheological properties have to be studied, hence multiple tests will be performed in order to acquire these results. Moreover, he binders ratio, the liquid to binder ratio, and the water to binder ratio will be kept constant throughout this work so that the only variable is the type of admixture used and its concentration to be able to fully understand the effect of each admixture.

3.2 Materials

3.2.1 Fly Ash (FA)

3.2.1.1 XRF-analysis

According to the XRF analysis, the fly ash used is made up of 55.8% silica (SiO_2), 23.7% aluminum-oxide (Al_2O_3), 6.16% Iron-oxide (Fe_2O_3), and other compounds in lower percentages. This is expected as fly ash is known for having high percentages of silicon (Si) and aluminum (Al). This is a type F fly ash as the CaO % is below 10%. Table 3.1 shows the chemical composition of the fly ash used.

Table 3.1: FA XRF analysis

Compound	Concentration %
SiO_2	55.8
Al_2O_3	23.7
Fe_2O_3	6.16
CaO	6.23
MgO	2.65
MnO	0.06
K_2O	1.36
TiO_2	1.16
SO_3	0.80
P_2O_5	0.88

3.2.1.2 XRD-analysis

An XRD analysis was done to analyze and identify the different crystalline phases of fly ash. Because the FA samples were partly amorphous, for quantification crystalline ZnO (zincite) was added as internal

standard. After observing the large humps between 10° and 90° 2θ in the sample, it is clear that the sample is mostly amorphous. The results are shown in table 3.2 and figure 3.1:

Table 3.2: XRD analysis of FA

Compound	**Wt%**
Quartz (SiO_2)	13 ± 1
Mullite ($Al_{1.272}Si_{0.728}O_{4.864}$	16 ± 1
Magnetite (Fe_3O_4)	<1
Calcite ($CaCO_3$)	<1
Amorphous	70

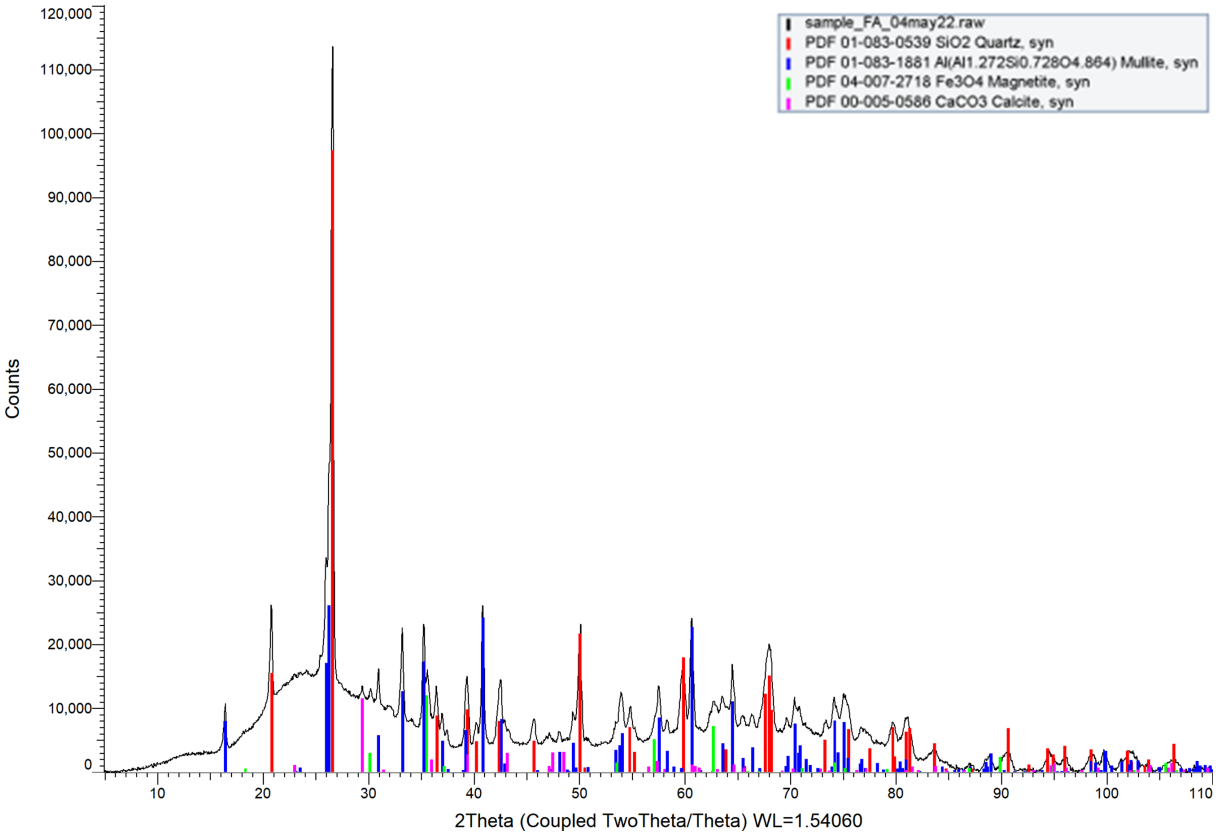

Figure 3.1: XRD analysis of FA

3.2.2 Ground-granulated Blast Furnace Slag (GGBFS)

3.2.2.1 XRF-analysis

According to the XRF, GGBFS composes of 34.5% silica (SiO_2), 38.1% calcium-oxide (CaO), 13.7% aluminum oxide (Al_2O_3), and smaller percentages of other compounds. The percentages are reasonable since GGBFS is known for being rich in calcium (Ca) and silicon (Si). Table 3.3 shows the XRF-analysis result of GGBFS.

Table 3.3: GGBFS XRF-analysis

Compound	Concentration %
SiO_2	34.5
Al_2O_3	13.7
Fe_2O_3	0.40
CaO	38.1
MgO	9.08
MnO	0.27
K2O	0.48
TiO_2	1.11
SO_3	1.69
Na_2O	0.46

3.2.2.2 XRD-analysis

An XRD analysis was done to analyze and identify the different crystalline phases of blast furnace slag. The sample appeared totally amorphous thus no ZnO was added. According to the results of the analysis the sample was amorphous. However, there was an unidentified peak at 32° 2θ. The result of the XRD is shown in figure 3.2:

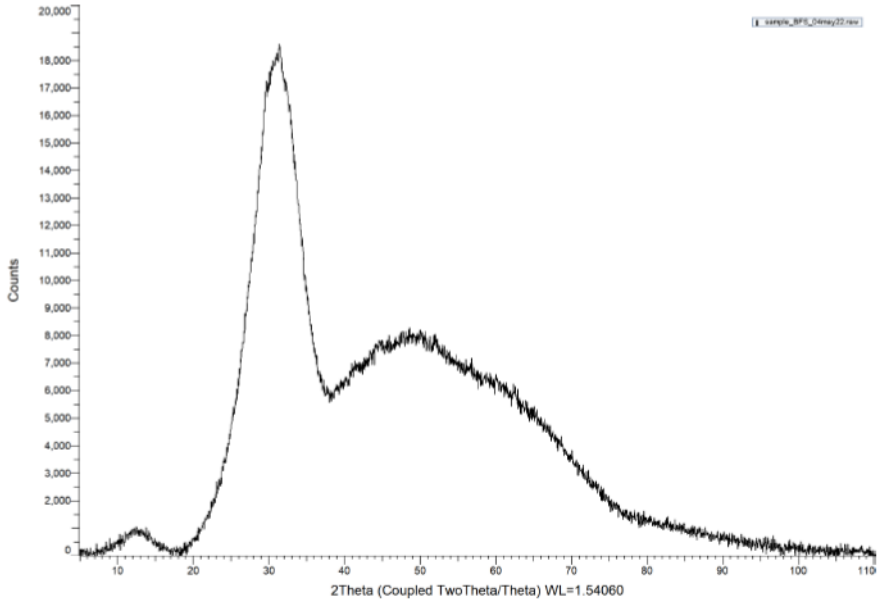

Figure 3.2: XRD analysis of BFS

3.2.3 Glass Wool (GW)

3.2.3.1 XRF-analysis

According to the XRF-analysis, GW composes of 60.1% silica (SiO_2), 15.9% sodium oxide (Na_2), 10.8% calcium-oxide (CaO), and other compounds in smaller concentrations. Glass wool is known for being rich in silicon (Si). Table 3.4 shows the XRF-analysis result of GW.

Table 3.4: GW XRF-analysis

Compound	Concentration %
SiO_2	60.1
Al_2O_3	6.83
Fe_2O_3	0.47
CaO	10.8
MgO	1.86
MnO	0.63
K_2O	0.49
TiO_2	1.42
SO_3	0.75
Na_2O	15.9

3.2.3.2 XRD-analysis

An XRD analysis was done to analyze and identify the different crystalline phases of glass wool. Because the GW samples were partly amorphous, for quantification crystalline ZnO (zincite) was added as internal standard. After observing the large humps between 10° and 90° 2θ in the sample, it is clear that the sample is mostly amorphous. The results are shown in table 3.5 and figure 3.3:

Table 3.5: XRD analysis of GW

Compound	Wt%
Quartz (SiO_2)	2 ± 1
Calcite ($CaCO_3$)	4 ± 1
Gibbsite ($Al(OH)_3 6$	7 ± 1
Rutile (TiO_2)	1 ± 1
Amorphous	86

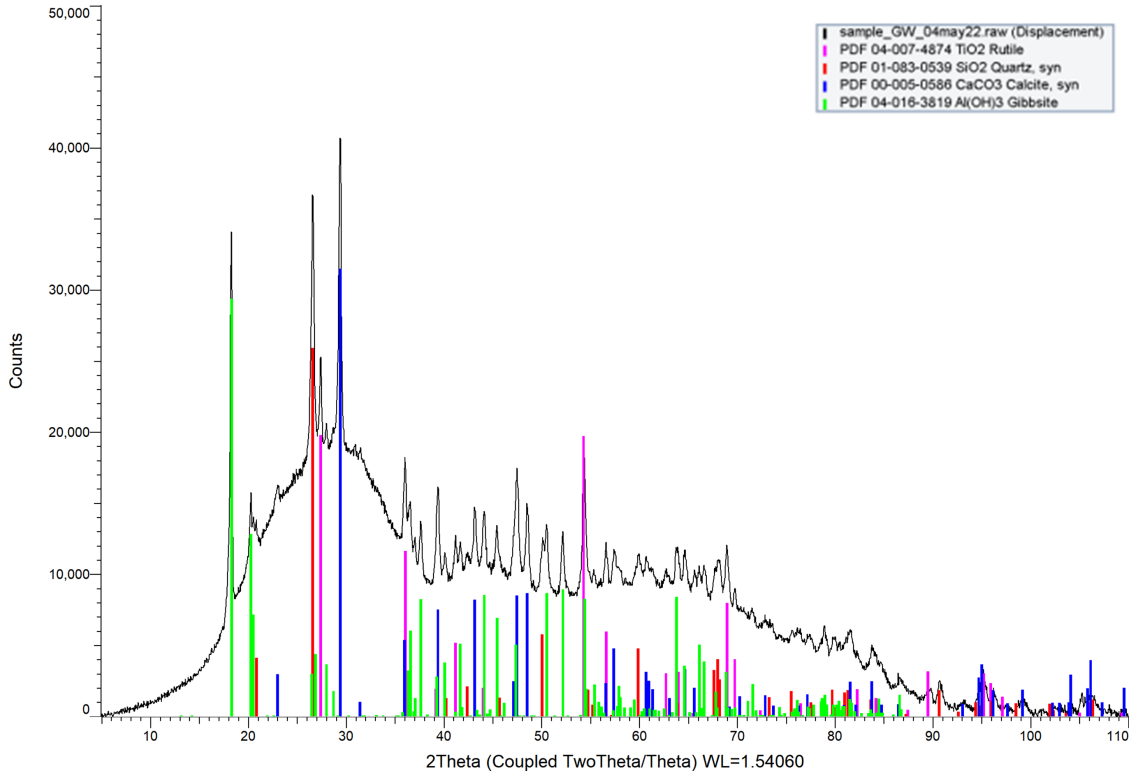

Figure 3.3: XRD analysis of GW

3.2.4 Initial Mix Design

The mixture that has to be prepared should have an initial setting time higher than 3 hours, open time higher than 2 hours, good strength development (40MPa), appropriate yield stress development (1400Pa) for 3D printing, suitable extrudability and buildability. The paste that will be used is based on the previous work done at the university. The paste proved to have good strength development but the problem was that it had short setting and open time which affected its printability. The mixture consists of 60% FA, 20% GGBFS, and 20% GW. The alkaline activator was composed of waterglass (Na_2SiO_3) and sodium hydroxide (NaOH) with a SiO_2/Na_2O ratio of 1.5. The binder ratio and the alkaline activators ratios will be fixed throughout the entire work. NaOH was added to the activator in pellets. Waterglass was supplied from PQ corporation with the following composition:

- SiO_2: 29-30.5%
- Na_2O: 14.5-15.5%

Table 3.6 shows the mix design of the mixture used:

Table 3.6: Mix Design: material percentages for a 300g sample

-	FA (g)	GGBFS (g)	GW (g)	Waterglass (g)	NaOH (g)	Water (g)	Liquid to binder ratio	SiO2/Na2O (activator)
M20S	180	60	60	90	6.4	23.6	0.4	1.5

3.2.4.1 Preparation and mixing procedure

First the alkaline activator by adding the NaOH pellets to the Waterglass liquid and they are mixed. This reaction is exothermic, hence the activator is left for 24h to cool down.

When paste is prepared, the dry materials are mixed for three minutes using the Hobart mixer, the alkaline activator solution is added to the dry materials and the entire mixture is mixed for three minutes at low speed. After that, the mixture is mixed at high speed (2) for on minute then back to slow mixing for another minute.

When mortar is used, the procedure is exactly the same up until the addition of the alkaline activator. Instead of mixing for three minutes, the mixture is mixed for one minute after adding the activator then standard sand (0.125-0.250 mm) is added and mixed for one minute. The mass of sand is the 1.1 x mass of the binder. Afterwards, 0.1 x the binder mass's of tap water is added and mixed for one minute. The last step is to keep mixing the mortar for two minutes same as before with the first minute at high speed then back to slow speed, then the sample is ready. The stage when the admixture is added varies depending on the admixture.

3.3 Test Methods

3.3.1 Setting time

To measure the initial and final setting time, a Vicat needle test [NEN-EN 480-2] will be done. The specimens will be prepared and tested at a temperature of 20 $\pm$ 2°C and a relative humidity of not less than 50%. The setting time is decided based on the depth of the Vicat needle. The needle is released and if the distance from the bottom to the needle is 4 $\pm$ 1mm then that's the initial setting time. When 2.5 $\pm$ 1mm of the needle is in the concrete then that's the final setting time. The test will be done two times for each mixture and averaged to make sure the setting time obtained is correct. The initial setting time is important for two reasons: it's an indication for the open time and it helps in figuring out how much mortar will be needed for the flowability test. This is because based on the initial setting time of the mixture, a specific amount of mortar can be prepared for the flowability test.

3.3.2 Flowability

The flowability will be measured using the mini-slump flow test also referred to as Hägermann flow table test. The test was done in accordance with the ASTM C230. The cone used to perform the test has dimensions of D_1 = 100 mm, D_2 = 60 mm, H = 70 mm. The cone will be filled with the mortar, then the cone will be lifted and the slump height will be measured. After that, the slump table will be dropped 25 times and the diameter of the spread will be measured from 4 different spots and then averaged. The time intervals at which the slump height and spread diameter were 10 and 20 minutes as the test was repeated twice for each mixture once with 20-minutes intervals and then the second time with 10-minutes intervals. The results then were averaged from both tests.

3.3.3 Slug-Test

This test will be done to measure the yield stress development of the mix. The concept behind this test is based on the specific gravity-induced non-Newtonian flow that occurs at the exit of a printing nozzle. This flow leads to the formation of drops that are called "slugs". The formation of slugs requires the nozzle to be far above the ground and that the yield stress is sufficiently high [94].

This kind of procedure was originally applied in the food-industry with fluids like ketchup or mayonnaise [95]. It was concluded by the authors that the mass of the slug is mostly influenced by the yield stress and later on by viscosity.

The formula used to calculate the yield stress is based on the assumption that extruded material is a pure plastic yield stress fluid. The formula used is:

$$\tau_c = \frac{g m_s}{\sqrt{3} S} \tag{3.1}$$

Where g is the earth gravitational constant, m_s (slug mass) = ρ*S*L_s where L_s is the slug length, S is the nozzle section ($\pi {R_0}^2$), and ρ is the concrete density [94].

The setup of the slug test is shown in fig 3.4. It consits of an extrusion gun, a white plastic container for the mortar to be placed in, a beaker to measure the volume, and a balance to measure the mass. The extrusion gun's speed was kept constant at speed 2. In the above mentioned paper [94], there were two procedures used: a manual slug test and an automated slug test. The setup used in this thesis was a replication of the manual slug test. The procedure was repeated every 10 minutes and the yield stress was calculated at every interval.

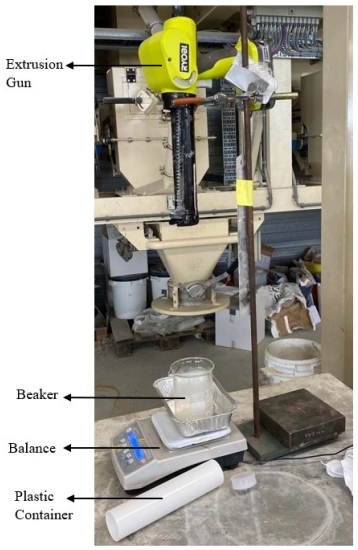

Figure 3.4: Setup of the Slug Test

The mass was measured by extruding 30 slugs and dividing the total mass by 30. The length of the slugs was measured by taping a ruler next to the nozzle and filming the extrusion process.

3.3.4 Compressive, Flexural, and Tensile Bond Strength

The general outcome of this thesis is the development of a mortar that can be used in the industry, hence the compressive and flexural strength are important parameters that have to be measured to see if they are within the European standards.

The test will be done according to the [NEN 5988] standards for compressive strength tests and [NEN-EN 14651+A1] for the flexural strength tests on prisms with dimensions of 160mmx40mmx40mm. The prisms will be sealed in plastic bags to prevent the loss of moisture, while being stored in a room with a temperature of 20°C and relative humidty above 95%. The samples will be tested on the 1^{st}, 7^{th}, 14^{th} and 28^{th} day. Moreover, rectangular prisms as shown in figure 3.5b with dimensions of 35mm x 35mm x 160mm will be cut from printed prisms as the one shown in figure 3.5a and tested in compression in the vertical and horizontal direction on the 7^{th} day. The vertical and horizontal directions are shown in figure 3.5a. These dimensions are not standard dimensions, however the width of nozzle used was 40mm, thus the cross-section dimensions decreased a bit after cutting.

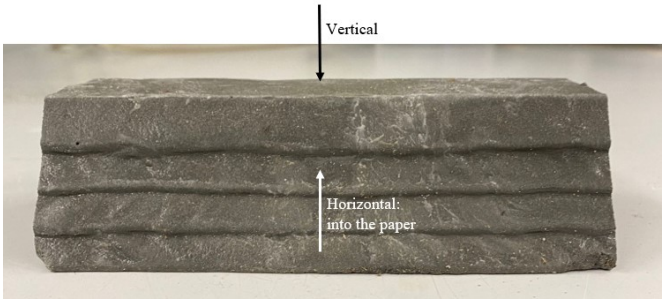

(a) 3D printed prism before cutting

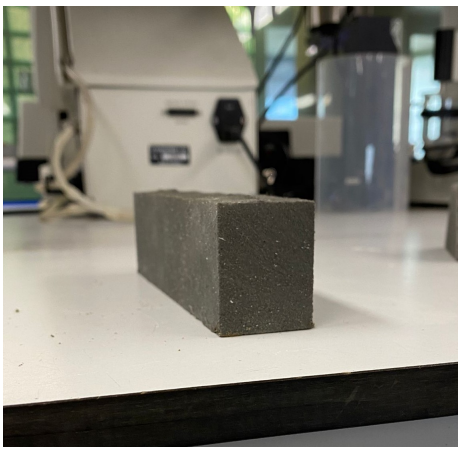

(b) 3D printed prism after cutting

Figure 3.5: 3D Printed Prisms

Then, a uni-axial tensile test was performed on the printed prism after it was cut to measure the tensile bond strength between the layers. The sample is shown in figure3.6a. 3 Samples with dimensions of 42mm x 20mm were used. The Instron 8872 was used to perform this test. The sample was glued to a metal plate from each side. Then a uni-axial force was applied using displacement control with a value of 0.1mm/s.

(a) Sample for tensile bond strength glued to the metal place from one side

(b) Setup of the Test with a sample after failure

Figure 3.6: Tensile Bond Strength Test Setup

3.3.5 Procedure of Tests

The procedure was divided into three stages:

1. Retarders
2. Viscosity modifying admixtures
3. 3D Printing

3.3.5.1 Retarders

The first stage will be adding the retarders to the alkaline activator and perform all the above mentioned tests. As mentioned earlier in section 2.2.1, the retarders that will be used are: sucrose, sodium chloride, and borax. The percentages of the retarders used are shown in table 3.7. These values are mass percentages of the admixture compared to the total mass of the binder.

Table 3.7: Retarder percentages

Sample	S0.75	S1	S1.5	N6	N7	N8	B4	B5	B6
Sucrose	0.75%	1.0%	1.5%	0%	0%	0%	0%	0%	0%
Sodium Chloride	0%	0%	0%	6.0%	7.0%	8.0%	0%	0%	0%
Sodium Borate	0%	0%	0%	0%	0%	0%	4.0%	5.0%	6.0%

However, the percentages changed throughout the thesis due to the results obtained. Table 3.8 shows all the percentages that were tested:

Table 3.8: Retarder percentages, SD: sucrose added to dry mix.

Sample	SD0.2	SD0.35	SD0.5	S0.5	SD0.6	S0.75	S1	SD1.5	S1.5	S2	S3	N3	N4	N5	N6	N7	N8	B1	B1.5	B2	B3	B4	B5	B6
Sucrose	0.20%	0.35%	0.50%	0.50%	0.60%	1%	1%	1.50%	1.50%	2%	3%	0%	0%	0%	0%	0%	0%	0%	0%	0%	0%	0%	0%	0%
Sodium Chloride	0%	0%	0%	0%	0%	0%	0%	0%	0%	0%	0%	3%	4%	5%	6%	7%	8%	0%	0%	0%	0%	0%	0%	0%
Sodium Borate	0%	0%	0%	0%	0%	0%	0%	0%	0%	0%	0%	0%	0%	0%	0%	0%	0%	1%	1.50%	2%	3%	4%	5%	6%

Firstly, the setting time and flowability tests were performed. Based on their results, the samples that did not achieve the desired values (setting time higher than 180 minutes, and a spread diameter of 150-200 mm) were eliminated. Afterwards, the development of yield stress will be tested using the slug test. From each retarder, the percentage that exhibited the best early-age and rheological properties was picked to be used in the next stage.

3.3.5.2 Viscosity modifying admixtures

The second stage is adding the viscosity modifying admixtures along with the retarders. As mentioned above in section 2.2.2, the viscosity modifying admixtures that will be used are attapulgite, sodium carboxymethyl starch, and xanthan gum. the mass percentages are shown in table 3.9.

Table 3.9: VMA's percentages, the percentages shown are mass percentages of the admixture compared to the total mass of the binder, except for the xanthan gum; it's the mass percentage compared to the mass of the alkaline activator.

Sample	SA	SX	NA0.75	NX0.4	0.75	BX0.4	C4	C5	C6
Nano-clay	0.75%	0%	0.75%	0%	0.75%	0%	0%	0%	0%
XG	0%	0.4% (of activator)	0%	0.4% (of activator)	0%	0.4% (of activator)	0%	0%	0%
CMS	0%	0%	0%	0%	0%	0%	4.0%	5.0%	6.0%

Nonetheless, the percentages of VMA's changed throughout the thesis due to the results obtained. Table 3.10 shows all the percentages that were tested:

Table 3.10: Percentages of VMA's tested, the percentages shown are mass percentages of the admixture compared to the total mass of the binder, except for the xanthan gum; it's the mass percentage compared to the mass of the alkaline activator.

Sample	NA0.75	NX0.4	NX0.2	NC0.5	NCM1	BA0.75	BX0.2	BC0.5	BC0.25	BCM1
Nano-Clay	0.75%	0%	0%	0%	0%	0.75%	0%	0%	0%	0%
XG	0%	0.40%	0.20%	0%	0%	0%	0.20%	0%	0%	0%
CMS	0%	0%	0%	0.50%	0%	0%	0%	0.50%	0.25%	0%
CMC	0%	0%	0%	0%	1%	0%	0%	0%	0%	1%

The test procedure here is the same as the one mentioned in stage 2. First the setting time and flowability tests were done, and based on their results some samples were eliminated. Then the slug test was done. Based on their results the samples that exhibited the best printability properties were picked for 3D printing.

3.3.5.3 Pumpability and 3D Printing

One mixture will be chosen based on its properties to be printed. The idea was to print a wall to test the buildability of the mixture. Firstly, a pumpability test was done to check if the mix can be pumped. The second aim of doing the pumpability test is to figure out which is the right speed of pumping based on the weight of the material that is pumped under each speed. Then based on the results of the pumpability test, the mixture will be printed. Secondly, the compressive and flexural strengths of the mortar were tested on the 1^{st}, 7^{th}, 14^{th}, and 28^{th} day. A wall will be printed in layers in which each layer has the dimensions of 1.4cm x 4cm x 90cm. The pumping speed will be 2. Then the flexural, compressive and tensile bond strength test of printed samples were tested.

4

The Effect of Retarders

This chapter will present and discuss the results of the mixtures with retarders only as mentioned in the procedure in section 3.3.5. The setting time, flowability, and yield stress development of the mixtures are shown in this chapter. There were two goals behind these tests; one was to study the effect of each retarder on the reference mixture, and second was to find out which retarder percentage is the optimum percentage. It was concluded that the mixtures with 4% sodium chloride and 3% borax showed the best early-age properties.

4.1 Reference Sample

The setting time, flowability, and yield stress development were measured for the reference sample that has no admixtures added. The results of these tests are shown below.

4.1.1 Setting time

The results of the setting time test done on the reference sample are shown in table 4.1:

Table 4.1: Setting time of the reference sample

Ref. sample	Initial setting time (min)	Final setting time (min)	Average initial setting time (min)	Average final setting time (min)
1	122	220	123	217.5
2	124	215		

4.1.2 Flowability Test (Mini-Slump)

The results of the flowability test done on the reference sample are shown in 4.1, figs. B.1a to B.1c and figs. B.2a and B.2b in appendix B.1:

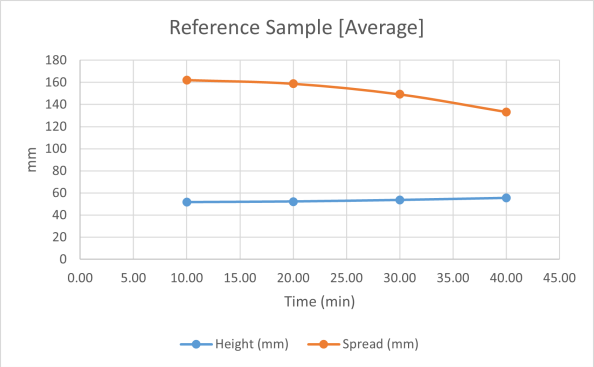

Figure 4.1: Reference Sample Slump Test

(a) Ref slump test

(b) Ref spread test

Figure 4.2: Flowability Test of the Reference Sample at the First Time Interval

4.1.3 Yield Stress Development

The slug test was performed on the reference sample to measure the yield stress development with time and when would the sample need too much pressure to be extruded through the nozzle. The results of slug test are shown in figure 4.3, and figure C.1a in appendix C.1:

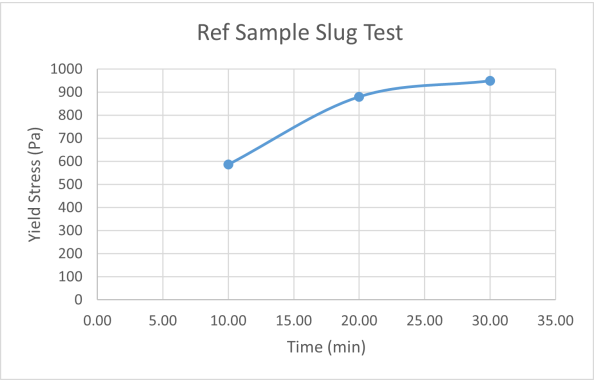

Figure 4.3: Ref slug test

Figure 4.4: Slug Test of the Ref Sample

The second reference sample is the sample that was printed by Ir. Irving. The only difference in that sample is that it had 0.75% attapulgite added to it. The results of the slug test are shown in figure 4.5, and figure C.1b in appendix C.1:

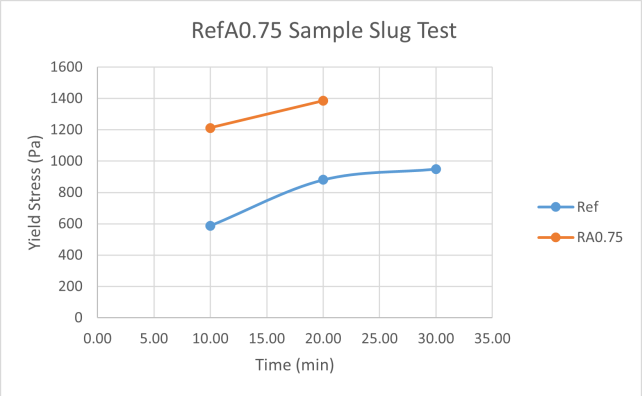

Figure 4.5: RefA0.75 slug test

Figure 4.6: Slug Test of the RefA0.75 Sample

4.2 Sucrose

Multiple sucrose mixtures were prepared in this stage. Each percentage was tested twice and the average initial and final setting time were taken. Sucrose was added to the already prepared alkaline solution then stirred for one hour. It was observed that after stirring if the alkaline solution is used with the binder, the paste will not be homogeneous. However, if the alkaline solution is left to rest for a day, when it's added to the binder the resulting paste is homogeneous. As mentioned in section 3.2.4.1, the dry materials (binder) are first mixed using the Hobart mixer for 3 minutes, then the alkaline solution with the sucrose was added and mixed for 3 minutes. Then the paste was mixed at speed 2 for one minute and then one more minute with slow mixing. For every test, 300g of binder were prepared. The results of the tests are shown in figure 4.7, and table A.1 in appendix A.1 for more exact numbers.

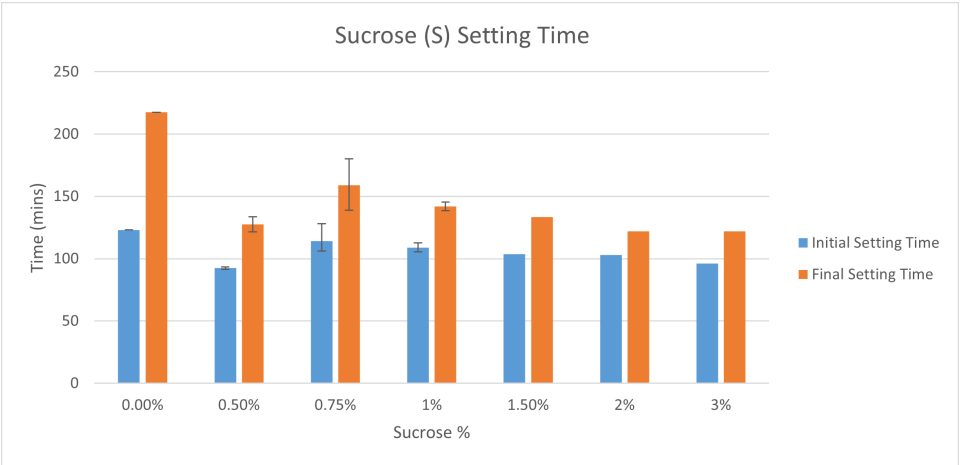

Figure 4.7: Initial and final setting times of sucrose samples

As shown in table A.1 and figure 4.7, none of the samples tested delayed the setting time. There is a trend in the results where both the initial and final setting time increased when the sucrose percentage increased from 0.5% to 0.75%. The initial setting time of S0.75 was the same as the reference sample, however its final setting time was reduced by 58.5 minutes. After the 0.75%, the higher the sucrose percentage is the lower are the initial and final setting time. S11 is in yellow because when the 1% sucrose was tested there was a difference in the results between the samples hence a third sample was tested and it turned out that S11 is the sample that was not accurate. The reason more samples were tested than what was originally planned is because the results of samples did not meet the expected results. Hence, the 0.5%, 2%, and 3% were also tested. The general outcome out of these tests was

that sucrose acts slightly as an accelerator instead of a retarder in this mix. S2 and S3 were tested only once as those samples were just to see if the addition of more sucrose would lead to a retardation effect.

More samples were prepared but this time sucrose was added to the dry mix instead of being added to the activator. The results are shown in figure 4.8, and table A.2 in appendix A.1. The samples were named SD(n) with the 'D' indicating dry mix.

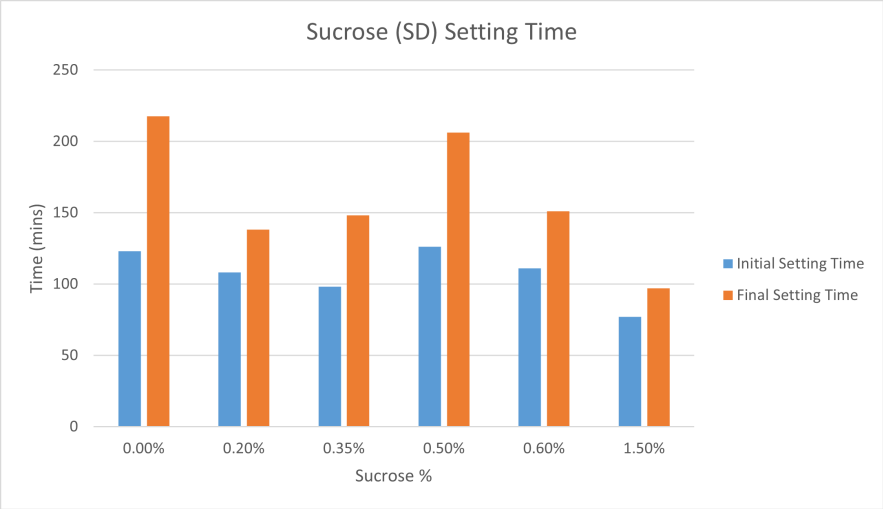

Figure 4.8: Initial and final setting times of sucrose samples (sucrose added to dry mix)

The results above shown that the even when sucrose is added to the dry mix it causes an acceleration effect with with the highest acceleration effect was in Sample SD1.5 which has 1.5% sucrose. However, only one sample showed a retardation effect which was sample SD0.5 which led to a delay of three minutes in the initial setting time but the final setting time was less compared to the reference sample. Thus, sucrose had mainly shown an acceleration effect rather than a retardation effect. Hence, sucrose will no longer be used in further tests because it did not achieve the results that were required.

As found in the state-of art literature in section 2.2.1.1, one of the proposed mechanisms of retardation was that sucrose retards the setting time by combining with Ca, Al, and Fe which lead to the formation of insoluble metal-organic complexes that covered fly ash particles and delayed the geopolymerization process.

Nevertheless, in this thesis, sucrose had no retardation effect on the paste and in most cases it actually accelerated the setting time. This could be explained by two reasons:

- the paste used composed of 60% fly ash, meaning that probably a bigger percentage of sucrose is needed to be able to cover all the fly ash particles and delay the geopolymerization. Moreover, one of the elements that sucrose combines with is Ca, and Ca is mostly found in slag, which is only 20% of the mix used, meaning that there is not enough Ca for sucrose to combine with to delay the setting time.
- The second proposed mechanism of retardation was that sucrose increases the viscosity leading to a delay in the initiation of the geopolymerization process. Moreover, viscosity is also affected by the SiO_2 content, and the binder used composes mostly of fly ash and glass wool whose main component is SiO_2. This could have lead to a very high viscosity that the samples were too hard.

Nonetheless, the first reasoning is probably the more reasonable one considering that low percentages of sucrose were tried and there was no delay in the setting time. However, higher percentages of sucrose were tested and none had an effect on the setting time meaning that more sucrose had to be added. But after a certain point too much addition of the admixture to get a positive result is not reasonable for the industry.

4.3 Sodium Chloride

4.3.1 Setting time

Multiple percentages of sodium chloride mixtures were prepared. Each percentage was tested once to obtain the initial and final setting time. NaCl was added to the already prepared alkaline solution then stirred for one hour. It was observed that with 6%, there was a small amount of NaCl that did not dissolve fully with the activator. As for the 7% and 8%, there was a bigger amount of precipitate. This was an indication that these concentrations will not be suitable for printing. As mentioned in section 3.2.4.1, the dry materials (binder) are first mixed using the Hobart mixer for 3 minutes, then the alkaline solution with the NaCl was added and mixed for 3 minutes. Then the paste was mixed at speed 2 for one minute and then one more minute with slow mixing. For every test 300g of binder were prepared. The results of the tests are shown in figure 4.9 and table A.3 in appendix A.2:

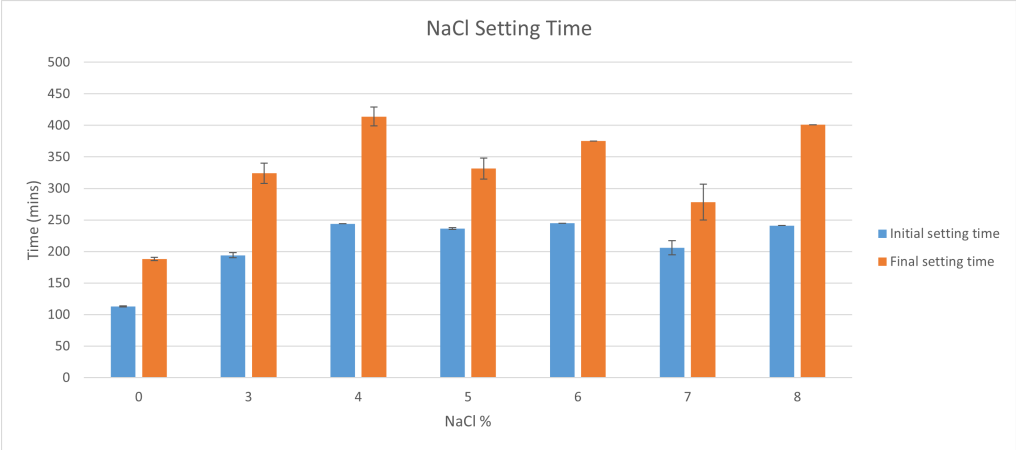

Figure 4.9: Initial and final setting times of NaCl samples

It can be observed in section 4.3, that the addition of NaCl effectively retards the setting time. Nevertheless, based on fig. 4.9, there is not a general trend in the delay of the setting time. The only thing that can be observed is that the addition of 4%-8%of NaCl delayed the initial setting time by almost the same amount of time. The reason the N7 sample was tested twice was to make sure that the obtained result was accurate since no trend was visible at that point. Both results confirmed that there was not a trend in the initial setting time as the percentage of NaCl increases. The drastic change happened when 3% NaCl was added to the mix where the delay in initial setting time was 50 minutes less compared to the N4 sample.

As mentioned in the state-of art literature in section 2.2.1.2, The mechanism behind the delay in setting time is the fact that the addition of NaCl lowers the pH, thus slowing down the reaction. Lowering the pH affects the solubility of soluble silica and the rate of slag dissolution is slowed down. Low pH also retards the kinetic reactions hence the alkali reaction requires more time [96]. Furthermore, the lower pH will slow down the breakdown of the Si-O-Si and Al-O-Si covalent bonds which will also retard the geopolymerization of fly ash [97].

A.R. Brough et al. [75] results indicated that the addition of 4% NaCl or less would lead to an acceleration in the setting time. However, as shown in table 4.2, the addition of 3% and 4% NaCl led to a delay in the setting time. This could be explained by two reasons:

- The slag content in the binder is 20%, meaning not much NaCl is needed to slow down the rate of slag dissolution.
- The presence of glass wool in the binder will also affect the setting time as GW is known for its low reactivity.

Based on these results, the N3 and N4 samples were chosen to be tested for flowability. This is due to the fact they both had an initial setting time higher than 180 minutes. Moreover, high percentages

of NaCl can be problematic because NaCl affects the strength development and if in a later stage, reinforcement was to be added, NaCl would negatively affect it.

4.3.2 Flowability Test (Mini-Slump)

As mentioned in section 4.3, two percentages of NaCl were chosen to be further studied; N3 and N4 (with 3% and 4% sodium chloride respectively). The test was done twice for each mixture and then averaged. The results are shown in figs. 4.10a, 4.10b, 4.12a and 4.12b, figs. B.3a to B.3d and B.5a to B.5c and figs. B.4a to B.4c, B.6a and B.6b in appendix B.2:

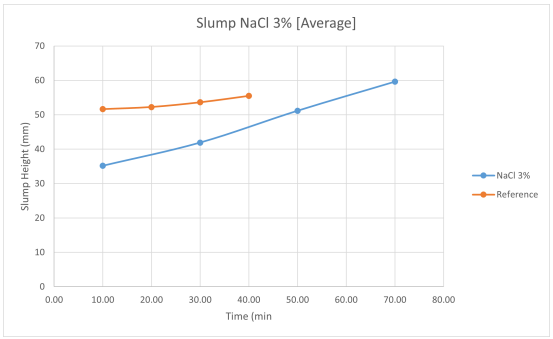

(a) NaCl 3% slump test [Slump]

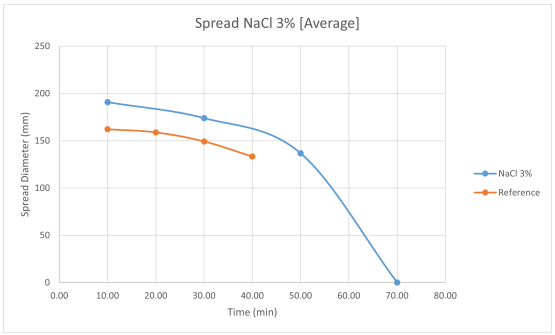

(b) NaCl 3% slump test [Spread]

Figure 4.10: NaCl 3% Slump Tests

(a) N3 slump test

(b) N3 spread test

Figure 4.11: Flowability Test of the N3 sample at the First Time Interval

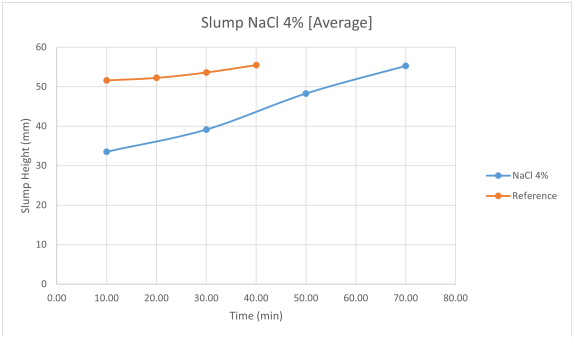

(a) NaCl 4% slump test [Slump]

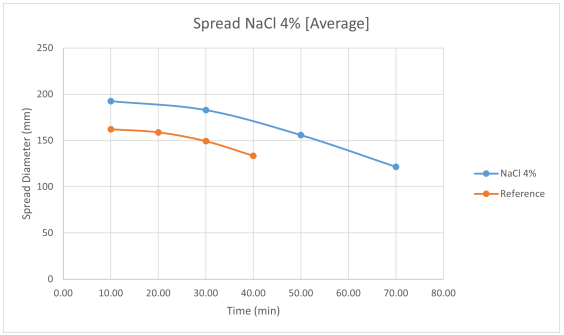

(b) NaCl 4% slump test [Spread]

Figure 4.12: NaCl 4% Slump Tests

(a) N4 slump test

(b) N4 spread test

Figure 4.13: Flowability Test of the N4 sample at the First Time Interval

Based on the results of the flowability tests, the addition of NaCl increased the flowability of the mixture. However, as shown in figs. 4.14 and 4.15, the mixtures lost flowability not so long after the reference sample lost its flowability. As the figures show, the reference sample lost its flowability after 40 minutes, while the N3 and N4 samples lost their flowability after 50 and 60 minutes respectively. This indicates that the initial setting time and the flowability of this alkali-activated mixture are not related to each other. Because the initial setting time of the mix is much higher than the flowability time.

It can also be observed that increasing the percentage of sodium chloride increases the time the mortar stays flowable. This also matches the setting time results as the the initial setting time of N4 was higher than N3.

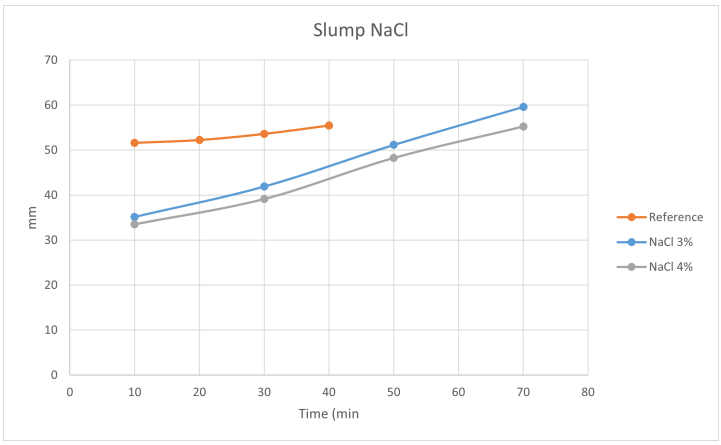

Figure 4.14: Slump of sodium chloride samples

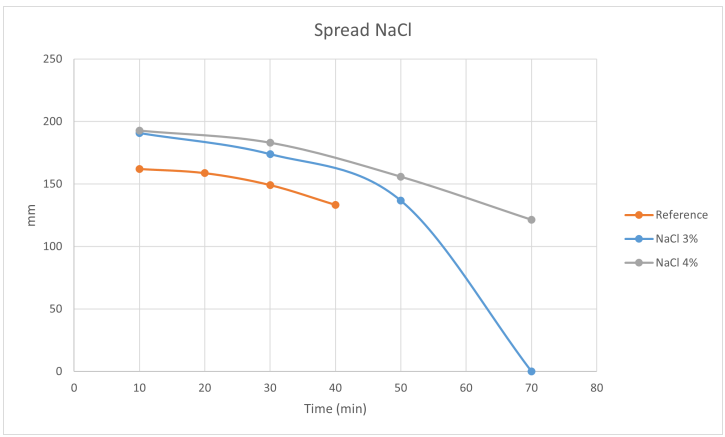

Figure 4.15: Spread of sodium chloride samples

The increase in flowability is due to the delay in the geopolymerization reaction. However, this small increase in the flowability could only be attributed to the fact that the lower pH induced by the sodium chloride slows the dissolution of the raw materials. And, a slower dissolution of raw materials leads to lower flowability.

The N4 sample was the more suitable sample to continue with as it had both a higher setting time and flowability time than the N3 sample. Furthermore, N4 had a spread diameter above 150mm for 10 minutes more than N3. Thus, the yield stress development test was carried on the N4 sample.

4.3.3 Yield Stress Development

The slug test was performed on the sample with 4% NaCl to see how does the yield stress develop with time and when would the sample need too much pressure to be extruded through the nozzle. This test was also done to be a reference to study the effect of the VMA's on the yield stress development. The results of slug test are shown in figure 4.16, and figure C.2a in appendix C.2:

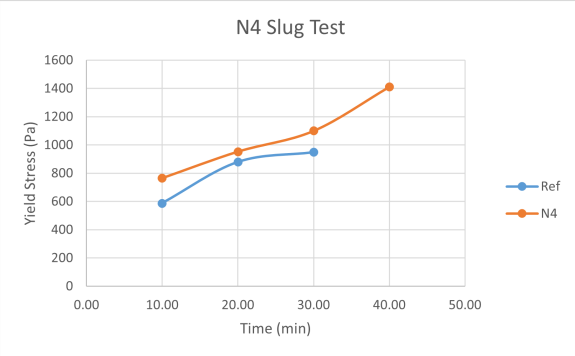

Figure 4.16: N4 slug test

Figure 4.17: Slug Test of the N4 Sample

It can be seen from figure 4.16, that the addition of NaCl increased both the yield strength over time and the time the mix remained extrudable compared to the reference sample. The reference sample required high pressure to be extruded from the beginning leading to the formation of slugs with lower length. This is because the speed of extrusion became less than the assigned speed because the mixture was too stiff, hence the slug had to withstand its self-weight for a longer period in the air hence it collapses faster. This leads to the conclusion that the yield stress of the mix is low because the slug length is the most influential factor in the yield stress formula.

It can be observed that the NaCl mix remained extrudable for 40 minutes. At the 50^{th} minute mark only 25 slugs were extruded under high pressure and that's why this was not recorded. The data is similar to the flowability test results as the sample started to lose flowability around 50 minutes after mixing. This indicates that the mixtures will lose extrudability before they completely lose flowability.

In stage 2, the N4 mixture will be used as it had the highest initial setting time among all the other sodium chloride samples, it maintained a spread diameter above 150mm for 50 minutes. However, the addition of Viscosity modifying admixtures is necessary as the yield stress was below 1400 Pa.

4.4 Sodium Borate (Borax)

4.4.1 Setting time

The 3 percentages mentioned in table 3.7 were prepared. Each percentage was tested once to obtain the initial and final setting time. Borax was added to the alkaline activator while it was being

prepared. It was observed that with 4%, 5%, 6%, there was a large amount of precipitate at the bottom. This was an indication that these concentrations will not be suitable for printing. However, it was tested to have an idea about its effect on the setting time. While with the samples with 3% borax and below there was no precipitation. As mentioned in section 3.2.4.1, the dry materials (binder) are first mixed using the Hobart mixer for 3 minutes, then the alkaline solution with the borax was added and mixed for 3 minutes. Then the paste was mixed at speed 2 for 4 minutes and then one more minute with slow mixing. The mixing procedure was changed here to try to make the mixture as homogeneous as possible because with the original way of mixing the paste was not homogeneous at all. For every test 300g of binder were prepared. The results of the tests are shown in table 4.2.

Table 4.2: Initial and final setting times of borax samples

Sample	Initial setting time (min)	Final setting time (min)	Average initial setting time (min)	Average final setting time (min)
B11	165	265	163.5	298.5
B12	190	350		
B13	162	332		
B1.51	224	354	231	359.5
B1.52	238	365		
B21	262	442	281	436.5
B22	300	431		
B31	>450	-	-	-
B41	>450	-	-	-
B51	>450	-	-	-
B61	>450	-	-	-

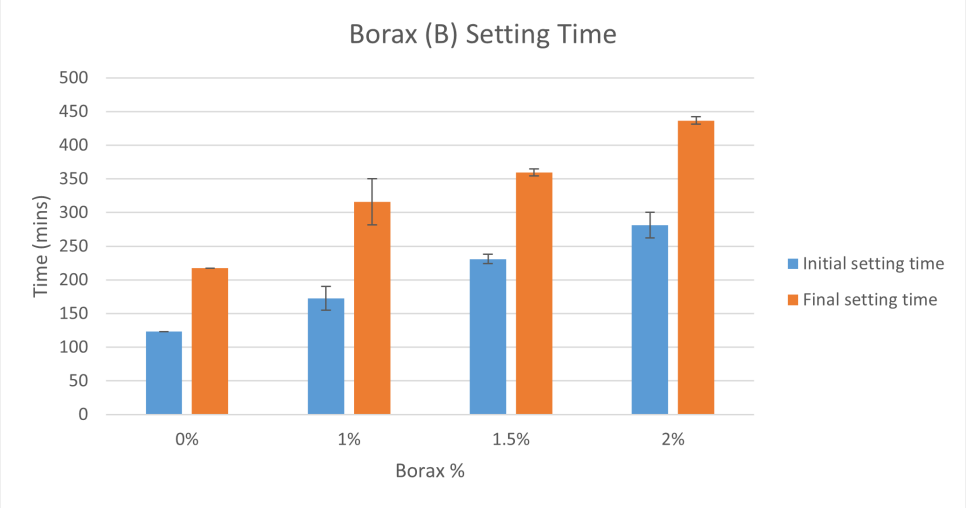

Figure 4.18: Initial and final setting times of borax samples

The addition of borax successfully delayed the setting time of the mix as observed in section 4.4. It is also observed that the delay in setting time increases with the increase of the borax percentage. This trend can be visually seen in figure 4.18.

It can be observed in table 4.2 that percentages of borax between 3% and 6% delay the initial setting for more than 7 hours. This much delay can be considered as negative because this means that the development of strength is really slow which could affect buildability later on.

However, it can be observed in table 4.2 that percentages between 1% and 2% have a reasonable effect on retarding the setting time. 1.5% and 2% of borax were the optimum percentages in this study because they led to an initial setting time of 231 minutes and 281 minutes respectively. This is also in indication of how sensitive the mix is to the percentage of borax added where a 0.5% difference led to a 50 minutes difference in setting time. This is also observed between the 1% and 1.5%, as there is a difference of 67.5 minutes.

As mentioned in the state-of art literature, borax retards the setting time by delaying the formation of Si-O-Al bonds. This indicates that the effect of Si-O-Al bonds is crucial on the setting time in this mix since a lower percentage of borax (compared to NaCl) was needed to delay the setting time critically.

It was also noticed during the mixing procedure that due to the addition of borax the mix needed one extra minute of fast mixing to be homogeneous enough. This was attributed to the fact that borax made the mix a bit dry that the mix could not form a doughy texture.

Since all the samples with 1.5% and above of borax had an initial setting time above 180 minutes, the B1.5, B2, and B3 were used to test flowability. These percentages were also chosen since they are more feasible on an industry scale as the percentages are not high hence cheaper and less effect on the strength development.

4.4.2 Flowability Test (Mini-Slump)

As mentioned in section 4.4, three percentages of borax were chosen to be further studied; B1.5, B2, and B3 (with 1.5%, 2%, and 3% of borax respectively). The test was done twice for each percentage and the average values were calculated. The results of the tests are shown in figs. 4.19a, 4.19b, 4.21a, 4.21b, 4.23a and 4.23b, figs. B.15a to B.15c, B.17a to B.17c and B.19a to B.19c and figs. B.16a, B.16b, B.18a, B.18b, B.20a and B.20b in appendix B.3:

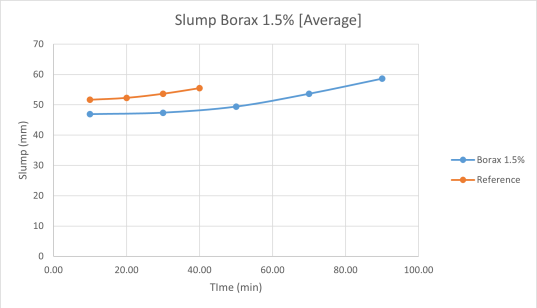

(a) Borax 1.5% slump test [Slump]

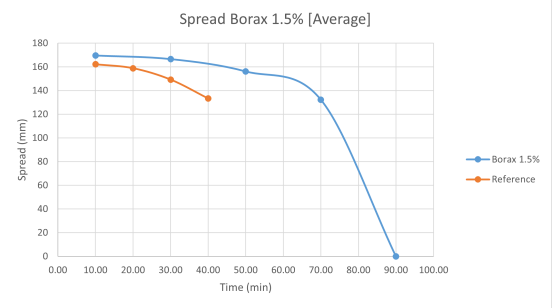

(b) Borax 1.5% slump test [Spread]

Figure 4.19: Borax 1.5% Slump Tests

(a) B1.5 slump test

(b) B1.5 spread test

Figure 4.20: Flowability Test of the B1.5 sample at the First Time Interval

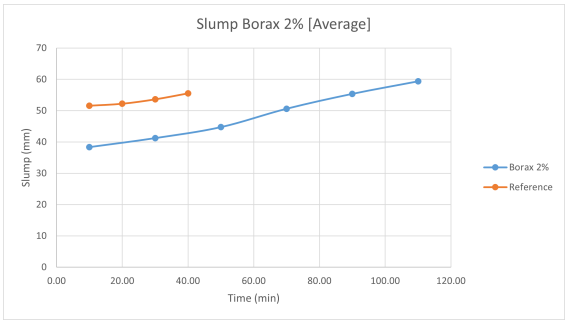

(a) Borax 2% slump test [Slump]

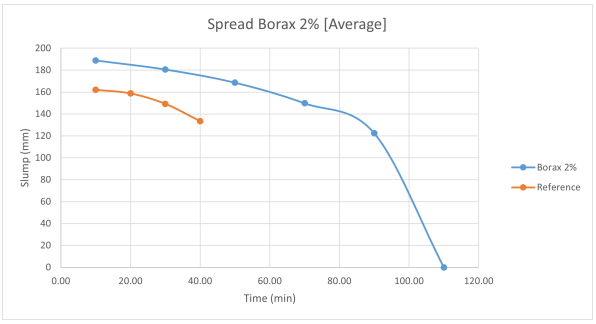

(b) Borax 2% slump test [Spread]

Figure 4.21: Borax 2% Slump Tests

(a) B2 slump test

(b) B2 spread test

Figure 4.22: Flowability Test of the B2 sample at the First Time Interval

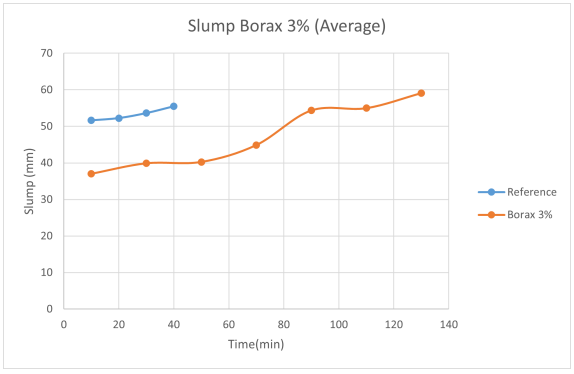

(a) Borax 3% slump test [Slump]

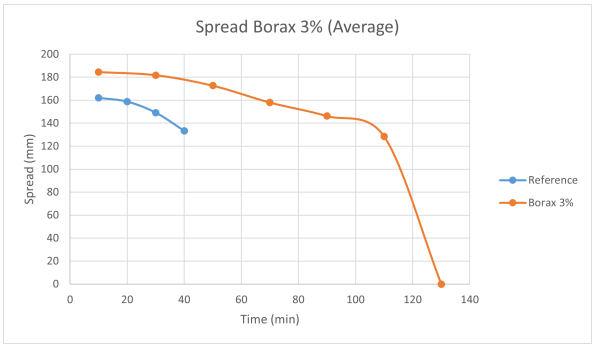

(b) Borax 3% slump test [Spread]

Figure 4.23: Borax 3% Slump Tests

(a) B3 slump test

(b) B3 spread test

Figure 4.24: Flowability Test of the B3 sample at the First Time Interval

It can be seen that the addition of borax increased the flowability of the mix. Furthermore, flowability increased when the percentage of borax increased. As mentioned in section 2.2.1.3, the addition of borax led to a delay in the setting time and increase in flowability. The increase in flowability can be attributed to the water-retaining nature of borax which improves flowability.

As shown in figs. 4.25 and 4.26, the addition of 1.5% borax almost doubled the flowability interval compared to the reference sample. While the addition of 2% kept the mortar flowable until almost the 100^{th} minute mark. This also confirms the earlier conclusion that the setting time and flowability of this mix are not related. The B3 sample remained flowable for 120 minutes which is 20 minutes more than the B2 sample. Looking back at the initial setting time of the B3 sample, it had an initial setting time of more than 450 minutes.

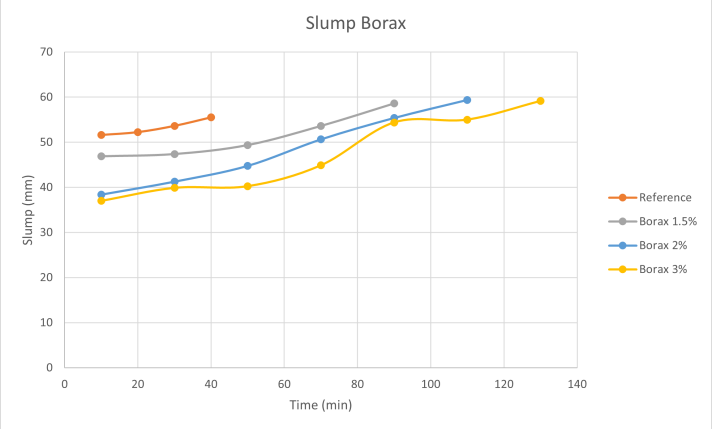

Figure 4.25: Slump of borax samples

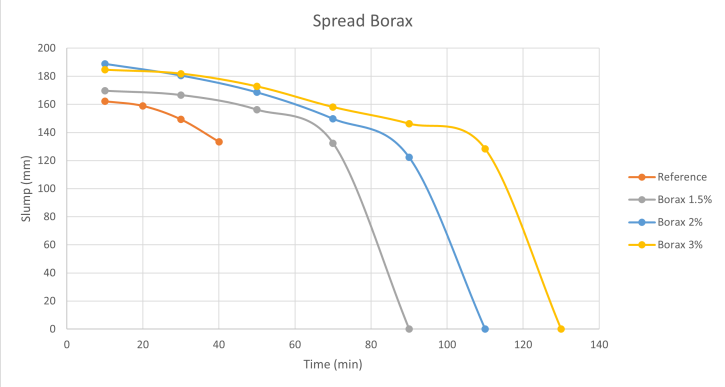

Figure 4.26: Spread of borax samples

Looking at the figure 4.25, B1.5 and B2 followed almost the same trend with the increase in slump, however, the B3 curve was a bit irregular. It can be seen that for the first 50 minutes slump almost remained the same, then it drastically changed until the 90 minute mark. Then, it became steady again until it reached the maximum slump after 130 minutes. This indicates that the delay in the Si-O-Al bonds formation was effective until the 50^{th} minute mark because after that the mixture started hardening quickly.

Furthermore, figure 4.26 shows all the borax samples follow the same trend when it comes to the decrease in the spread diameter. However, the only odd result was that the spread of the B2 sample was higher than the B3 sample after the first 10 minutes. This could be attributed to the fact that 3% borax led to a more dry mixture hence its spread diameter was slightly less than the B2 sample. But in the end, the B3 sample as shown maintained flowability for a longer period of time than B2. Nevertheless,

due to the fact that B3 sample had an initial setting time of more than 450 minutes, it would be a bit hard to calibrate the optimum percentage of VMA's needed. Hence, for the setting time tests the B2 sample was used.

Based on the results above, the B3 sample was the optimum mixture to move on with to the yield stress development test. This is because it maintained a spread diameter above 150mm for the longest time compared to the other samples and had an initial setting above 180 minutes.

4.4.3 Yield Stress Development

The slug test was performed on the sample with 3% borax to see how does the yield stress develop with time and when would the sample need too much pressure to be extruded through the nozzle. The results of slug test are shown in figure 4.27, and figure C.3a in appendix C.3:

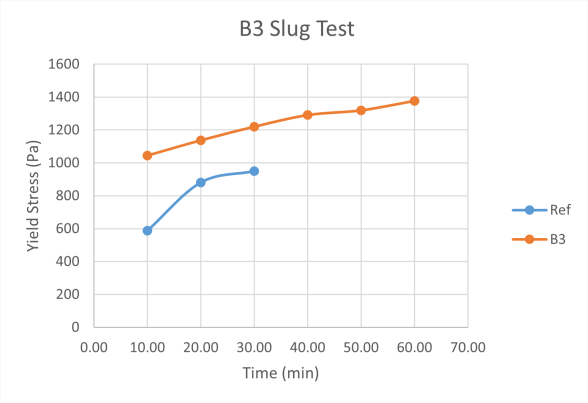

Figure 4.27: B3 slug test

Figure 4.28: Slug Test of the B3 Sample

The addition of 3% borax led to an increase in the extrudability time by 30 minutes compared to the reference sample. It can also be observed from figure 4.27 that there was also an increase in the yield stress of the sample from the start. However, during extrusion it was observed that the sample needed a lot of pressure to be extruded. Hence, the addition of borax led to an increase in the shear of the sample. This could be a sign that the mixture will not be printable as it lost extrudability almost 60 minutes before it lost its flowability in the slump test.

This confirms what was observed by [79] that borax also affects the rheological properties. They mentioned that there was an increase in viscosity with shear rate. Meaning that while extruding, the mix's viscosity increased and this could be the explanation for why the mix lost its extrudability at almost half the flowability time. This is an indication that this percentage of borax could be too high with the addition of VMA's as the viscosity is already high.

That's why the slug test was repeated with the B2 mixture to check if the viscosity under shear will be less. The sample lost extrudability after around 50 minutes. Hence, the tests were continued with 3% of borax. However, the percentages of attapulgite and cellulose that will be added were changed to a lower percentage so that the viscosity will not be too high for extrusion.

Nevertheless, due to the negative results of slug test of the sample, it was decided to change the liquid to binder ratio to 0.45 instead of 0.4. As the addition of more alkaline activator can improve the workability of the mix and solve the dryness problem that borax led to.

Based on figure 4.29, the yield stress significantly improved. This confirms that due to the difficulty in extrusion of the B3 mix with 0.4 liquid to binder ratio, the yield stress values did not represent that actual stress values. Increasing the activator percentage indeed improved the workability of the solution

as it was easily extruded.

However, the extrusion time was the same for both B3 and B3lb as they were both extrudable for 60 minutes only meaning that the workability improved only for the time that mix was extrudable. The second observation, is that due to the difference in viscosity under shearing, the mix borax did not lose its extrudability when the slump height was 50mm or the spread diameter was 150mm. This means that the correlation between the flowability and yield stress test is not the same for the all mixes. Lastly, with the N4 samples, extrudability was lost when the yield stress was around 1600 Pa, but the B3lb mix reached 1979.16 Pa before losing extrudability. This means that there is not a standard value for the yield stress before losing extrudability as it differs between different mixes.

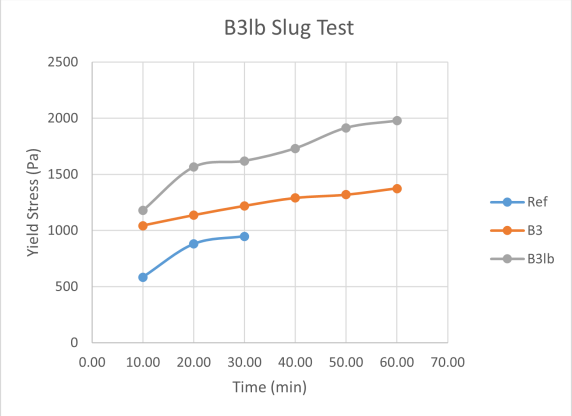

Figure 4.29: B3lb slug test

Figure 4.30: Slug Test of the B3lb Sample

4.5 Sodium Carboxymethyl Starch (CMS)

As mentioned in table 3.5, 3 percentages (4%, 5%, and 6%) were to be tested. However, after preparing the paste with 4% CMS, the paste was too dry to test indicating that this percentage of CMS is way too high for the amount of activator used. The results of the mixtures prepared are shown in table 4.3:

Table 4.3: Initial and final setting times of CMS samples, A: CMS added to activator instead of the dry mix

Sample	Initial setting time (min)	Final setting time (min)
C11	102	230
C12A	60	230
C0.51	113	243
C0.11	102	152

CMS was added to the dry mix prior to mixing. However, in sample C12A the CMS was added to the activator and mixed until fully dissolved. The results indicated that there is no retardation in the setting time. This could be explained by the fact that the CMS retards the setting time by covering the slag particles which slows down the reaction between the activator and slag, and the binder used here contains only 20% slag which could be the reason why CMS did not delay the setting. Thus, from this point onwards, CMS was considered only as a viscosity modifying admixture.

5

The Effect of Viscosity Modifying Admixtures

This chapter will present and discuss the results of the mixtures with both retarders and viscosity modifying admixtures as mentioned in the procedure in section 3.3.5. The setting time, flowability, and yield stress development of the mixtures are shown in this chapter. There were two goals behind these tests; one was to study the effect of each viscosity modifying admixture on the mixtures with retarders, and second was to find out which mixture shows the optimum properties for printing. It was concluded that the mixture with 3% borax and 0.5% attapulgite exhibited the best properties for printing.

5.1 Nano-Clay (Attapulgite)

5.1.1 Attapulgite with Sodium Chloride

5.1.1.1 Setting Time

The setting time of N4 was tested with the addition of 0.75% nano-clay. The results of the test are shown in figure 5.1, and table A.4 in appendix A.2:

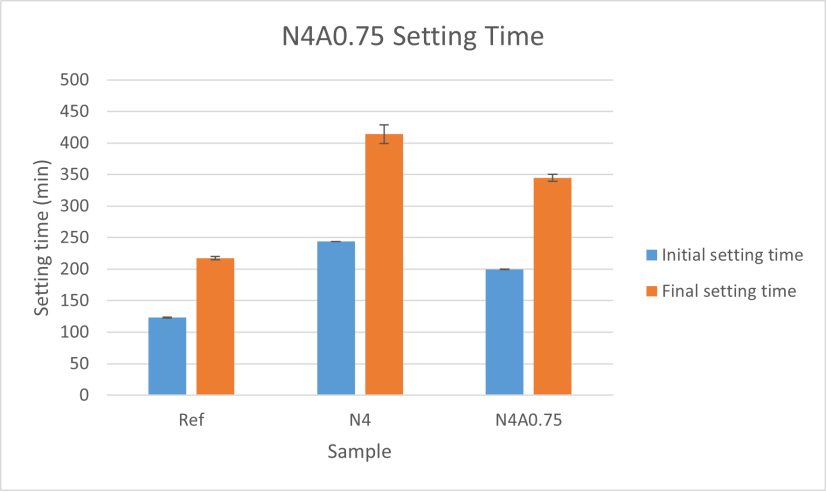

Figure 5.1: Initial and final setting time of N4A0.75

The addition of nano-clay led to a 44.5 minutes and 69.5 minutes decrease in the initial and final setting time respectively. the decrease in initial setting time could be understandable since attapulgite is known for reducing the open time of mortar. However, attapulgite does not change the reaction

mechanisms so the only reason this could have happened is that this percentage of attapulgite is too high for the NaCl percentage used. The only way to improve the setting time would be to increase the percentage of sodium chloride but 4% is already high hence it's not reasonable to change it. It was decided not to change the percentage of attapulgite because 0.75% was found as the optimum percentage for this mix.

5.1.1.2 Flowability Test (Mini-Slump)

The test was done for the sample prepared in section 5.1 with 4% NaCl and 0.75% nano-clay. The results of the flowability test are shown in figs. 5.2a and 5.2b, figs. B.7a to B.7c and figs. B.8a and B.8b in appendix B.2:

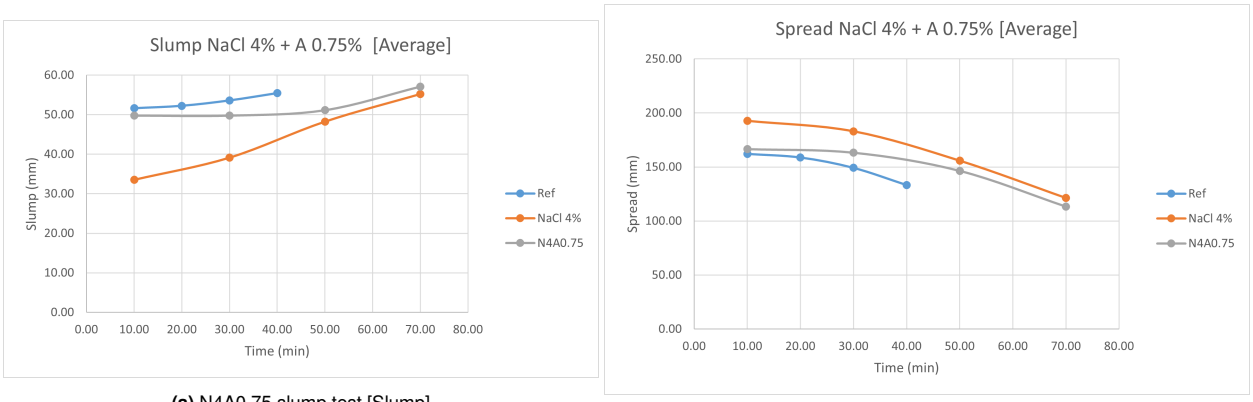

(a) N4A0.75 slump test [Slump]

(b) N4A0.75 slump test [Spread]

Figure 5.2: N4A0.75 Slump Tests

(a) N4A0.75 slump test

(b) N4A0.75 spread test

Figure 5.3: Flowability Test of the N4A0.75 sample at the First Time Interval

Attapulgite improves the workability by increasing the flocculation rate of geopolymer by the dipole-dipole interactions. This was proved as the slump value increased compared to the N4 sample meaning that the mortar became more viscous which is what was expected. The mortar's slump was almost constant for 50 minutes at around 50mm height. At the 70^{th} minute mark, the slump of both the N4A0.75 and N4 was almost the same and then they both lost flowability after that. This indicates that attapulgite does not increase the flowability duration, it just improves the viscosity and the yield strength which is discussed later.

As for the spread diameter, the addition of the attapulgite led to a decrease in the diameter. Up until the 50^{th} minute, the spread was higher than or almost 150mm which is the value that was determined earlier to be the lower range for 3D printing. Nevertheless, this value is only an assumption because the only way to check if a mortar is printable is actually printing it. Furthermore, as seen in figure 5.2b, the

N4A0.75 sample followed the same trend as the N4 sample where the spread diameter was almost constant until the first 30 minutes, then it majorly decreased.

5.1.1.3 Yield Stress Development

The slug test was performed on the sample with 4% NaCl and 0.75% attapulgite to see how does the yield stress develop with time and when would the sample need too much pressure to be extruded through the nozzle. The results of slug test are shown in figure 5.4, and figure C.2b in appendix C.2:

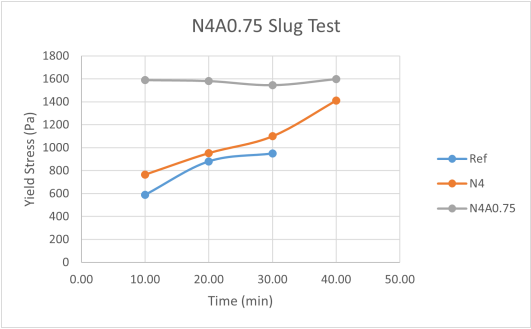

Figure 5.4: N4A0.75 slug test

Figure 5.5: Slug Test of the N4A0.75 Sample

As expected, the addition of nano-clay led to the increase in yield stress. Based on figure 5.4, the mix's yield stress remained almost constant until the mix lost its extrudability. This also matches the results of the flowability test as it can be seen in figure B.7b that N4A0.75 had almost the same slump height and spread diameter in the first 40 minutes.

Even though that the nano-clay significantly improved the yield stress, it was still extrudable for the same amount of time as the N4 sample. This is explained by the fact that when the shear rate is high (during extrusion) the mixture loses a bit of its viscosity and because of the lubrication layer formed due to the shear-induced particle migration hence extrudability was not affected.

5.1.2 Attapulgite with Sodium Borate (Borax)

5.1.2.1 Setting Time

The setting time of B2 was tested with the addition of 0.75% nano-clay. The results of the test are shown in figure 5.6, and table A.8 in appendix A.3:

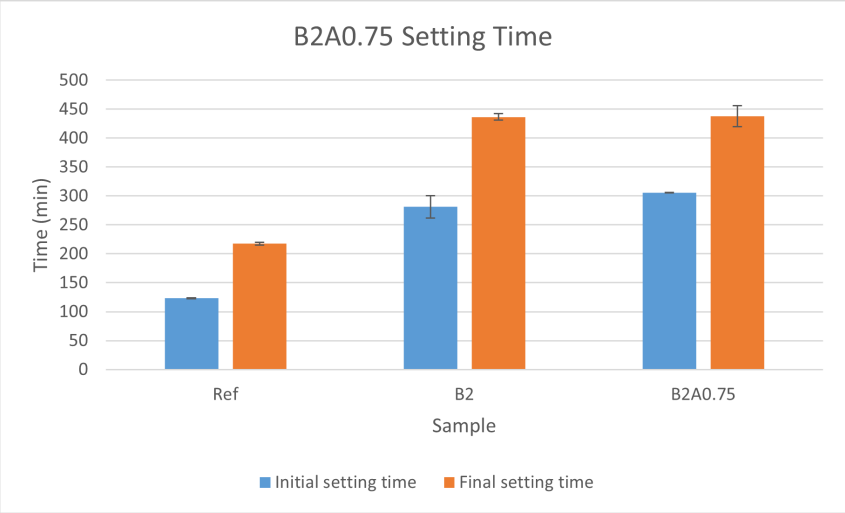

Figure 5.6: Initial and final setting time of B2A0.75

The addition of attapulgite led to a 24.5 minutes increase in the initial setting time and a 1.5 minutes increase in the final setting time. This increase in the setting time can be attributed to one of two things: the combination of borax and attapulgite causes a change in the reaction of the materials leading to a further delay in the setting time, or the formation of water-molecules as a by-product of the condensation reaction which was observed by Muthukrishnan [61]. However, since the setting time was not affected drastically, 0.75% of attapulgite is indeed the optimum percentage.

5.1.2.2 Flowability Test (Mini-Slump)

The test was done for the mix containing 3% borax and 0.75% nano-clay. The results of the flowability test are shown in figs. 5.7a and 5.7b, figs. B.21a to B.21c and figs. B.22a and B.22b in appendix B.3:

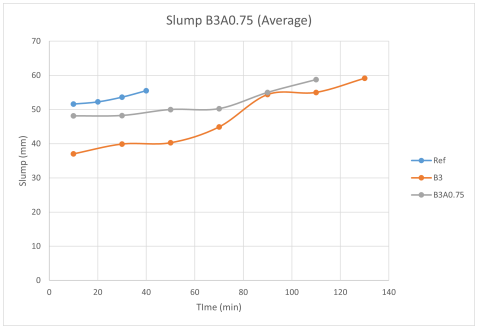

(a) B3A0.75 slump test [Slump]

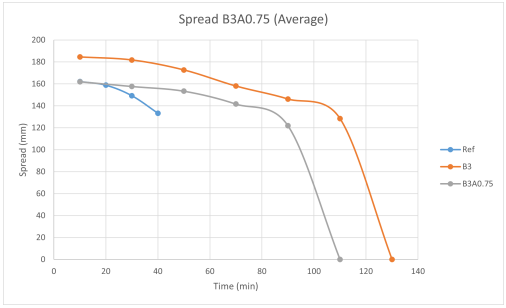

(b) B3A0.75 slump test [Spread]

Figure 5.7: B3A0.75 Slump Tests

(a) B3A0.75 slump test

(b) B3A0.75 spread test

Figure 5.8: Flowability Test of the B3A0.75 sample at the First Time Interval

It can be seen from figs. 5.7a and 5.7b that the mix lost its flowability after 90-100 minutes. This means that the addition of nano-clay increased the yield strength of the mixture to a point where it lost flowability before the reference sample with 3% borax. Looking at figure 5.7a, both the B3 and the B3A0.75 sample had the same behaviour in the beginning where the slump remained almost the same for the first 50 minutes. However, for the B3A0.75 sample the slump remained the same for an extra 20 minutes. This means that attapulgite helped maintain the viscosity of the mix for a longer period of time. Furthermore, the addition of attapulgite increased the slump of the mixture by 10mm. This is an indication that the yield strength and viscosity of the mixture were increased.

Based on figure 5.7b, the addition of attapulgite reduced the spread diameter by 20mm, also indicating the increase of viscosity and yield strength. However, since the mixture lost its flowability before the b3 sample, this means that this percentage of attapulgite was too high for this percentage of borax. This means that more borax should be added to maintain the flowability so that it remains as the B3 sample.

5.1.2.3 Yield Stress Development

The slug test was performed on the sample with 3% borax and 0.5% attapulgite to see how does the yield stress develop with time and when would the sample need too much pressure to be extruded through the nozzle. The results of slug test are shown in figure 5.9, and figure C.4a in appendix C.3:

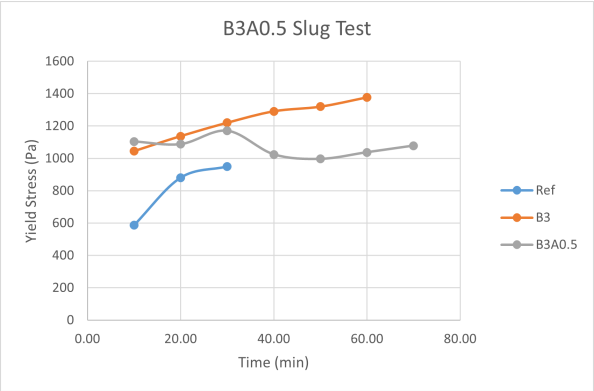

Figure 5.9: B3A0.5 slug test

Figure 5.10: Slug Test of the B3A0.5 Sample

It can be observed from figure 5.9 that the addition of attapulgite did not improve the yield stress but in fact it made it worse. The only positive outcome was that the mix was extrudable for an extra 10 minutes. However, there is no clear trend in the figure and that has to do with the fact that the mix needed too much pressure from the start to be extruded. This affected the speed of extrusion as it became lower and the slugs were sheared for a longer time so their length was small. From visual observation, the mix had good yield stress hence this is one of the drawbacks of this test that if the mixture needs more pressure that what the extrusion gun can provide, the results will not be accurate.

It was also concluded that attapulgite usually keeps the yield stress almost the same from start to beginning. The difference in yield stress between the lowest and highest value is 173 Pa. This was also the case for the N4A0.75 sample were the yield stress values were very close. This conclusion is also proved by the results of the flowability test. The slump values were similar for the first 60 minutes meaning that the yield stress was almost the same in this period which is also confirmed by the slug test.

Due to the results of the slug test, the liquid to binder ratio was changed to 0.45 as was done with the B3 sample. The results are shown in Chapter 6.

5.2 Xanthan Gum (XG)

5.2.1 Xanthan Gum with Sodium Chloride

5.2.1.1 Setting Time

The setting time of N4 was tested with the addition of xanthan gum. A second percentage of XG (0.2%) was tested because the results of N4X0.4 showed a big drop in both the initial and final setting time. The results of the tests are shown in figure 5.11, and table A.5 in appendix A.2:

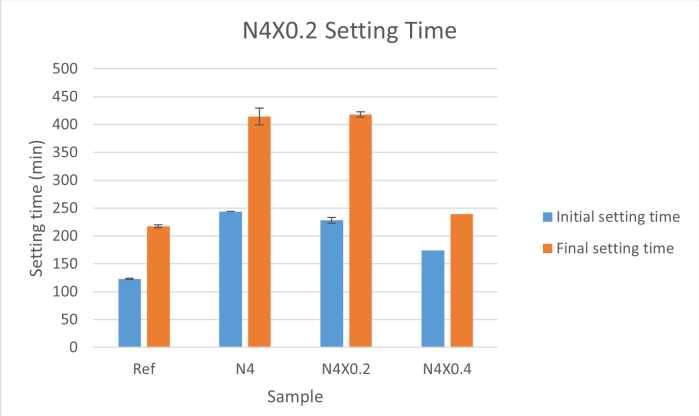

Figure 5.11: Initial and final setting time of N4X

The addition of 0.4% xanthan gum decreased the initial and final setting time drastically compared to the N4 sample. This could be due to the fact that the addition of xanthan gum increases the viscosity of the activating solution leading to a more dry paste which is what was observed during mixing. Hence, it was decided to lower the percentage to 0.2% which significantly improved the initial and final setting time. The initial setting time was 16 minutes lower compared to the N4 sample while the final setting time was actually 4 minutes more. Thus, 0.2% of xanthan gum is the optimum percentage for this mix.

5.2.1.2 Flowability Test (Mini-Slump)

The test was done for the sample prepared in section 5.2 with 4% NaCl and 0.2% XG. The results of the flowability test are shown in figs. 5.12a and 5.12b, figs. B.9a to B.9c and figs. B.10a and B.10b in appendix B.2:

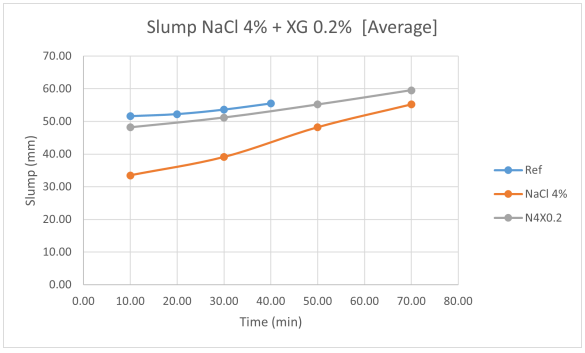

(a) N4X0.2 slump test [Slump]

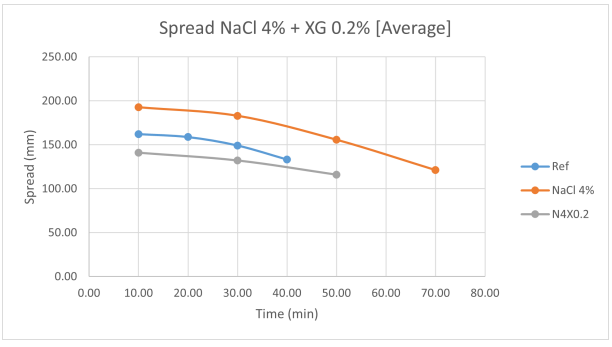

(b) N4X0.2 slump test [Spread]

Figure 5.12: N4X0.2 Slump Tests

(a) N4X0.2 slump test

(b) N4X0.2 spread test

Figure 5.13: Flowability Test of the N4X0.2 sample at the First Time Interval

The addition of xanthan gum severely affected the flowability of the mortar. It can be seen from figs. 5.12a and 5.12b that the mortar lost flowability after 50 minutes which is less than the N4 sample. The slump height almost linearly increases throughout the whole experiment from 48.25 until 60. Furthermore, the spread diameter was also affected extremely to a point where it was even lower than the spread of the reference sample. The spread never even reached the 150mm point which is a bad sign when it comes to the printability of this mix. However, these results contradict what was reported in literature [90, 91], that the addition of xanthan gum increases the marsh cone flow time. This can only be explained by the fact that different activating solutions and binders are used in this work and the mentioned papers. As mentioned earlier there are a lot of factors that influence the effect of admixtures and that's why there has not been any concrete research about their effects.

5.2.1.3 Yield Stress Development

The slug test was performed on the sample with 4% NaCl and 0.2% xanthan gum to see how does the yield stress develop with time and when would the sample need too much pressure to be extruded through the nozzle. The results of slug test are shown in figure 5.14, and figure C.2c in appendix C.2:

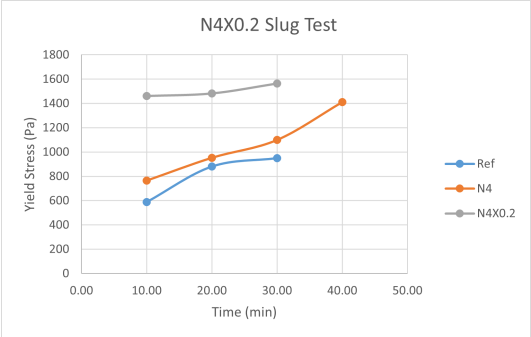

Figure 5.14: N4X0.2 slug test

Figure 5.15: Slug Test of the N4X0.2 Sample

it can be seen that the addition of xanthan gum led to the loss of extrudability after 30 minutes which is less than both the N4 and N4A0.75 mixes. Even though, the N4X0.2 started with a lower yield stress than N4A0.75 the pressure needed for extrusion was higher. This also matches the results of the flowability test as the N4X0.2 sample had the least flowability time among all the N4 mixes. This concludes that the addition of xanthan gum with sodium chloride is not a suitable combination for 3D printing. As the addition of xanthan gum negatively affected the flowability and extrudability which are important factors for printing.

5.2.2 Xanthan Gum with Sodium Borate (Borax)

5.2.2.1 Setting Time

The setting time of B2 was tested with the addition of 0.2% xanthan gum. The results of the test are shown in figure 5.16, and table A.9 in appendix A.3:

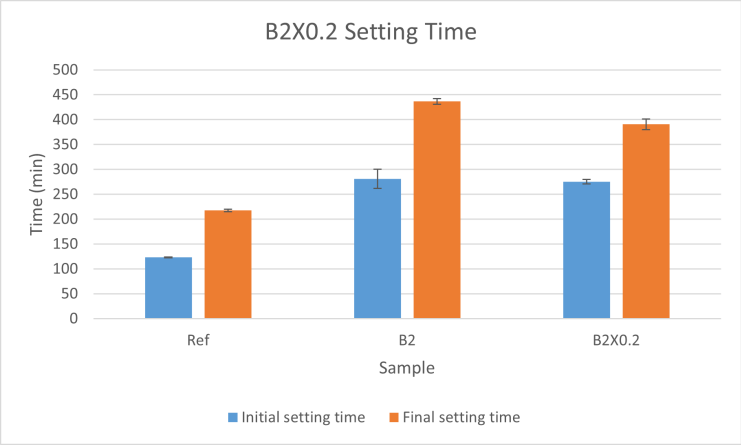

Figure 5.16: Initial and final setting time of B2X0.2

The addition of 0.2% xanthan gum did not affect the initial setting as it only decreased by 5.5 minutes compared to the B2 sample. However, the final setting time was a bit affected as it decreased by 46 minutes. Since, the initial setting was not affected no changes had to be done as the initial setting time is what matters in this research. This also indicates that the 0.2% is also the optimum percentage for this mix.

5.2.2.2 Flowability Test (Mini-Slump)

The test was done for the mix containing 3% borax and 0.2% XG. The results of the flowability test are shown in figs. 5.17a and 5.17b, figs. B.24a to B.24c and figs. B.25a and B.25b in appendix B.3:

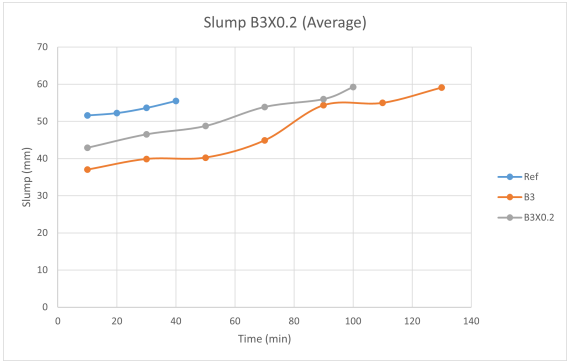

(a) B3X0.2 slump test [Slump]

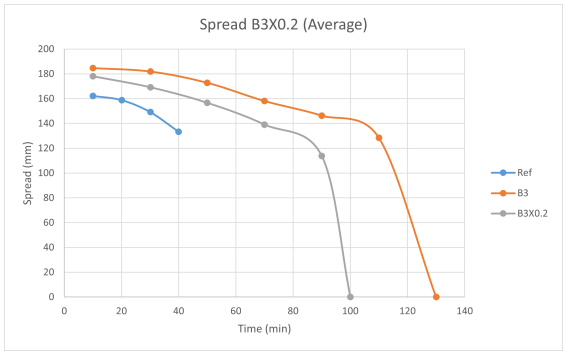

(b) B3X0.2 slump test [Spread]

Figure 5.17: B3X0.2 Slump Tests

(a) B3X0.2 slump test

(b) B3X0.2 spread test

Figure 5.18: Flowability Test of the B3X0.2 sample at the First Time Interval

It can be seen from figs. B.25a and B.25b that the addition of xanthan gum led to the loss of flowability after 90 minutes. This is an indication that more borax should be added to counteract the increase in yield strength and viscosity due to the xanthan gum. Looking at figure 5.17a, the mixture followed the same behaviour as the B3 sample. Nevertheless, it lost its flowability 30 minutes before the B3 sample. Xanthan gum led to an increase of 10mm in the slump compared to the B3 sample. Only at the 90^{th} minute mark they had almost the same slump.

Based on figure 5.17b, both B3X0.2 and B3 had almost the same spread diameter after 10 minutes. However, the B3X0.2's spread decreased faster than the B3 sample after that. There was almost a 20mm difference at all times. This indicates that xanthan gum's effect gradually increases over time as it started with a very small effect on the spread then later on with time it had a much bigger effect.

5.2.2.3 Yield Stress Development

The B3X0.2 sample was only extrudable for the first 10 minutes. There is no clear correlation between this and the results from the slump test. This indicates that the sample with xanthan gum behaves differently when its sheared. This could also mean that with the addition of xanthan gum the viscosity of the mix increases when sheared.

Nevertheless, these results confirmed what was concluded earlier that the addition of xanthan gum is not suitable for this mix as it affected its printability properties negatively. This probably has to do with the type of activator used in this thesis as its already viscous due to the high amount of sodium silicate. Another important factor is that the addition of borax led to a dry mix this is also an important reason why xanthan gum had this negative effect.

5.3 Sodium Carboxymethyl Starch (CMS)

5.3.1 Sodium Carboxymethyl Starch with Sodium Chloride

5.3.1.1 Setting Time

The setting time of N4 was tested with the addition of 0.5% CMS. The results of the test are shown in figure 5.19, and table A.6 in appendix A.2:

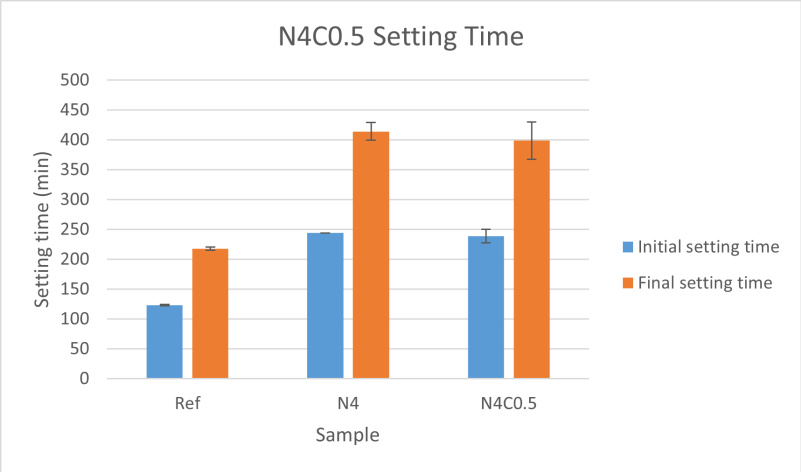

Figure 5.19: Initial and final setting time of N4C0.5

The addition of 0.5% CMS did not affect the setting time in a big way as the initial setting time decreased only by 5.5 minutes compared to the N4 sample. Moreover, the final setting time decreased but 15.5 minutes.

5.3.1.2 Flowability Test (Mini-Slump)

The test was done for the sample prepared in section 5.3 with 4% NaCl and 0.5% CMS. The results of the flowability test are shown in figs. 5.20a and 5.20b, figs. B.11a to B.11c and figs. B.12a and B.12b in appendix B.2:

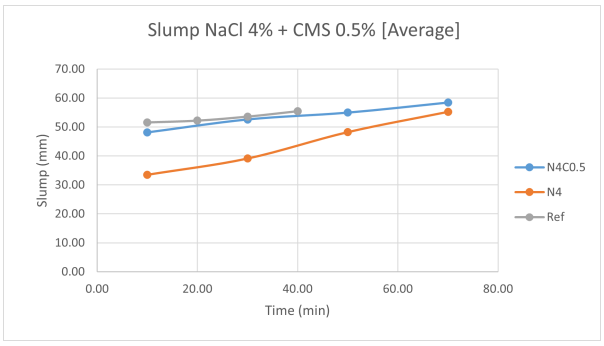

(a) N4C0.5 slump test [Slump]

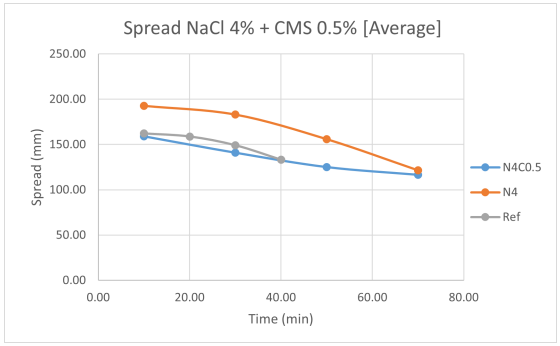

(b) N4C0.5 slump test [Spread]

Figure 5.20: N4C0.5 Slump Tests

(a) N4C0.5 slump test

(b) N4C0.5 spread test

Figure 5.21: Flowability Test of the N4C0.5 sample at the First Time Interval

CMS also lowered the flowability of the N4 mortar drastically, but it lost its flowability at the same time as the N4 sample. However, the slump height was almost the same as the reference sample which is not a good indication. And same goes for the spread diameter as the spread was lower than the reference sample. At the 10 minute mark, it was above 150mm but then it went below it which is a small indication that this mortar might not be very suitable for printing. This confirms that indeed CMS leads to a decrease in the fluidity hence the drop in flowability.

5.3.1.3 Yield Stress Development

The slug test was performed on the sample with 4% NaCl and 0.5% CMS to see how does the yield stress develop with time and when would the sample need too much pressure to be extruded through the nozzle. The results of slug test are shown in figure 5.22, and figure C.2d in appendix C.2:

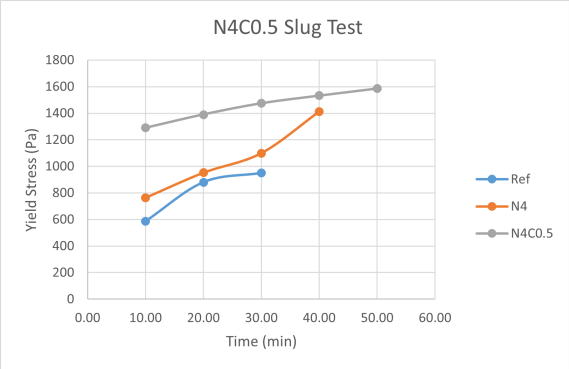

Figure 5.22: N4C0.5 slug test

Figure 5.23: Slug Test of the N4C0.5 Sample

It can be seen from figure 5.22, that the addition of CMS increased the yield stress of the mix. It can also be observed that the mix remained extrudable for 50 minutes which is higher than all the previous samples. Regardless of the fact that the yield stress increased, the mix remained extrudable which can be explained by the fact that under shearing, the molecules will move in a parallel direction to the shear force causing a decrease in viscosity during extrusion and an ease of sliding.

However, this result contradicted the flowability test results. As, shown in figs. 5.44 and 5.45, N4C0.5 was the sample with the second worst flowability. The mix started with a high slump height and low spread diameter indicating high viscosity or yield stress. Nevertheless, according to the results of the slug test, the mix started with a lower yield stress than all the previous samples and then it increased gradually. This could only be attributed to the loss in viscosity during shearing and the parallel movement of the particles which was mentioned above.

5.3.2 Sodium Carboxymethyl Starch with Sodium Borate (Borax)

5.3.2.1 Setting Time

The setting time of B2 was tested with the addition of 0.5% CMS. The results of the test are shown in figure 5.24, and table A.10 in appendix A.3:

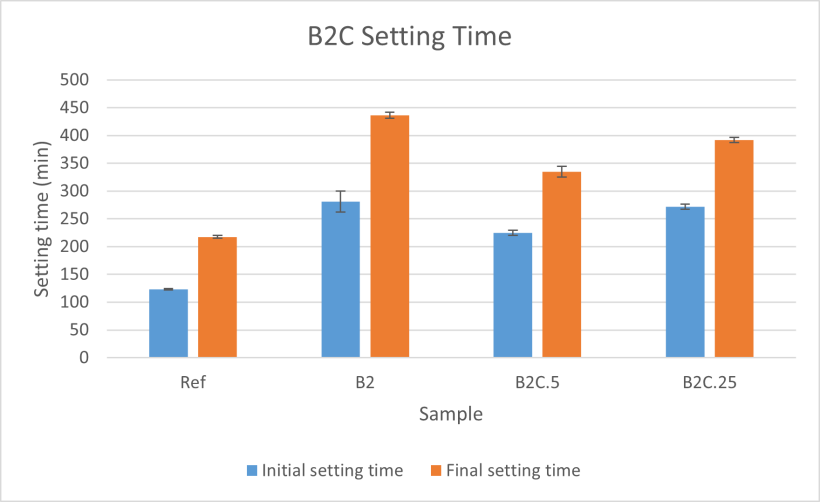

Figure 5.24: Initial and final setting time of B2C

The addition of 0.5% CMS decreased the initial and final setting time by 56.5 and 102 minutes respectively compared to the B2 sample. Furthermore, during mixing the paste was too dry and needed more mixing time which confirms that CMS lowers the fluidity. Thus, it was chosen to lower the percentage to 0.25% which improved the setting time quite nicely. The initial setting time was only 9.5 minutes lower compared to the B2 sample while the final setting time was 45 minutes less. In spite of that, for the same reasoning mentioned above no changes were done because the initial setting time is the critical point in this thesis which was not affected so this percentage was chosen to be the optimum percentage when borax is added.

5.3.2.2 Flowability Test (Mini-Slump)

The test was done for the mix containing 3% borax and 0.25% CMS. The results of the flowability test are shown in figs. 5.25a and 5.25b, figs. B.26a to B.26c and figs. B.27a and B.27b in appendix B.3:

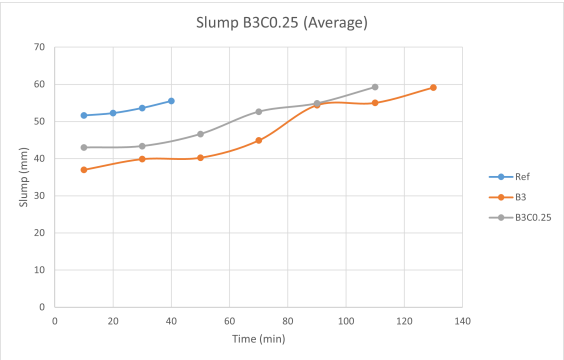

(a) B3C0.25 slump test [Slump]

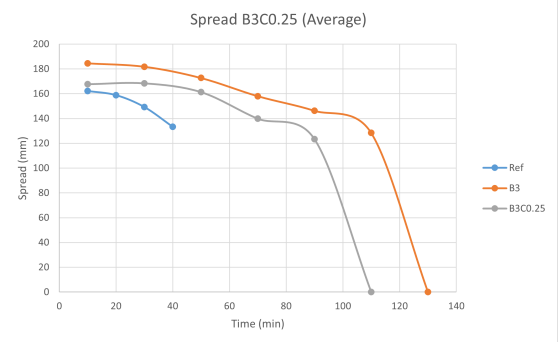

(b) B3C0.25 slump test [Spread]

Figure 5.25: B3C0.25 Slump Tests

(a) B3C0.25 slump test

(b) B3C0.25 spread test

Figure 5.26: Flowability Test of the B3C0.25 sample at the First Time Interval

Looking at figure 5.25a, the addition of CMS led to a loss in flowability after 100 minutes, which is 20 minutes less than the B3 sample. This indicates that more borax should be added since the increase in yield strength and viscosity reduced the flowability time of the mix. It also led to an increase in slump of 5-8mm compared to the B3 sample, which further confirms the increase in yield strength and viscosity.

Based on figure 5.25b, the mix maintained its spread diameter for the first 50 minutes. After that, it started to decrease up until the point it lost flowability. At most time there was a difference of 10-15mm in spread between this mix and the B3, proving that CMS had an effect on both the yield strength development and the viscosity.

5.3.2.3 Yield Stress Development

The slug test was performed on the sample with 3% borax and 0.25% CMS to see how does the yield stress develop with time and when would the sample need too much pressure to be extruded through the nozzle. The results of slug test are shown in figure 5.27, and figure C.5a in appendix C.3:

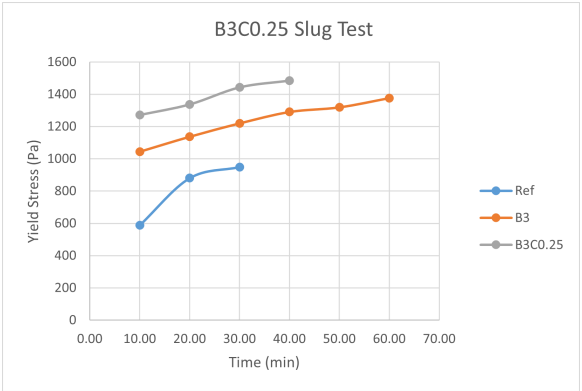

Figure 5.27: B3C0.25 slug test

Figure 5.28: Slug Test of the B3C0.25 Sample

It can be observed from figure 5.39 that the addition of CMS improved the yield strength of the mix. However, extrudability was lost 20 minutes before the B3 sample. However, for this period of 40 minutes, extrudability was significantly improved as the mix did not need high pressure to be extruded. The same behaviour was observed in the N4C0.5 sample where the sample remained perfectly extrudable as the yield stress increased. The only drawback was that extrudability was lost in 40 minutes.

Due to these results, the liquid to binder ratio was changed to 0.45 and the test was repeated. The results are shown in figure 5.29, and figure C.5b in appendix C.3:

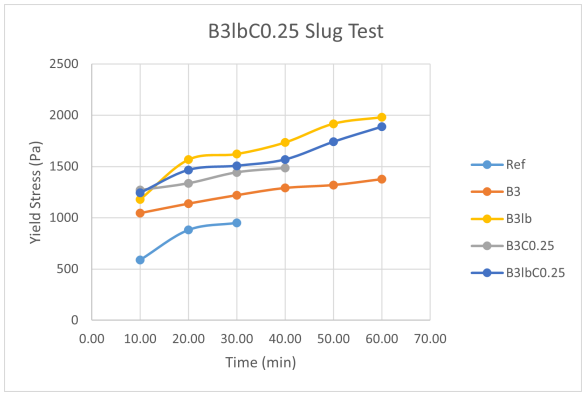

Figure 5.29: B3lbC0.25 slug test

Figure 5.30: Slug Test of the B3lbC0.25 Sample

When the liquid to binder ratio was increased to 0.45, the extrudability time remained the same as the B3lb sample, the only difference is in the yield stress development where the yield stress values were actually less than the B3lb sample which means that this percentage of CMS did not improve the yield stress. Furthermore, looking at figure 5.29, extrudability was lost when the yield stress reached 1888.87 Pa which is almost 100 Pa less than both the B3lb and B3lbA0.5 mixes which further indicates that the addition of CMS had an unusual effect on the B3lb mix.

5.4 Sodium Carboxymethyl Cellulose (CMC)

5.4.1 Sodium Carboxymethyl Cellulose with Sodium Chloride

5.4.1.1 Setting Time

The setting time of N4 was tested with the addition of 1% CMC. The results of the test are shown in figure 5.31, and table A.7 appendix A.2:

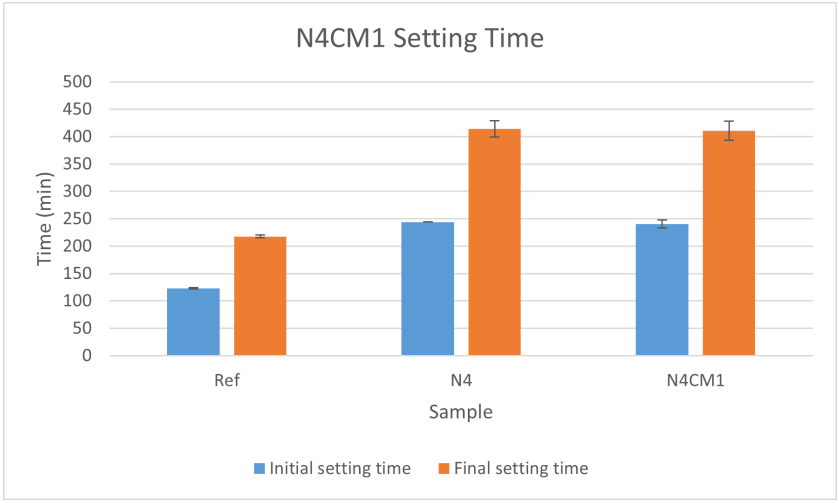

Figure 5.31: Initial and final setting time of N4CM1

CMC was added a very late stage of the thesis as a trial. It was supplied in three different viscosities (30mPa, 500mPa, and 3000mPa). The CMC used was the one with the lowest viscosity (30mPa) as there was already a problem noticed in the workability of the mixes.

It can be seen from figure 5.31 that the addition of CMC had a very small effect on the setting time. The initial and final setting time were both lower by 3.5 minutes than the N4 sample. This is an indication that this percentage of CMC is optimal for the percentage of NaCl added as the setting time was not changed.

5.4.1.2 Flowability Test (Mini-Slump)

The test was done for the sample prepared in section 5.3 with 4% NaCl and 1% CMC. The results of the flowability test are shown in figs. 5.32a and 5.32b, figs. B.13a to B.13c and figs. B.14a and B.14b in appendix B.2:

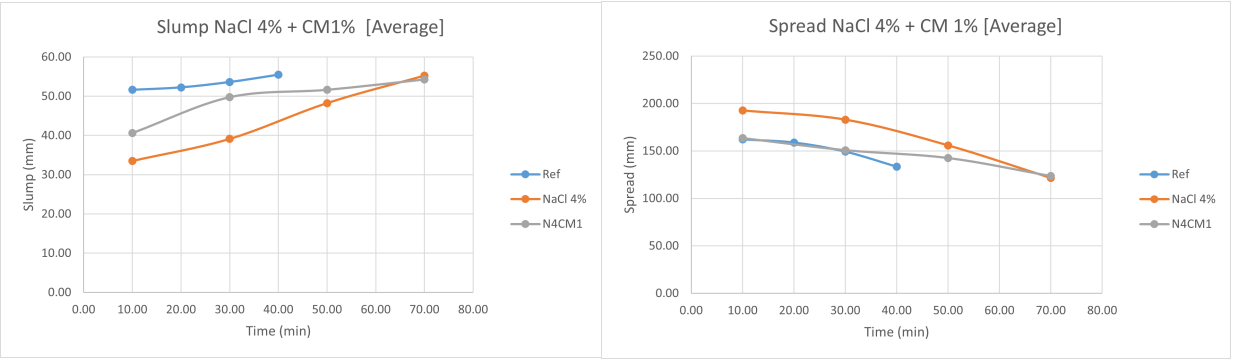

(a) N4CM1 slump test [Slump]

(b) N4CM1 slump test [Spread]

Figure 5.32: N4CM1 Slump Tests

(a) N4CM1 slump test

(b) N4CM1 spread test

Figure 5.33: Flowability Test of the N4CM1 sample at the First Time Interval

CMC led to the decrease in flowability compared to the N4 mix. Nevertheless, The mixture lost its flowability at the same time the N4 sample did. Based on figure 5.32a, it can be seen that up to the 10^{th} minute, the mix was quite flowable as the slump height was 40.6mm but then there was a jump in the slump height at it reached 49.75mm. This is an indication that CMC does not have a big effect on the yield stress and viscosity in the beginning.

However, the spread diameter results did not match the slump height results as the diameter was the same as the reference sample for the first 30 minutes. This could mean that CMC's influence on the yield stress is higher than its influence on the viscosity.

5.4.1.3 Yield Stress Development

The slug test was performed on the sample with 4% NaCl and 1% CMC to see how does the yield stress develop with time and when would the sample need too much pressure to be extruded through the nozzle. The results of slug test are shown in figure 5.34, and figure C.2e in appendix C.2:

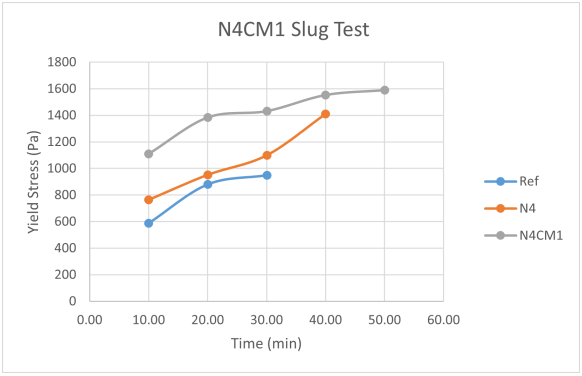

Figure 5.34: N4CM1 slug test

Figure 5.35: Slug Test of the N4CM1 Sample

The results of the slug-test showed that the addition of CMC increased the yield stress of the mix as shown in figure 5.34. It can also be observed that the extrudability time also increased by 10 minutes. Meaning that CMC and CMS have almost the same effect on extrudability even though that their trend of increase in yield stress is different. The difference is that after 10 minutes, N4CM1 had a much lower yield stress than N4C0.5, but from the 20^{th} minute mark and onwards they both had almost the same yield stress.

5.4.2 Sodium Carboxymethyl Cellulose with Sodium Borate (Borax)

5.4.2.1 Setting Time

The setting time of B2 was tested with the addition of 1% CMC. The results of the test are shown in figure 5.36, and table A.12 in appendix A.3:

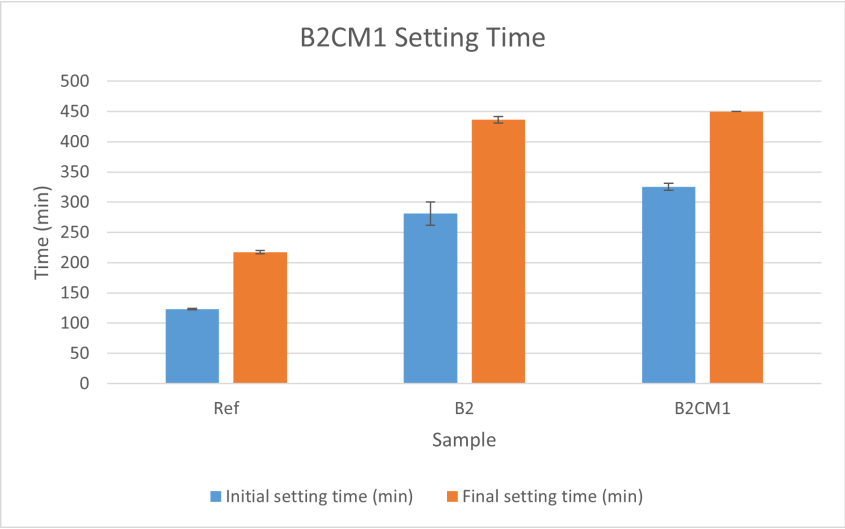

Figure 5.36: Initial and final setting time of B2CM1

The addition of 1% CMC led to an increase in both the initial and final setting time compared to the B2 sample. The initial and final setting time were increased by 44.5 and 13.5 minutes respectively. This is an indication that the decrease of fluid loss property of CMC can lead to also an increase in the initial setting time which could be also an increase in open time.

5.4.2.2 Flowability Test (Mini-Slump)

The test was done for the sample prepared in section 5.3 with 3% borax and 1% CMC. The results of the flowability test are shown in figs. 5.37a and 5.37b, figs. B.28a to B.28c and figs. B.29a and B.29b in appendix B.3:

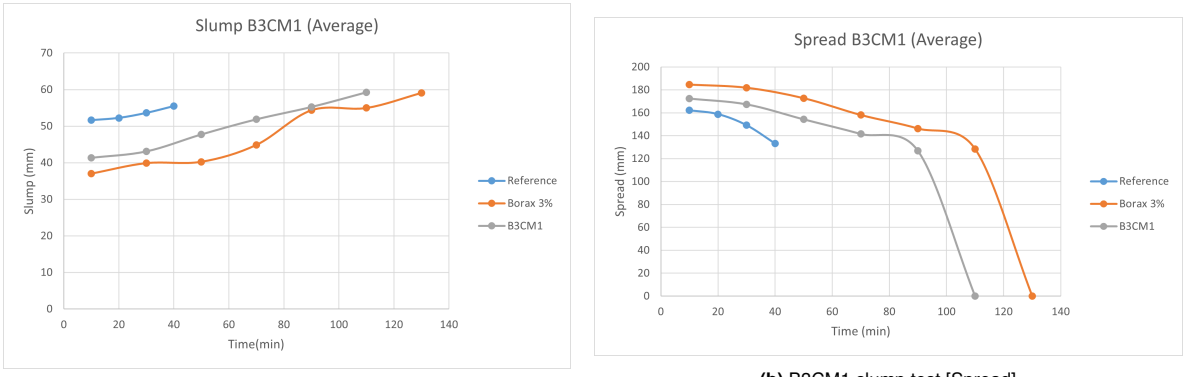

(a) B3CM1 slump test [Slump]

(b) B3CM1 slump test [Spread]

Figure 5.37: B3CM1 Slump Tests

(a) B3CM1 slump test

(b) B3CM1 spread test

Figure 5.38: Flowability Test of the B3CM1 sample at the First Time Interval

Based on figure 5.37a, the addition of CMC led to a loss in flowability after 100 minutes which is 20 minutes before the B3 sample. This means that this percentage of borax is not sufficient for maintaining the flowability of the mix. Based on the slump height values, CMC improved the viscosity and potentially the yield stress of the mix as the values were higher than the B3 sample. It's noticeable that CMC increased the slump height in a steady pace meaning that it gradually increases the viscosity.

Looking at figure 5.37b, the spread diameter was less than the B3 sample further confirming that CMC improved the yield strength of the mix. There was a difference of almost 15-20mm in diameter between the B3CM1 and B3 mixes. Furthermore, the trend in the decrease of the diameter of B3CM1 and B3 is the same.

5.4.2.3 Yield Stress Development

The slug test was performed on the sample with 3% borax and 0.75% CMC to see how does the yield stress develop with time and when would the sample need too much pressure to be extruded through the nozzle. The results of slug test are shown in figure 5.39, and figure C.6a in appendix C.3:

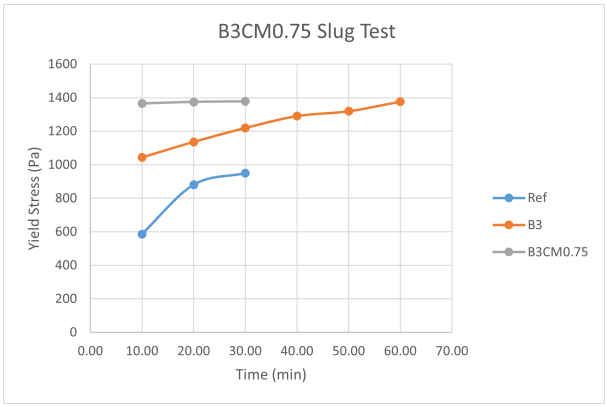

Figure 5.39: B3CM0.75 slug test

Figure 5.40: Slug Test of the B3CM0.75 Sample

It can be observed from figure 5.39 that the yield stress was improved as it started with value higher by 321 Pa than the B3 sample. However, the mix lost its extrudability 30 minutes before the B3 sample. It can also be seen that the yield stress was almost the same for this period indicating that the addition of CMC is good for the thixotropy of this mix.

Due to these results, the liquid to binder ratio was changed to 0.45 and the test was repeated. The results are shown in figure 5.41, and figure C.6b in appendix C.3:

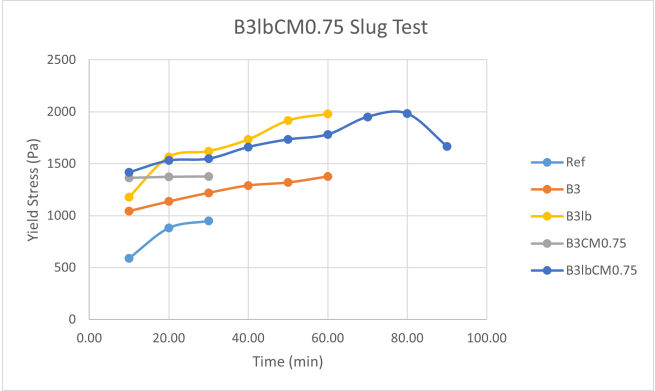

Figure 5.41: B3lbCM0.75 slug test

Figure 5.42: Slug Test of the B3lbCM0.75 Sample

When the liquid to binder ratio was increased to 0.45, It can be seen from figure 5.41 that the extrudability time was extended by 30 minutes compared to the B3lb mix. Furthermore, the same trend was observed were the B3lb mix had lower yield stress after the first 10 minutes but then it was higher for the remaining period of time. Nevertheless, their yield stress values were almost the same for the first 40 minutes. Furthermore, after 80 minutes there was a drop in the yield stress which was due to the fact that the mix needed higher pressure to be extruded. But if we look at the yield stress value before the drop, it was 1982.25 Pa which is also very similar to the yield stress value at which both B3lb and B3lbA0.5 lost their extrudability.

5.5 Overview

5.5.1 VMA's with Sodium Chloride

5.5.1.1 Setting Time

The overall setting time results are shown in figure 5.43. It can be seen that CMC and CMS had the least effect on the initial setting compared to the other VMA's. This is important because the percentage of the retarder is fixed, hence it is essential that the percentage of the VMA's does not affect the initial setting time drastically. With this in mind, the addition of attapulgite led to a big drop in the initial setting time thus this percentage is a bit high for this percentage of sodium chloride.

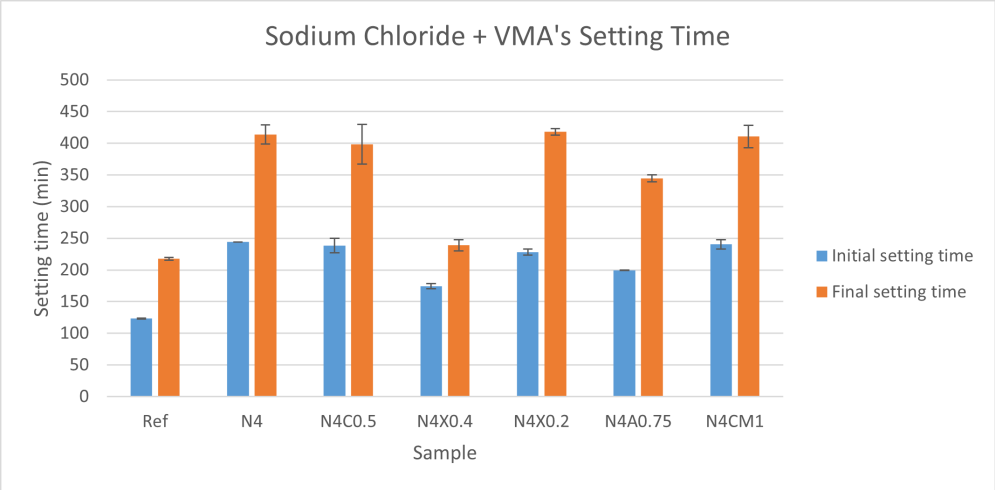

Figure 5.43: Initial and final setting time of all N4 Samples

5.5.1.2 Flowability

The figs. 5.44 and 5.45 below show all the N4 samples and the samples with the viscosity modifying admixtures. It is visible from the figures that CMC had the least effect on slump and it can be said that the effect it had is positive since the mortar was viscous enough. As said earlier, these results are only small indications of the printability of the mixes but with the presented data N4A0.75 is the only mix that be printed easily. While N4X0.2 and N4C0.5 data shows that they have high viscosity which will probably cause printing problems due to their pumpability. When it comes to N4CM1, it could also have good pumpability and buildability as the slump height was less than the other VMA's but still higher than N4 meaning good viscosity. Moreover, the spread diameter was smaller than the rest of the VMA's which could indicate higher yield stress which is needed for good buildability.

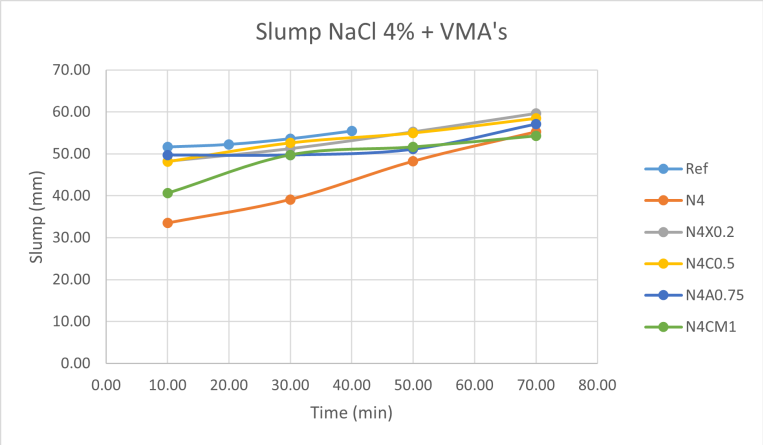

Figure 5.44: Slump of all Sodium Chloride Samples

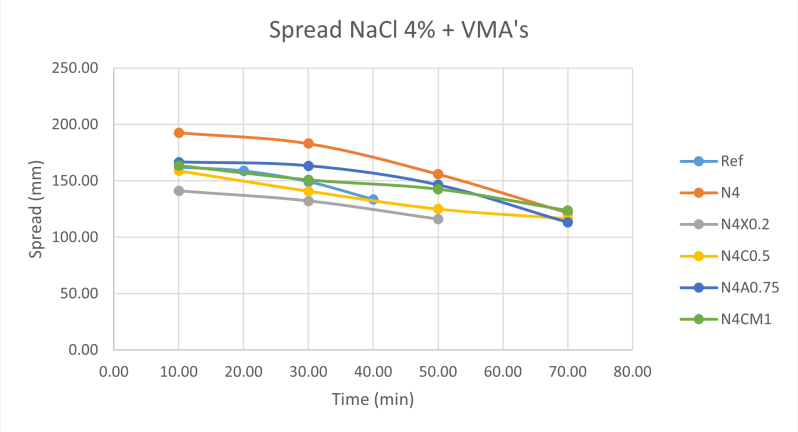

Figure 5.45: Spread of all Sodium Chloride Samples

5.5.1.3 Yield Stress Development

Figure 5.46 shows the yield stress development of all the sodium chloride samples. It can be observed that N4C0.5 had the best extrudability as it was extrudable for a longer period of time with a high yield stress indicating promising buildability properties. However, N4A0.75 is the most promising mixture when it comes to buildability as it had the highest yield stress from the start and it maintained the same stress throughout its entire extrudability time. The obvious conclusion from this graph is that all the VMA's improved the yield stress development of the reference sample and the N4 sample.

A trend was noticed which is that usually the mixtures lose their extrudability when they reach a slump height above 50mm and a spread diameter below 150mm. The only sample that contradicted this trend was the N4C0.5 which as mentioned earlier could only be explained by the shearing rate effect on the viscosity during extrusion.

However, a similar trend regarding the yield stress value could not be observed between all the mixtures. Even though that all the N4 samples with VMA's lost their extrudability when they had a yield stress of almost 1600 Pa. While, the reference and N4 sample lost their extrudability at 949.4 Pa and 1411.3 Pa respectively. The reason behind this is that each mix requires a different extrusion speed and pressure and the behaviour under shearing is different between them hence it cannot be said that at a certain yield stress value, extrudability will be lost.

Based on the results of the yield stress test performed on the RA0.75 mix, all the N4 samples with the addition of VMA's would be printable. This is based on the fact that the RA0.75 mix was printed by Ir. Irving Flores without any problems except for the short open time. While based on its yield stress test, it needed very high pressure for extrusion as after 10 minutes of mixing only 23 slugs were extruded and after 20 minutes, only 10 slugs were extruded meaning that it had already lost its extrudability. While all the N4 samples with VMA's were easily extruded.

Furthermore, RA0.75 exhibited very good buildability properties as 15 layers were printed vertically which is the max. height that can be reached with 3D printer. However, the buildability potential of the N4 mixes with VMA's cannot be predicted based on the yield stress values comparison. This is because the RA0.75 yield stress values for sure do not represent the actual yield stress value since it needed high pressure to be extruded. Thus, the shape retention and buildability of all the mixes cannot be predicted based on the yield stress values obtained.

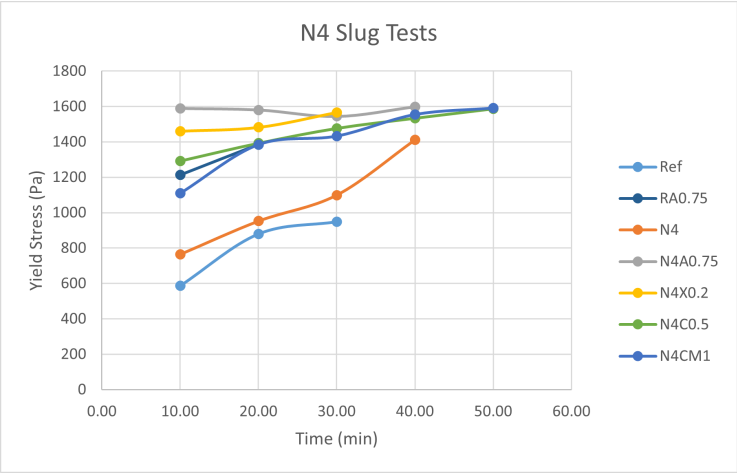

Figure 5.46: Yield Stress Development of all Sodium Chloride Samples

5.5.2 VMA's with Sodium Borate

5.5.2.1 Setting Time

The overall setting time results are shown in figure 5.47. It can be observed that CMC and attapulgite had the best effect regarding the effect on the initial setting as they both increased the initial and final setting time. The percentages of all the VMA's used were all optimal as their effect on the initial setting time was minimal.

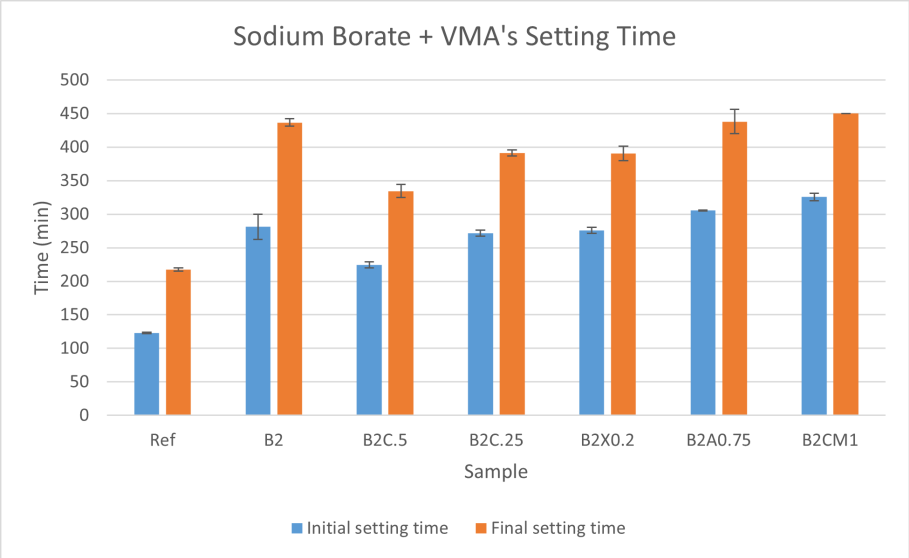

Figure 5.47: Initial and final setting time of all B2 samples

5.5.2.2 Flowability

Below, figs. 5.48 and 5.49 show all the B3 mixes with the different VMA's used. It can be observed that all 4 VMA's decreased the flowability time of the mix. Xanthan gum had the highest effect on flowability as it decreased the flowability time by 30 minutes compared to the B3 sample. While CMS and attapulgite both decreased it by 20 minutes.

Based on the slump results in the first 50 minutes, attapulgite had the biggest effect on the mix as it had the highest slump value compared to B3, B3X0.2, B3C0.25, and B3CM1. Nevertheless, after that both B3X0.2, B3C0.25, and B3CM1 had higher slump than B3A0.75 and this was explained earlier by the fact the xanthan gum, CMS, and CMC's effect on the yield strength and viscosity gradually increases over time. This was not the case for attapulgite, as it can be seen that for the first 70 minutes there was a very slight change in slump. Thus, based on the slump results attapulgite had the most positive effect on the mix.

Based on the spread diameter results, again in the first 50 minutes, the addition of attapulgite had the biggest effect as it had the lowest spread value out of all samples. For the first 20 minutes B3A0.75 had the same spread as the reference sample, meaning that this percentage of attapulgite completely cancelled out the effect of borax.

Nevertheless, both B3A0.75 and B3C0.25 had the same behaviour when it came to the spread diameter, because for the first 50 minutes there was a slight difference in the spread values. While, B3X0.2 started with the highest spread diameter compared to B3A.75, B3C0.25, and B3CM1, but then its spread diameter decreased sharply up until it reached the 0 mark at 100 minutes.

Based on these results it is hard to judge which VMA had a better effect between attapulgite and CMS. This is due to the fact that as mentioned above up until the 50^{th} minute mark they had a stable spread with B3C0.25 having a slightly higher spread diameter. After that, both samples had the same spread diameter up until they lost flowability. Thus, the effect on buildability can only be investigated with actually printing both mixes.

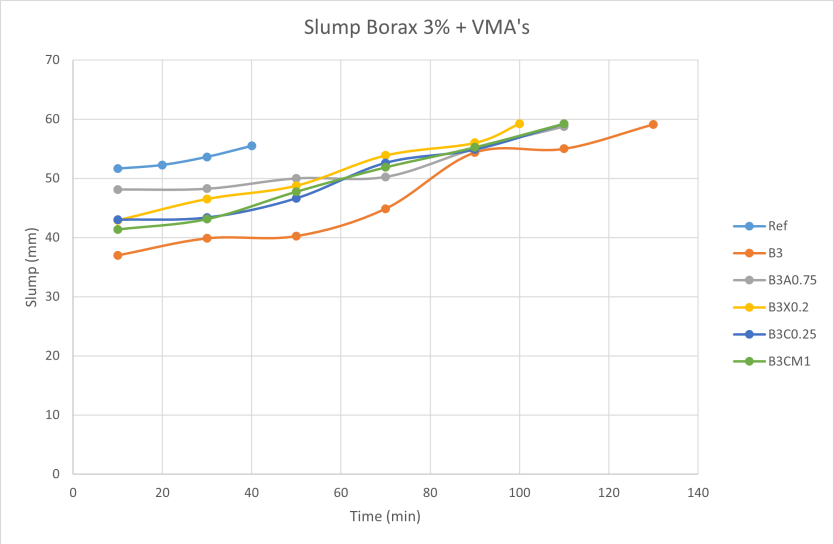

Figure 5.48: Slump of all borax samples

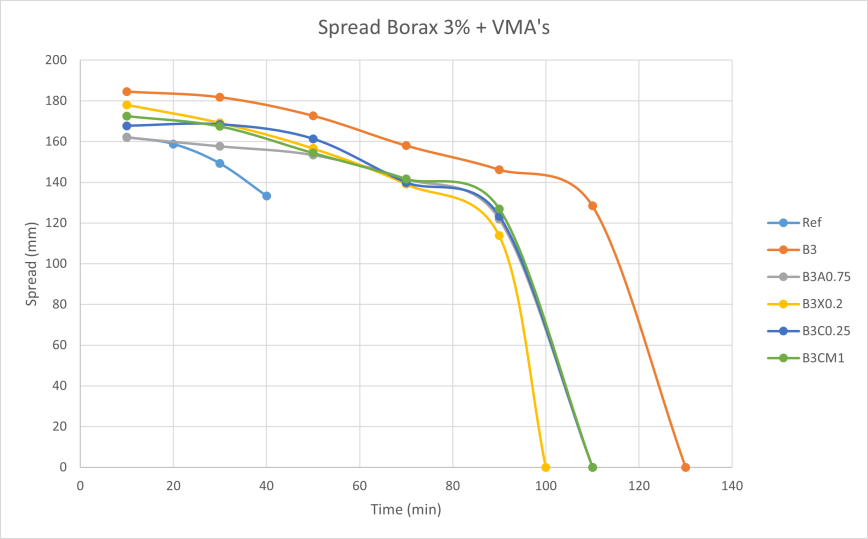

Figure 5.49: Spread of all borax samples

5.5.2.3 Yield Stress Development

Based on figure 5.50, the addition of VMA's decreased the extrudability time except for attapulgite as it increased it by 10 minutes. However, when it comes to yield stress development, attapulgite had a negative effect on the yield stress which can only be explained by the pressure needed for extrusion. Both CMS and CMC had a positive effect when it comes to the yield stress as they both improved the yield stress development compared to the B3 sample.

When it comes to printability, based on the yield stress test results of the RA0.75 mix, all the B3 mixes should be printable. Nevertheless, no conclusions can be made regarding their buildability due to the inaccuracy in the yield stress results of the RA0.75 mix.

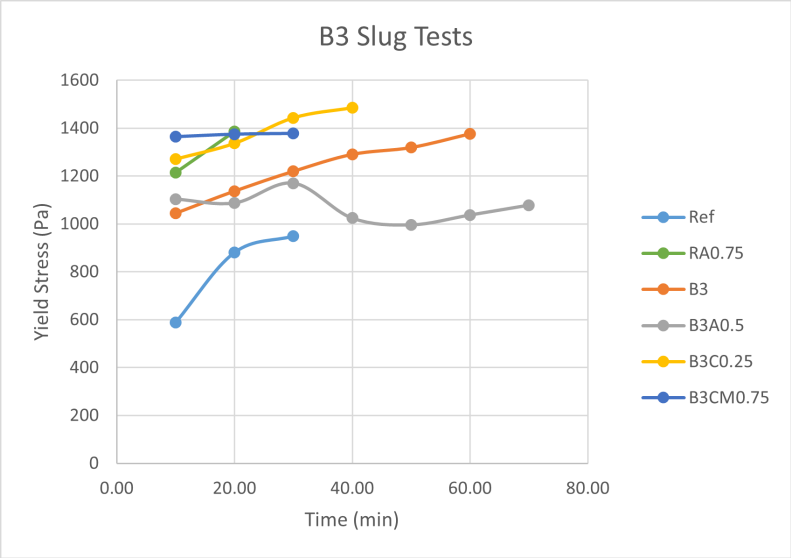

Figure 5.50: Slug of all borax samples

Based on figure 5.51, the addition of attapulgite had the best effect when it comes to the extrudability time, while CMC had the best effect when it comes to yield stress development. Furthermore, when it comes to printability, all the B3lb mixes should be printable as they were all extruded with ease.

These results confirmed that the increase in the liquid to binder ratio improved the workability of the mix. It has been reported that increasing either the water content or the alkaline activator content will improve workability. Nevertheless, it comes at a price as the compressive strength will decrease. G.Khali et al [98] indicated that increasing the activator content has a lower effect on the strength than adding water, hence why it was decided to increase the activator content to improve the workability and increase the open time.

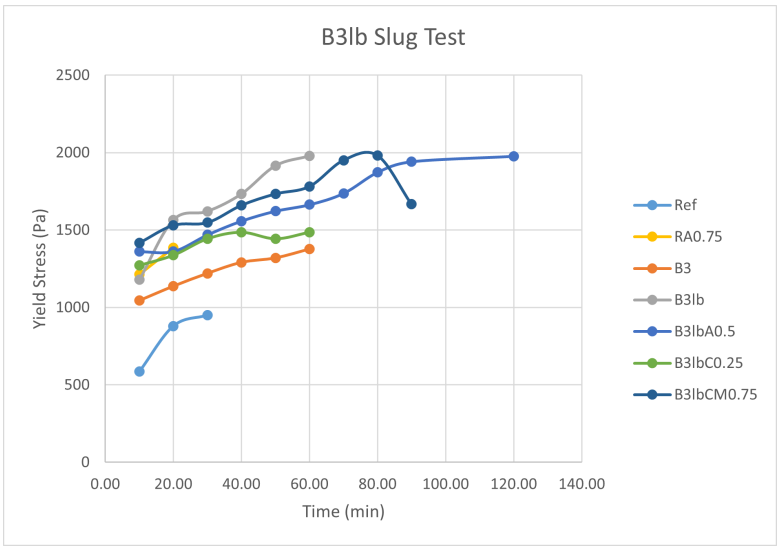

Figure 5.51: Slug of all borax (l/b=0.45) samples

6

Final Mixture: B3lbA0.5

The B3lbA0.5 mix was chosen for printing for two significant reasons:

- It had the longest extrudability time among all the other mixes which was two hours. This is one of the research goals of this research which was developing a mixture that has an open time of 2 hours or more. Based on the fact that the mixture was extrudable for 2 hours means that it definitely has an open time longer than two hours since the RA0.75 mix had an open time of 50 minutes while with the yield stress test it was only extrudable for almost 20 minutes.
- The yield stress development obtained from the yield stress test showed relatively good results since [94] indicated that a yield stress of 1400 Pa is good for buildability.

Below all the tests results of the B3lbA0.5 mixture are presented.

6.1 Flowability Test (Mini-Slump)

The flowability test was done to have an indication about the flowability behaviour to check when to stop the printing process. This was carried out so to avoid the risk of the mortar hardening inside the pump. The results of the flowability test are shown in figs. 6.1a and 6.1b and table B.23 in appendix B.3:

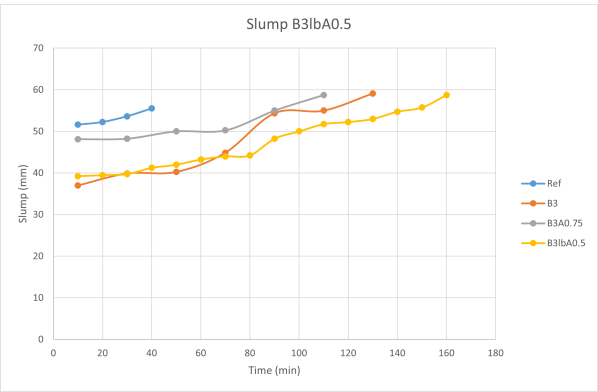

(a) B3lbA0.5 slump test [slump]

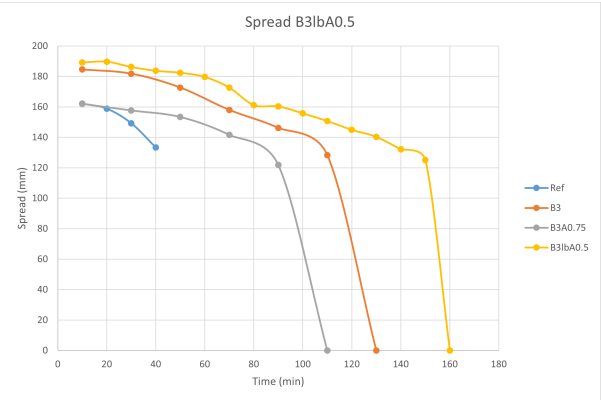

(b) B3lbA0.5 slump [Spread]

Figure 6.1: B3lbA0.5 Slump Test

(a) B3lbA0.5 slump test

(b) B3lbA0.5 spread test

Figure 6.2: Flowability Test of the B3lbA0.5 sample at the First Time Interval

It can be seen from figs. 6.1a and 6.1b that the flowability time increased to 150 minutes which is 30 and 50 minutes more than the B3 and B3A0.75 samples respectively. Looking at the slump height, there is no big difference between the B3lbA0.5 and B3A0.75 samples up until the 70th minute. After that, the the B3lbA0.5's slump height remained lower which has to do with the increase in the liquid to binder ratio. As for the spread diameter, the difference between them was small up until the 60th minute. This means the increase in the activator percentage slowed down the loss in flowability that was occurring after 60-70 minutes from mixing. This could lead to the conclusion that the liquid to binder ratio does not affect flowability for the for the first 60 minutes. It only starts to have an effect after that point by slowing down the loss in flowability with the increase in its value. Furthermore, it can be seen that the flowability remained constant up until the 80^{th} minute giving a margin of 80 minutes of safely printing without any risks to the pump.

6.2 Yield Stress Development

The results of the yield stress development test are shown in figure 6.3, and figure C.4b in appendix C.3:

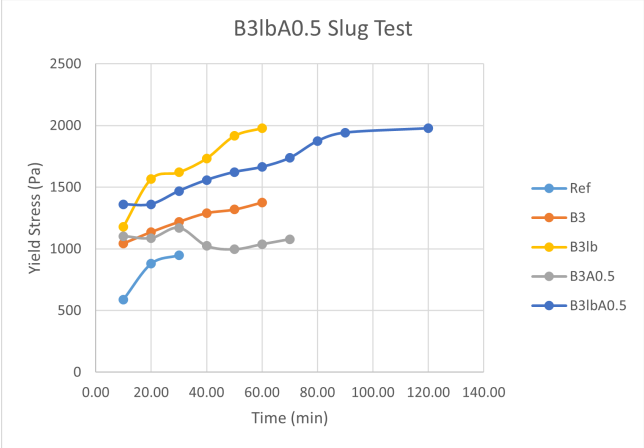

Figure 6.3: B3lbA0.5 slug test

Figure 6.4: Slug Test of the B3lbA0.5 Sample

It can be seen from the graph that the extrudability time significantly improved as it reached 2 hours compared to the B3lb. However, the yield stress development is slower than than the B3lb mix as the yield stress was only higher after 10 minutes then the B3lb mix always had higher yield stress. Nevertheless, as seen in figure 6.3 the B3lbA0.5 mix had higher yield stress than B3, B3A0.5 and ref mixes. Although, this does not necessarily mean that the B3lbA0.5 would have better buildability as the yield stress values of the B3, B3A0.5 and ref mixes may not actually represent their actual yield stress values. Furthermore, it can be observed that the mix lost it extrudability when it reached a yield stress of 1977.78 Pa which is very similar to the value when the B3lb mix lost its extrudability. Moreover, the

mixture lost its extrudability 30 minutes before it lost its flowability. This behaviour has been noticed many times, hence extrudability is always lost before the loss of flowability.

6.3 Pumpability and 3D Printing

The pumpability test was done for the B3lbA0.5 sample. The results are shown in table 6.1 and figure 6.5

Table 6.1: B3lbA0.5 Pumpability Test

B3lbA0.5 Pumpability Test						
Speed	**Mass (g)**	**Mass/10 (g/s)**	**Density (g/L)**	**Volume (L/s)**	**d (mm)**	**V/d (V/mm.s)**
Speed 1	not pumpable	-	-	-	-	-
Speed 2	303.8	31.895	2.04	15.63	25	0.63
	334.1					
AVG	318.95					
Speed 3	399.1	40.275	2.04	19.74	25	0.79
	406.4					
AVG	402.75					
Speed 4	513	54.92	2.04	26.92	25	1.08
	585.4					
AVG	549.2					
Speed 5	686.6	69.635	2.04	34.13	25	1.37
	706.1					
AVG	696.35					

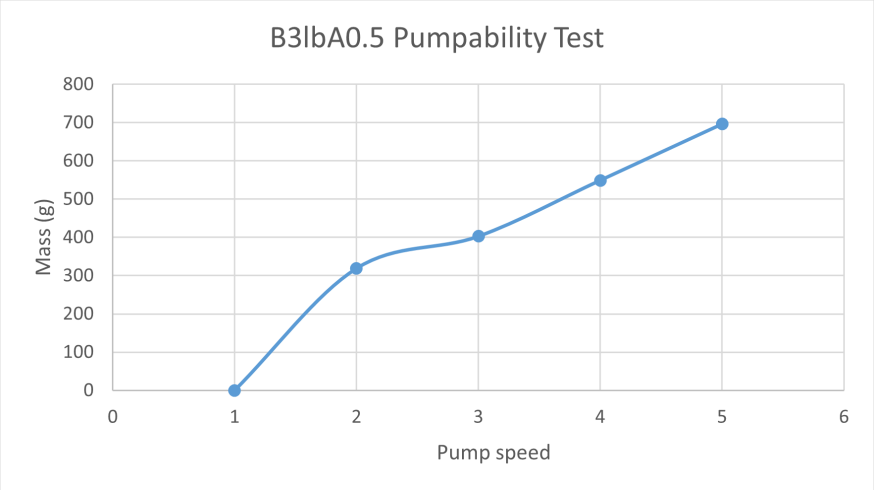

Figure 6.5: B3lbA0.5 Pumpability Test

According to the pumpability test results seen in figure 6.5, the mixture was not pumpable at speed 1. This means that the mixture's yield stress is too high for this speed. Nevertheless, at speed's 2-5, the mixture was pumped easily, thus the mixture is printable.

The printed wall using B3lbA0.5 shown in figure 6.6:

Figure 6.6: B3lbA0.5 Printed Wall

As can be seen in figure 6.6 the printed wall had 10 layers. The printing was stopped because further printing would have led to the collapsing of the wall. The B3lbA0.5 mixture has less buildability than RefA0.75 as 15 layers were printed using the RefA0.75 mixture as shown in figure 6.7. Nevertheless, this outcome was expected since the reaction is retarded due to the borax and there is less attapulgite in the mixture than the reference mixture. Moreover, the mixture was easily pumped thus the percentage of attapulgite can probably be increased back to 0.75% to improve the buildability of the mixture.

Coming back to the flowability and yield stress development tests, it can be concluded that a spread diameter above 180mm could be too high for buildability purposes. Which means that a spread diameter between 150-180mm could ensure that a mixture shows good buildability properties. As for the yield stress, indeed a yield stress of 1400 Pa insures good flowability of the material. Nevertheless, it's still too low to withstand the self-weight. Based on the printing process, the mixture stayed in the pump for 60 minutes after mixing, meaning that a yield stress above 1600 Pa would be required to have better buildability.

There were also two reasons that affected the printing process: the distance between the nozzle and the printing surface and the nozzle itself. The distance from the nozzle till the printing surface was considered a bit high for this mixture. The distance affects the buildability as the concrete will cause further deformation to the layer under it. The second problem was the nozzle itself as it was slightly rotating while printing which led sometimes to the layers to be printed at an angle which so the layers were not totally aligned.

Figure 6.7: RefA0.75 Printed Wall

6.4 Flexural and Compressive Strength Tests

The tests were carried out on cast and printed samples. First, The flexural and compressive strength test for the B3lbA0.5, B3lb, and reference cast samples were carried out. The results are shown in figs. 6.8a and 6.8b, and tables D.1 to D.3 in appendix D:

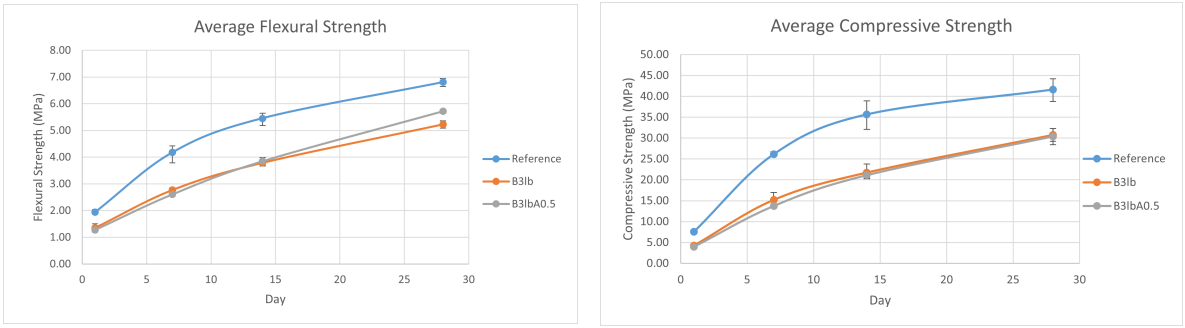

(a) B3lbA0.5 flexural strength test

(b) B3lbA0.5 compressive strength test

Figure 6.8: Flexural and Compressive Strength Test of B3lbA0.5

Based on the results of the flexural and compressive strength tests shown in figs. 6.8a and 6.8b, the change in liquid to binder ratio and the addition of borax led to a decrease in the flexural and compressive strength. It can be seen that the flexural and compressive strength test of B3lb and B3lbA0.5 are almost the same at all time meaning that the attapulgite has no effect on the strength development. The only visible difference was the flexural strength at the 28^{th} day where the B3lbA0.5 had a slightly higher flexural strength. The flexural strength of B3lbA0.5 increased from 0.66% at the 1^{st} day to 0.84% at the 28^{th} day compared to the reference sample. While the compressive strength of B3lbA0.5 increased from 0.53% at the 1^{st} day to 0.73% at the 28^{th} day. This is probably the effect of borax as it slows down the strength development in the early stages then it increases but it is still less than the reference sample which is the effect of the increased amount of activator. The compressive strength of B3lbA0.5 is equivalent to C25/30. However, the flexural strength of B3lbA0.5 is equivalent to C45/55. This is a typical result for geopolymer concrete where the compressive strength is always less than the flexural strength.

Flexural and compressive strength test were carried out on printed prisms on the 7^{th} day after printing. The results of the compressive and flexural strength tests done on printed prism compared with the cast prism results are shown in figs. 6.9a and 6.9b and tables D.4 and D.5 in appendix D:

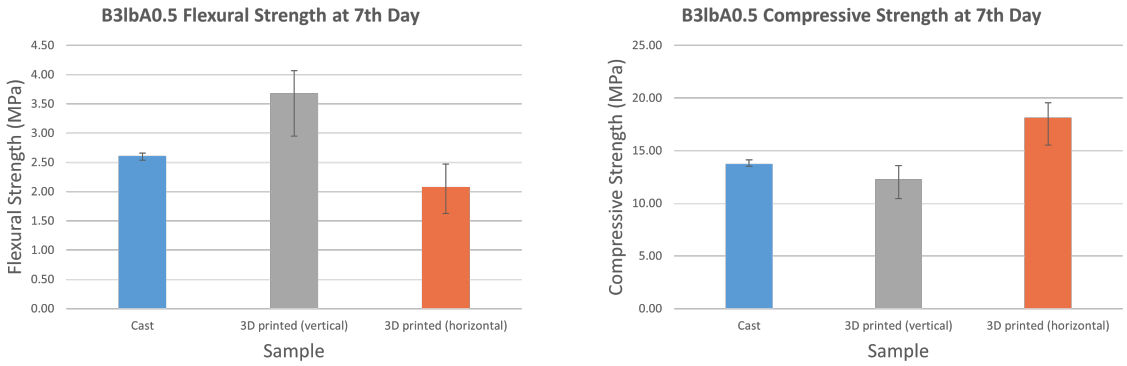

(a) Printed B3lbA0.5 sample flexural strength test

(b) Printed B3lbA0.5 compressive strength test

Figure 6.9: Flexural and Compressive Strength Test of Printed B3lbA0.5 Samples

Based on the results shown in 6.9a, It can be seen that the flexural strength of the 3D printed prism tested in the vertical direction is the highest compared to the cast prism and 3D printed prism tested in the horizontal direction by 0.29% and 0.43% respectively. This means that printed prisms behave in an anisotropic way as the flexural strength changes based on the direction of the test. This has to do with the region that is subjected to the maximum bending moment in the test. Nevertheless, in both the vertical and horizontal directions, the maximum bending stress should occur in the bulk of the concrete. Hence, the results should be close but in this case the only reasonable explanation is that the interface layer influenced the results in a way. Moreover, it's reasonable that the printed prism had higher flexural

strength as it has been proven that the porosity of cast concrete is higher than 3D printed concrete, and this higher porosity leads to a decrease in the flexural strength.

Nevertheless, based on the results shown in 6.9b, the compressive strength of 3D printed cube tested in the horizontal direction was higher than both the cast cube and the 3D printed cube tested in the vertical direction by 0.24% and 0.32% respectively. Normally cast cubes have higher compressive strength than 3D printed cubes because of the interface layer at it is usually the weak link in printed prisms so it leads to failure faster. Nevertheless, as was shown in the tensile bond test, the failure happened near the glue which means the interface is not the weaker link which explains why the cube tested in the horizontal direction had the highest compressive strength.

6.5 Tensile Bonding Strength Test

The test was done on the 4^{th} day after printing. The results of the tests are shown in figs. 6.10a to 6.10c:

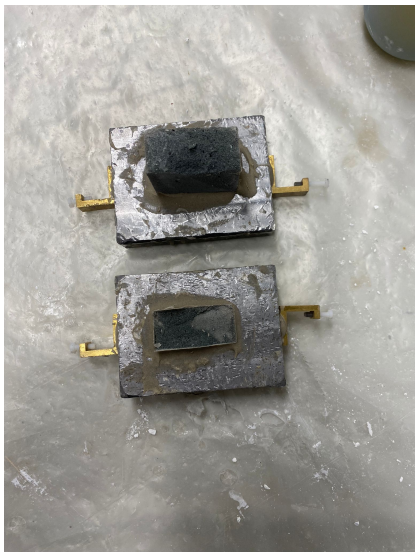

(a) B3lbA0.5 uni-axial test (1)

(b) B3lbA0.5 uni-axial test (2)

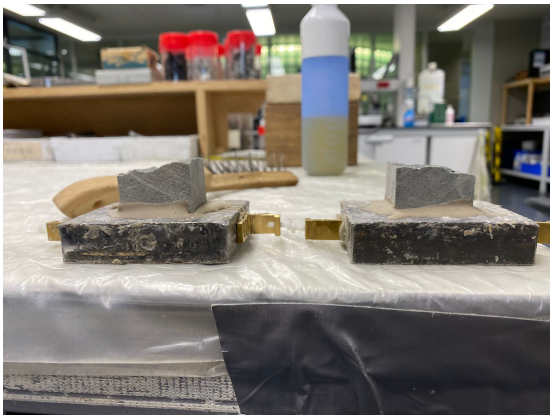

(c) B3lbA0.5 uni-axial test (3)

Figure 6.10: B3lbA0.5 Uni-axial Test

Based on the results of the tensile bond strength test shown in figs. 6.10a to 6.10c, the first two samples failed near the glue. This location of the crack indicates that the bond between the layers is strong. This could be explained by the adhesive nature of geopolymer and the effect of attapulgite as it

increases the cohesion of the mixture. This result was also achieved by Zainab [85] as her sample also failed near the glue due to the use of attapulgite. One other factor that could have influenced this failure is the heat induced by the glue which leads to extra stress buildup near it. The average tensile strength for the samples is 0.69 MPa.

6.6 Conclusion

The B3lbA0.5 mixture showed acceptable printability and buildability properties. The mixture's initial results were in range of the required values as the initial setting time was higher than 3 hours, the spread diameter was between 150-200mm for almost 130 minutes, and the yield stress reached 1400 Pa after 20 minutes. Nevertheless, after printing it was concluded that a spread diameter between 150-180mm, and a yield stress above 1600 Pa would be better to ensure better buildability. hence, the addition of more attapulgite would prove to be beneficial to both in enhance the buildability and strengthen the interface between the layers. As shown in the uni-axial test, failure happened near the glue which meant that the interface layer was stronger due to the addition of attapulgite. Moreover, as shown in the flexural and compressive strength results, the difference in strength between the cast and printed mixtures is not high, and depending on the direction of applying the load the printed mixture can show higher strength than the cast mixture.

7

Conclusions and Recommendations

7.1 Conclusions

Multiple conclusions can be drawn from the work done in this thesis. Regarding the tests that were done in this thesis, the setting time test is not a good indicator for printing properties. This is due to the fact that all of the mixes lost their flowability or extrudability a long time before their initial setting time. The only outcome that can be drawn from the setting time test is if an admixture does have an effect on the mix or not. Furthermore, the setting time test was used in this thesis to calibrate the percentage of VMA's used based on the their effect in reducing the initial setting time. This was the case because the retarder percentage was fixed when the VMA's were added, thus the VMA's percentage should not reduce the initial setting time because that would mean that the yield stress became too high for extrudability.

However, slump and slug tests are a good indicator of the material's behaviour regarding printability and flowability. It was deduced that the slump height can be an indicator of the mixtures' viscosity, while the spread diameter can show the mixtures' yield stress development. As for the slug test, it is most definitely the closest test to printing. This is because the material is extruded during the test so it experiences shearing which can indicate the full extent of the VMA's effect on the mixtures because VMA's alter the material's behaviour under shearing.

A correlation between the slump and slug tests could not be found for all the mixtures. The one constant is that extrudability is always lost before the loss of flowability. Usually the loss of the extrudability occurs 20 minutes before the loss of flowability. It was only noticeable with the sodium chloride samples with added VMA's. They all lost their extrudability in the slug test when the slump height value was 50mm and the spread diameter was 150mm. However, for the borax samples, there was no correlation between the results of both tests. This has to do with the fact that the thixotropic behaviour of each mixture is different depending on the retarder added. Furthermore, the slug test does not give the actual yield stress values when the mixture needs high pressure to be extruded. This is one of the drawbacks of the slug test, as the diameter of the nozzle and the pressure that can be provided do not represent the pressure than can be given by a printer's pump. This was validated by the fact that the RA0.75 sample lost its extrudability after 15-20 minutes with the slug test. However, the mixture was printable for 50 minutes. .

One of the most important conclusions is agreeing with what most researchers already implied which is that there is no way to be sure about the effect of retarders with alkali-activated material. There is no way to generalize the effect of a certain admixture and usually the results obtained will only be for the specific mixture they were tested on. This has to do with the fact that there are a lot of factors that influence the effect of admixtures, like the precursors used, their percentage in the total binder, the alkali activator used, the molarity of the activator, the liquid to binder ratio, and the water content. To further elaborate on this, in section 2.2.1.1, the effect of sucrose as a retarder was reported. Nevertheless, when it was added to the mixture used in this thesis, it did not have a retarding effect at all. Furthermore,

when it comes to the percentages of the admixtures used, none of the percentages of admixtures used in this thesis are the same as the ones reported in the literature. Thus, this further confirms that the admixtures topic is complicated when it comes to alkali-activated materials as there are a lot of factors that influence their effect.

Both sodium chloride and sodium borate had a retarding effect on the mixture. However, less percentages were needed than the ones mentioned in literature. For sodium chloride, it was reported that with a percentage lower than 4% it would act as an accelerator and that the optimum percentage is 6% but this was not the case. Percentages from 3%-8% were tested. They all exhibited a retarding effect with 4% being the optimum as it led to the biggest delay in initial setting time. Sodium Chloride also enhanced the flowability of the mixtures. Two percentages of sodium chloride were tested with the flowability test: 3% and 4%. The mix with 4% NaCl had better flowability meaning that with the increase in NaCl percentage, flowability will be better. Sodium Chloride also enhanced the extrudability of the mixture, as the mix was extrudable for a longer period of time compared to the reference sample during the slug test.

Borax had a bigger effect on the setting time than NaCl as less percentages of borax compared to NaCl led to a bigger delay in the setting time. The percentages of borax tested ranged from 1-6%. They all showed a delay in the setting time of the mixture. Also, it was concluded that the delay in setting time increases as the percentage of borax increases. Also, based on the slump tests, the addition of borax increased the flowability of the mixture, and flowability increases with the increase in the borax percentage. According to the results of slug test, borax also increased the extrudability time of the mixture. However, the mixture required high to be extruded during the test. And in general, the addition of borax led to having a dry paste. Although, when the liquid to binder ration was increased to 0.45, the mixture was easily extruded. however, increasing the activator content did not affect the extrudability time. This means that the increase in the activator content only affected workability.

The second part of this thesis was to check if the chosen retarders and VMA's can work side by side to simultaneously increase the open time and enhance the viscosity and yield stress for better buildability. It was concluded that nano-clay (attapulgite), sodium carboxymethyl starch (CMS), and sodium carboxymethyl cellulose are compatible with both sodium chloride and borax. However, xanthan gum led to a severe decrease in flowability and led to the dryness of the mixtures.

The addition of attapulgite led to a decrease in fluidity but it improved the yield stress development while maintaining the same flowability and extrudability time. It was noticed that attapulgite increases the viscosity and yield stress up to a certain point and then stays at the same value for around 40-50 minutes then the values start to change again or in case of extrudability it stops being extrudable. However, this property was not noticed when the liquid to binder ratio was increased to 0.45. However, when the liquid to binder ratio was increased to 0.45, B3lbA0.5 was extrudable for double amount the time B3lb was extrudable and it was flowable for 150 minutes. Moreover, based on the results of the slug tests, attapulgite improved the thixotropy of the mixture as the mixture had relatively high yield stress but it was still extrudable meaning that under shearing its viscosity decreases which is optimum for 3D printing.

When it comes to xanthan gum, the increase in viscosity and yield stress was too high for this mixture that it negatively affected both its flowability and yield stress development. This is due to the fact that xanthan gum is mixed with the alkaline activator which increases it viscosity even more, when in fact the activator is already viscous due to sodium silicate.

Sodium carboxymethyl starch did not delay the setting time of the mixture, it only affected its viscosity meaning that for this mixture CMS can only work as a VMA. CMS improved the thixotropy of the mixture. It reduced the flowability of the mixture but improved its viscosity and yield stress. It is good for thixotropy because even with high yield stress values and low flowability, the mixture was still easily extruded. This means that under shearing the mixture loses its viscosity which is suitable for printing. Nevertheless, the percentage of CMS added has to be well studied before as it was noticed that amounts higher than 0.5% of the binder in this case led to severe dryness of the mixture.

Sodium carboxymethyl cellulose had a positive effect on the viscosity and yield stress of the mixture.

It increased the yield stress of the mixture while maintaining its extrudability. This means that CMC also enhanced the thixotropic behaviour of the mixture. Furthermore, when added to the B3lb sample, it lead to an increase in the extrudability time by 1.5 times the extrudability time of the B3lb sample. However, the mechanism behind this behaviour is not known as it still have not been studied. In the end, it can be said that borax had the biggest influence on the setting time while attapulgite and CMC had the best influence on the thixotropy of the mixture.

The compressive strength of the cast B3lbA0.5 is 30.49 MPa after 28 days so it didn't reach the value (40 MPa)that was looked for. Moreover, the compressive strength of the cast, and printed cubes tested on the 7^{th} day in the vertical and horizontal direction were 13.76 MPa, 12.28, MPa, and 18.13 MPa respectively. Assuming that the difference between the value will be the same, the values on the 28^{th} day would be, 30.49 MPa, 27.15 MPa, and 40.08 MPa. This indicates that this mixture can be used in structural applications. The mixture showed good buildability properties as 10 layers were printed. However, the buildability could be improved with the increase of the attapulgite's percentage. Furthermore, the buildability of the mixture does not only depend on the mixture itself but also the speed of printing, the height between the nozzle and the printing surface and the nozzle itself. It was also concluded that the compressive and flexural strength of the printed concrete could be higher than cast concrete based on the direction of testing due to the influence of the interface layer. In this case, the interface layer did not affect the strength negatively as it was not the weakest link.

7.2 Recommendations

- Decreasing the percentage of borax added to 2.5% or 2% while keeping the liquid to binder ratio at 0.45. This would improve the flexural and compressive strength of the mixture while having sufficient flowability and a long open time.
- Increasing the water to binder ratio of the mortar because it will improve flowability and increase the open time. This is a recommended since maybe less percentage of water would need to be added than the activator percentage that was added when the liquid to binder ratio was increased to 0.45. This may lead to a better flexural and compressive strength development of the mixture.
- Increase the percentage of attapulgite to 0.75% to further improve the mixture's buildability.
- Conducting an isothermal calorimetry test to further understand the behaviour of the mixture with each different admixture based on the heat generated at each stage. Moreover, the width of the dissolution peak can indicate the loss of flowability which could aid in finding the reason why flowability is lost a long time before the initial setting time.
- To further understand the reaction mechanisms of the admixtures and their effect on the early-age properties, an SEM test can be done to visually inspect the reactions, and an FTIR test to study which chemical bonds are being formed.

References

[1] Pierre-Claude Aıtci an. “Cements of yesterday and today: Concrete of tomorrow”. In: *Cement and Concrete Research* 30 (Sept. 2000), pp. 1349–1359. DOI: 10.1016/S0008-8846(00)00365-3.

[2] Provis et al. “Geopolymers and Related Alkali-Activated Materials”. In: *Annual Review of Materials Research* 44.1 (2014), pp. 299–327. DOI: 10.1146/annurev-matsci-070813-113515.

[3] Ei Thwe, Dilip Khatiwada, and Alexandros Gasparatos. “Life cycle assessment of a cement plant in Naypyitaw, Myanmar”. In: *Cleaner Environmental Systems* 2 (Dec. 2020), p. 100007. DOI: 10.1016/j.cesys.2020.100007.

[4] Worldometer. *Netherlands CO2 Emissions*. 2016. URL: https://www.worldometers.info/co2-emissions/netherlands-co2-emissions/.

[5] Harpa Birgisdottir and Freja Nygaard Rasmussen. *Introduction to LCA of Buildings*. English. 1st ed. Trafik-og Byggestyrelsen, 2016.

[6] Government NL. *climate deal makes halving carbon emissions feasible and affordable*. 2019. URL: https://www.government.nl/latest/news/2019/06/28/climate-deal-makes-halving-carbonemissions-feasible-and-affordable.

[7] European Commission. *Construction and demolition waste*. 2008. URL: https://environment.ec.europa.eu/topics/waste-and-recycling/construction-and-demolition-waste_en.

[8] Naim Sedira et al. “A review on mineral waste for chemical-activated binders: mineralogical and chemical characteristics”. In: (2017).

[9] Wool2Loop. *The Project*. 2020. URL: https://www.wool2loop.eu/en/project/.

[10] Ming Xia and Jay Sanjayan. “Method of formulating geopolymer for 3D printing for construction applications”. In: *Materials & Design* 110 (2016), pp. 382–390. ISSN: 0264-1275. DOI: https://doi.org/10.1016/j.matdes.2016.07.136. URL: https://www.sciencedirect.com/science/article/pii/S0264127516310437.

[11] Behrokh Khoshnevis et al. “Experimental investigation of contour crafting using ceramics materials”. In: *Rapid Prototyping Journal* 7 (Mar. 2001), pp. 32–42. DOI: 10.1108/13552540110365144.

[12] Sungwoo Lim et al. “Fabricating construction components using layer manufacturing technology”. In: *Proc Int Conf Glob Innov Constr* (Jan. 2009), pp. 512–520.

[13] E.M. Sachs et al. “Three-dimensional printing techniques”. In: (1993).

[14] Giovanni Cesaretti et al. “Building Components for an Outpost on the Lunar Soil by Means of a Novel 3D Printing Technology”. In: *Acta Astronautica* 93 (Jan. 2014), pp. 430–450. DOI: 10.1016/j.actaastro.2013.07.034.

[15] TU Eindhoven. *first resident of 3d printed concrete house in Eindhoven receives key*. 2021. URL: https://www.tue.nl/en/our-university/departments/biomedical-engineering/the-department/news/news-overview/30-04-2021-first-resident-of-3d-printed-concrete-house-in-eindhoven-receives-key/#top.

[16] Urbanist. *Made in China: World’s First 3D-Printed Apartment Complex*. 2015. URL: https://weburbanist.com/2015/01/20/made-in-china-worlds-first-3d-printed-apartment-complex/.

[17] Jingchuan Zhang et al. “A review of the current progress and application of 3D printed concrete”. In: *Composites Part A: Applied Science and Manufacturing* 125 (July 2019), p. 105533. DOI: 10.1016/j.compositesa.2019.105533.

[18] Duxson et al. “Geopolymer technology: the current state of the art”. In: *Journal of Materials Science* 9 (May 2007), p. 2917. DOI: 10.1007/s10853-006-0637-z.

[19] Joseph Davidovits. “Properties of geopolymer cements”. In: *First international conference on alkaline cements and concretes*. Vol. 1. Kiev State Technical University Kiev, Ukraine. 1994, pp. 131–149.

[20] Jordi Payá et al. “Application of alkali-activated industrial waste”. In: Jan. 2019, pp. 357–424. ISBN: 9780081024805. DOI: 10.1016/B978-0-08-102480-5.00013-0.

[21] Navid Ranjbar et al. “Hardening evolution of geopolymers from setting to equilibrium: A review”. In: *Cement and Concrete Composites* 114 (2020), p. 103729. ISSN: 0958-9465. DOI: https://doi.org/10.1016/j.cemconcomp.2020.103729. URL: https://www.sciencedirect.com/science/article/pii/S0958946520302353.

[22] Juho Yliniemi et al. “Utilization of Mineral Wools as Alkali-Activated Material Precursor”. In: *Materials* 9 (Apr. 2016), p. 312. DOI: 10.3390/ma9050312.

[23] John L. Provis et al. “X-ray microtomography shows pore structure and tortuosity in alkali-activated binders”. In: *Cement and Concrete Research* 42.6 (2012), pp. 855–864. ISSN: 0008-8846. DOI: https://doi.org/10.1016/j.cemconres.2012.03.004. URL: https://www.sciencedirect.com/science/article/pii/S0008884612000579.

[24] Andrzej Cwirzen. “Properties of SCC with industrial by-products as aggregates”. In: Jan. 2020, pp. 249–281. ISBN: 9780128173695. DOI: 10.1016/B978-0-12-817369-5.00010-6.

[25] İsa Yüksel. “Blast-furnace slag”. In: Jan. 2018, pp. 361–415. ISBN: 9780081021569. DOI: 10.1016/B978-0-08-102156-9.00012-2.

[26] John L Provis and Jan Stephanus Jakob Van Deventer. *Geopolymers: structures, processing, properties and industrial applications*. Elsevier, 2009.

[27] Fernández Jiménez and Ana María. “Cementos de escorias activadas alcalinamente: influencia de las variables y modelización del proceso”. 2000. URL: http://hdl.handle.net/10486/13323.

[28] Caijun Shi, Della Roy, and Pavel Krivenko. *Alkali-activated cements and concretes*. CRC press, 2003.

[29] I. Garcia-Lodeiro, A. Palomo, and A. Fernández-Jiménez. “3 - Crucial insights on the mix design of alkali-activated cement-based binders”. In: *Handbook of Alkali-Activated Cements, Mortars and Concretes*. Ed. by F. Pacheco-Torgal et al. Oxford: Woodhead Publishing, 2015, pp. 49–73. ISBN: 978-1-78242-276-1. DOI: https://doi.org/10.1533/9781782422884.1.49. URL: https://www.sciencedirect.com/science/article/pii/B9781782422761500034.

[30] Rizhao Steel Holding Group. *Product center*. URL: https://www.rizhaosteel.com/kf/344.htm.

[31] A. Fernández-Jiménez, J.G. Palomo, and F. Puertas. “Alkali-activated slag mortars: Mechanical strength behaviour”. In: *Cement and Concrete Research* 29.8 (1999), pp. 1313–1321. ISSN: 0008-8846. DOI: https://doi.org/10.1016/S0008-8846(99)00154-4. URL: https://www.sciencedirect.com/science/article/pii/S0008884699001544.

[32] Shao-Dong Wang, Karen L. Scrivener, and P.L. Pratt. “Factors affecting the strength of alkali-activated slag”. In: *Cement and Concrete Research* 24.6 (1994), pp. 1033–1043. ISSN: 0008-8846. DOI: https://doi.org/10.1016/0008-8846(94)90026-4. URL: https://www.sciencedirect.com/science/article/pii/0008884694900264.

[33] P. Wang, V. Rudert, and R. Trettin. “Effect of Fineness and Particle Size Distribution of Granulated Blast-Furnace Slag on the Hydraulic Reactivity in Cement Systems”. In: *Advances in Cement Research - ADV CEM RES* 17 (Jan. 2005), pp. 161–167. DOI: 10.1680/adcr.2005.17.4.161.

[34] Shao-Dong Wang et al. “Alkali-activated slag cement and concrete: a review of properties and problems”. In: *Advances in Cement Research* 7.27 (1995), pp. 93–102. DOI: 10.1680/adcr.1995.7.27.93. URL: https://doi.org/10.1680/adcr.1995.7.27.93.

[35] I. Garcia-Lodeiro, A. Palomo, and A. Fernández-Jiménez. “2 - An overview of the chemistry of alkali-activated cement-based binders”. In: *Handbook of Alkali-Activated Cements, Mortars and Concretes*. Ed. by F. Pacheco-Torgal et al. Oxford: Woodhead Publishing, 2015, pp. 19–47. ISBN: 978-1-78242-276-1. DOI: https://doi.org/10.1533/9781782422884.1.19. URL: https://www.sciencedirect.com/science/article/pii/B9781782422761500022.

[36] A. Allen, J. Thomas, and H. Jennings. “Composition and density of nanoscale calcium–silicate–hydrate in cement”. In: *Nature Materials* 6 (2007), pp. 311–316. DOI: 10.1038/nmat1871. URL: https://doi.org/10.1038/nmat1871.

[37] A. Palomo, M.W. Grutzeck, and M.T. Blanco. “Alkali-activated fly ashes: A cement for the future”. In: *Cement and Concrete Research* 29.8 (1999), pp. 1323–1329. ISSN: 0008-8846. DOI: https://doi.org/10.1016/S0008-8846(98)00243-9. URL: https://www.sciencedirect.com/science/article/pii/S0008884698002439.

[38] Glukhovsky V. “Ancient, modern and future concretes”. In: *First International Conference Alkaline Cements and Concretes, Kiev, Ukraine* (1994), pp. 1–8.

[39] Alibaba. URL: https://www.alibaba.com/product-detail/Fly-Ash_62021137075.html.

[40] A Fernández-Jiménez and A Palomo. “Characterisation of fly ashes. Potential reactivity as alkaline cements”. In: *Fuel* 82.18 (2003), pp. 2259–2265. ISSN: 0016-2361. DOI: https://doi.org/10.1016/S0016-2361(03)00194-7. URL: https://www.sciencedirect.com/science/article/pii/S0016236103001947.

[41] A. Fernández-Jiménez and A. Palomo. “Composition and microstructure of alkali activated fly ash binder: Effect of the activator”. In: *Cement and Concrete Research* 35.10 (2005), pp. 1984–1992. ISSN: 0008-8846. DOI: https://doi.org/10.1016/j.cemconres.2005.03.003. URL: https://www.sciencedirect.com/science/article/pii/S0008884605000864.

[42] Juho Yliniemi et al. “Utilization of Mineral Wools as Alkali-Activated Material Precursor”. In: *Materials* 9 (Apr. 2016), p. 312. DOI: 10.3390/ma9050312.

[43] “Woodhead Publishing Series in Energy”. In: *Materials for Energy Efficiency and Thermal Comfort in Buildings*. Ed. by Matthew R. Hall. Woodhead Publishing Series in Energy. Woodhead Publishing, 2010, pp. xix–xx. ISBN: 978-1-84569-526-2. DOI: https://doi.org/10.1016/B978-1-84569-526-2.50031-1. URL: https://www.sciencedirect.com/science/article/pii/B9781845695262500311.

[44] Wikipedia. URL: https://en.wikipedia.org/wiki/Glass_wool.

[45] Juho Yliniemi et al. “Influence of activator type on reaction kinetics, setting time, and compressive strength of alkali-activated mineral wools”. In: *Journal of Thermal Analysis and Calorimetry* 144 (Apr. 2020). DOI: 10.1007/s10973-020-09651-6.

[46] J. Yliniemi et al. “Nanostructural evolution of alkali-activated mineral wools”. In: *Cement and Concrete Composites* 106 (2020), p. 103472. ISSN: 0958-9465. DOI: https://doi.org/10.1016/j.cemconcomp.2019.103472. URL: https://www.sciencedirect.com/science/article/pii/S0958946519313150.

[47] Tuomas Kohvakka. *Glass wool as geopolymer raw material: Milling process waste with Mil-Tek IC60 screw mill*. 2020. URL: https://www.theseus.fi/handle/10024/354586.

[48] Zhenming Li et al. “Early-age properties of alkali-activated slag and glass wool paste”. In: *Construction and Building Materials* 291 (2021), p. 123326. ISSN: 0950-0618. DOI: https://doi.org/10.1016/j.conbuildmat.2021.123326. URL: https://www.sciencedirect.com/science/article/pii/S0950061821010862.

[49] Paul Awoyera and Adeyemi Adesina. “A critical review on application of alkali activated slag as a sustainable composite binder”. In: *Case Studies in Construction Materials* 11 (2019), e00268. ISSN: 2214-5095. DOI: https://doi.org/10.1016/j.cscm.2019.e00268. URL: https://www.sciencedirect.com/science/article/pii/S2214509519302098.

[50] Shabarish Patil, Veeresh Karikatti, and Manojkumar Chitawadagi. “Granulated Blast-Furnace Slag (GGBS) based Geopolymer concrete - Review Concrete - Review”. In: *International Journal of Advanced Science and Engineering* 5 (Aug. 2018), p. 879. DOI: 10.29294/IJASE.5.1.2018.789-885.

[51] Marija Nedeljković, Zhenming Li, and Guang Ye. “Setting, Strength, and Autogenous Shrinkage of Alkali-Activated Fly Ash and Slag Pastes: Effect of Slag Content”. In: *Materials* 11.11 (2018). ISSN: 1996-1944. URL: https://www.mdpi.com/1996-1944/11/11/2121.

[52] Smolcyk H.G. “Structure et characterisation des laitiers”. In: *7th International Congress of the Chemistry of Cement* 1 (1980), pp. 1–16.

[53] Shao-Dong Wang and Karen L. Scrivener. “Hydration products of alkali activated slag cement”. In: *Cement and Concrete Research* 25.3 (1995), pp. 561–571. ISSN: 0008-8846. DOI: https://doi.org/10.1016/0008-8846(95)00045-E. URL: https://www.sciencedirect.com/science/article/pii/000888469500045E.

[54] Da-Wang Zhang et al. “The study of the structure rebuilding and yield stress of 3D printing geopolymer pastes”. In: *Construction and Building Materials* 184 (Sept. 2018), pp. 575–580. DOI: 10.1016/j.conbuildmat.2018.06.233.

[55] Hui Zhong and Mingzhong Zhang. “3D printing geopolymers: A review”. In: *Cement and Concrete Composites* 128 (2022), p. 104455. ISSN: 0958-9465. DOI: https://doi.org/10.1016/j.cemconcomp.2022.104455. URL: https://www.sciencedirect.com/science/article/pii/S0958946522000506.

[56] Qaisar Munir, Riku Peltonen, and Timo Kärki. “Printing Parameter Requirements for 3D Printable Geopolymer Materials Prepared from Industrial Side Streams”. In: *Materials* 14 (Aug. 2021), p. 4758. DOI: 10.3390/ma14164758.

[57] Jacques Kruger, Stephan Zeranka, and Gideon van Zijl. “An ab initio approach for thixotropy characterisation of (nanoparticle-infused) 3D printable concrete”. In: *Construction and Building Materials* 224 (2019), pp. 372–386. ISSN: 0950-0618. DOI: https://doi.org/10.1016/j.conbuildmat.2019.07.078. URL: https://www.sciencedirect.com/science/article/pii/S0950061819317507.

[58] C. Leonelli and M. Romagnoli. “6 - Rheology parameters of alkali-activated geopolymeric concrete binders”. In: *Handbook of Alkali-Activated Cements, Mortars and Concretes*. Ed. by F. Pacheco-Torgal et al. Oxford: Woodhead Publishing, 2015, pp. 133–169. ISBN: 978-1-78242-276-1. DOI: https://doi.org/10.1533/9781782422884.2.133. URL: https://www.sciencedirect.com/science/article/pii/B978178242276150006X.

[59] Ian Morrison. “Dispersions”. In: *Kirk-Othmer Encyclopedia of Chemical Technology*. John Wiley & Sons, Ltd, 2003. ISBN: 9780471238966. DOI: https://doi.org/10.1002/0471238961.0409191613151818.a01. eprint: https://onlinelibrary.wiley.com/doi/pdf/10.1002/0471238961.0409191613151818.a01. URL: https://onlinelibrary.wiley.com/doi/abs/10.1002/0471238961.0409191613151818.a01.

[60] Mingxu Chen et al. “Rheological parameters, thixotropy and creep of 3D-printed calcium sulfoaluminate cement composites modified by bentonite”. In: *Composites Part B: Engineering* 186 (Apr. 2020), p. 107821. DOI: 10.1016/j.compositesb.2020.107821.

[61] Shravan Muthukrishnan, Sayanthan Ramakrishnan, and Jay Sanjayan. “Effect of alkali reactions on the rheology of one-part 3D printable geopolymer concrete”. In: *Cement and Concrete Composites* 116 (2021), p. 103899. ISSN: 0958-9465. DOI: https://doi.org/10.1016/j.cemconcomp.2020.103899. URL: https://www.sciencedirect.com/science/article/pii/S0958946520304030.

[62] Biranchi Panda, Cise Unluer, and Ming Jen Tan. “Extrusion and rheology characterization of geopolymer nanocomposites used in 3D printing”. In: *Composites Part B: Engineering* 176 (2019), p. 107290. ISSN: 1359-8368. DOI: https://doi.org/10.1016/j.compositesb.2019.107290. URL: https://www.sciencedirect.com/science/article/pii/S1359836819331579.

[63] Chenchen Sun et al. “3D extrusion free forming of geopolymer composites: Materials modification and processing optimization”. In: *Journal of Cleaner Production* 258 (Mar. 2020), p. 120986. DOI: 10.1016/j.jclepro.2020.120986.

[64] Ali Kazemian et al. “Construction-scale 3D printing: shape stability of fresh printing concrete”. In: *International Manufacturing Science and Engineering Conference*. Vol. 50732. American Society of Mechanical Engineers. 2017, V002T01A011.

[65] Guowei Ma, Zhijian Li, and Li Wang. “Printable properties of cementitious material containing copper tailings for extrusion based 3D printing”. In: *Construction and Building Materials* 162 (2018), pp. 613–627. ISSN: 0950-0618. DOI: https://doi.org/10.1016/j.conbuildmat.2017.12.051. URL: https://www.sciencedirect.com/science/article/pii/S0950061817324546.

[66] Zhanzhao Li et al. “Fresh and Hardened Properties of Extrusion-Based 3D-Printed Cementitious Materials: A Review”. In: *Sustainability* 12.14 (2020). ISSN: 2071-1050. DOI: 10.3390/su12145628. URL: https://www.mdpi.com/2071-1050/12/14/5628.

[67] Civil Digital. *What is an Admixture | Functions of Admixtures*. 2013. URL: https://civildigital.com/what-are-admixtures/.

[68] A. M. Pailere. “Application of admixtures in concrete”. In: *The International Union of Testing and Research Laboratories for Materials and Structures,* ().

[69] America’s Cement Manufacturers. *Chemical Admixtures*. URL: https://www.cement.org/cement-concrete/concrete-materials/chemical-admixtures.

[70] John Provis and Jannie Deventer. *Alkali Activated Materials: State-of-the-Art Report, RILEM TC 224-AAM*. Jan. 2014. ISBN: 978-94-007-7671-5. DOI: 10.1007/978-94-007-7672-2.

[71] engr.psu.edu. *Use of Water Reducers, Retarders, and Superplasticizers.* URL: https://www.engr.psu.edu/ce/courses/ce584/concrete/library/materials/Admixture/AdmixturesMain.htm#:.

[72] Shin Hau Bong et al. “Efficiency of Different Superplasticizers and Retarders on Properties of ‘One-Part’ Fly Ash-Slag Blended Geopolymers with Different Activators”. In: *Materials* 12 (Oct. 2019), p. 3410. DOI: 10.3390/ma12203410.

[73] Andri Kusbiantoro et al. “Development of Sucrose and Citric Acid as the Natural based Admixture for Fly Ash based Geopolymer”. In: *Procedia Environmental Sciences* 17 (Dec. 2013), 596–602. DOI: 10.1016/j.proenv.2013.02.075.

[74] Lateef N. Assi, Edward (Eddie) Deaver, and Paul Ziehl. “Using sucrose for improvement of initial and final setting times of silica fume-based activating solution of fly ash geopolymer concrete”. In: *Construction and Building Materials* 191 (2018), pp. 47–55. ISSN: 0950-0618. DOI: https://doi.org/10.1016/j.conbuildmat.2018.09.199. URL: https://www.sciencedirect.com/science/article/pii/S0950061818323869.

[75] A.R Brough et al. “Sodium silicate-based alkali-activated slag mortars: Part II. The retarding effect of additions of sodium chloride or malic acid”. In: *Cement and Concrete Research* 30 (Sept. 2000), pp. 1375–1379.

[76] Aaron R. Sakulich et al. “Mechanical and microstructural characterization of an alkali-activated slag/limestone fine aggregate concrete”. In: *Construction and Building Materials* 23.8 (2009), pp. 2951–2957. ISSN: 0950-0618. DOI: https://doi.org/10.1016/j.conbuildmat.2009.02.022. URL: https://www.sciencedirect.com/science/article/pii/S0950061809000622.

[77] Linglei Zhang et al. “Effect of retarders on the early hydration and mechanical properties of reactivated cementitious material”. In: *Construction and Building Materials* 212 (July 2019), pp. 192–201. DOI: 10.1016/j.conbuildmat.2019.03.323.

[78] Arnab Kumar Sinha and Sudip Talukdar. “Enhancement of the properties of silicate activated ultrafine-slag based geopolymer mortar using retarder”. In: *Construction and Building Materials* 313 (2021), p. 125380. ISSN: 0950-0618. DOI: https://doi.org/10.1016/j.conbuildmat.2021.125380. URL: https://www.sciencedirect.com/science/article/pii/S0950061821031214.

[79] Jixiang Wang et al. “Setting controlling of lithium slag-based geopolymer by activator and sodium tetraborate as a retarder and its effects on mortar properties”. In: *Cement and Concrete Composites* 110 (2020), p. 103598. ISSN: 0958-9465. DOI: https://doi.org/10.1016/j.cemconcomp.2020.103598. URL: https://www.sciencedirect.com/science/article/pii/S0958946520300901.

[80] Huajie Liu, Jay G. Sanjayan, and Yuhuan Bu. “The application of sodium hydroxide and anhydrous borax as composite activator of class F fly ash for extending setting time”. In: *Fuel* 206 (2017), pp. 534–540. ISSN: 0016-2361. DOI: https://doi.org/10.1016/j.fuel.2017.06.049. URL: https://www.sciencedirect.com/science/article/pii/S0016236117307573.

[81] M Lachemi et al. “Performance of new viscosity modifying admixtures in enhancing the rheological properties of cement paste”. In: *Cement and Concrete Research* 34.2 (2004), pp. 185–193. ISSN: 0008-8846. DOI: https://doi.org/10.1016/S0008-8846(03)00233-3. URL: https://www.sciencedirect.com/science/article/pii/S0008884603002333.

[82] M Palacios and RJ Flatt. “Working mechanism of viscosity-modifying admixtures”. In: *Science and Technology of Concrete Admixtures*. Elsevier, 2016, pp. 415–432.

[83] Stefan Chaves Figueiredo et al. “An approach to develop printable strain hardening cementitious composites”. In: *Materials & Design* 169 (2019), p. 107651. ISSN: 0264-1275. DOI: https://doi.org/10.1016/j.matdes.2019.107651. URL: https://www.sciencedirect.com/science/article/pii/S0264127519300887.

[84] Yu Chen et al. “The Effect of Viscosity-Modifying Admixture on the Extrudability of Limestone and Calcined Clay-Based Cementitious Material for Extrusion-Based 3D Concrete Printing”. In: *Materials* 12 (Apr. 2019), p. 1374. DOI: 10.3390/ma12091374.

[85] Zainab Aldin. *3D printing of geopolymer concrete*. 2019. URL: http://resolver.tudelft.nl/uuid:7862fc20-7b66-40ca-957a-7bca1ec20e54.

[86] Biranchi Panda and M.J. Tan. “Experimental study on mix proportion and fresh properties of fly ash based geopolymer for 3D concrete printing”. In: *Ceramics International* 44 (Mar. 2018). DOI: 10.1016/j.ceramint.2018.03.031.

[87] Shiho Kawashima et al. “Study of the mechanisms underlying the fresh-state response of cementitious materials modified with nanoclays”. In: *Construction and Building Materials* 36 (2012), pp. 749–757. ISSN: 0950-0618. DOI: https://doi.org/10.1016/j.conbuildmat.2012.06.057. URL: https://www.sciencedirect.com/science/article/pii/S0950061812004497.

[88] Stephen B. Johnson, Adrian S. Russell, and Peter J. Scales. “Volume fraction effects in shear rheology and electroacoustic studies of concentrated alumina and kaolin suspensions”. In: *Colloids and Surfaces A: Physicochemical and Engineering Aspects* 141.1 (1998), pp. 119–130. ISSN: 0927-7757. DOI: https://doi.org/10.1016/S0927-7757(98)00208-8. URL: https://www.sciencedirect.com/science/article/pii/S0927775798002088.

[89] Gautam Singhvi et al. “Xanthan gum in drug delivery applications”. In: *Natural Polysaccharides in Drug Delivery and Biomedical Applications* (2019).

[90] Abdelilah Aboulayt et al. “Stability of a new geopolymer grout: Rheological and mechanical performances of metakaolin-fly ash binary mixtures”. In: *Construction and Building Materials* 181 (2018), pp. 420–436. ISSN: 0950-0618. DOI: https://doi.org/10.1016/j.conbuildmat.2018.06.025. URL: https://www.sciencedirect.com/science/article/pii/S0950061818314156.

[91] Abdelilah Aboulayt et al. “Alkali-activated grouts based on slag-fly ash mixtures: From early-age characterization to long-term phase composition”. In: *Construction and Building Materials* 260 (2020), p. 120510. ISSN: 0950-0618. DOI: https://doi.org/10.1016/j.conbuildmat.2020.120510. URL: https://www.sciencedirect.com/science/article/pii/S0950061820325150.

[92] Limenglu Ma et al. “Evaluation of Self-degradability of Sodium Carboxymethyl Cellulose (CMC) in Alkali-activated Cementitious Materials for Geothermal Wells”. In: ().

[93] Shin Hau Bong et al. “Method of Optimisation for Ambient Temperature Cured Sustainable Geopolymers for 3D Printing Construction Applications”. In: *Materials* 12.6 (2019). URL: https://www.mdpi.com/1996-1944/12/6/902.

[94] Nicolas Ducoulombier et al. “The “Slugs-test” for extrusion-based additive manufacturing: Protocol, analysis and practical limits”. In: *Cement and Concrete Composites* 121 (2021), p. 104074. ISSN: 0958-9465. DOI: https://doi.org/10.1016/j.cemconcomp.2021.104074. URL: https://www.sciencedirect.com/science/article/pii/S0958946521001438.

[95] P. Coussot and F. Gaulard. “Gravity flow instability of viscoplastic materials: The ketchup drip”. In: *Phys. Rev. E* 72 (3 2005), p. 031409. DOI: 10.1103/PhysRevE.72.031409. URL: https://link.aps.org/doi/10.1103/PhysRevE.72.031409.

[96] A. Fernández-Jiménez and F. Puertas. “Effect of activator mix on the hydration and strength behaviour of alkali-activated slag cements”. In: *Advances in Cement Research* 15.3 (2003), pp. 129–136. DOI: 10.1680/adcr.2003.15.3.129. URL: https://doi.org/10.1680/adcr.2003.15.3.129.

[97] VD Glukhovsky, GS Rostovskaja, and GV Rumyna. “High strength slag-alkaline cements”. In: *Proceedings of the seventh international congress on the chemistry of cement*. Vol. 3. 1980, pp. 164–168.

[98] Mohamed G. Khalil et al. “Performance of geopolymer mortar cured under ambient temperature”. In: *Construction and Building Materials* 242 (2020), p. 118090. ISSN: 0950-0618. DOI: https://doi.org/10.1016/j.conbuildmat.2020.118090. URL: https://www.sciencedirect.com/science/article/pii/S0950061820300957.

A

Appendix A: Setting Time Results

For more exact results, the tables below show all the results of the setting time tests done.

A.1 Sucrose

Table A.1: Initial and final setting times of sucrose samples

Sample	Initial setting time (min)	Final setting time (min)	Average initial setting time (min)	Average final setting time (min)
S0.51	97	127	92.5	127.5
S0.52	88	128		
S0.751	115	165	114	159
S0.752	113	153		
S11	123	163	102	131.5
S12	101	141		
S13	103	122		
S1.51	107	137	103.5	133.5
S1.52	100	130		
S21	103	122	103	122
S22	-	-		
S31	96	122	96	122
S32	-	-		

Table A.2: Initial and final setting times of sucrose samples (sucrose added to dry mix)

Sample	Initial setting time (min)	Final setting time (min)
SD0.2	108	138
SD0.35	98	148
SD0.5	126	206
SD0.6	111	151
SD1.5	77	97

A.2 Sodium Chloride (NaCl)

Table A.3: Initial and final setting times of NaCl samples

Sample	Initial setting time (min)	Final setting time (min)	Average initial setting time (min)	Average final setting time (min)
N31	198	308	194	324
N32	190	340		
N41	244	444	244	429
N42	244	414		
N51	235	315	236.5	331.5
N52	238	348		
N61	245	375	245	375
N71	217	307	206	278.5
N72	195	250		
N81	241	401	241	401

Table A.4: Initial and final setting time of N4A0.75

Sample	Initial setting time (min)	Final setting time (min)	Average initial setting time (min)	Average final setting time (min)
N4A0.751	200	350	199.5	344.5
N4A0.752	199	339		

Table A.5: Initial and final setting time of N4X

Sample	Initial setting time (min)	Final setting time (min)	Average initial setting time (min)	Average final setting time (min)
N4X0.21	233	423	228	418
N4X0.22	223	413		
N4X0.41	170	230	174	239
N4X0.42	178	248		

Table A.6: Initial and final setting time of N4C0.5

Sample	Initial setting time (min)	Final setting time (min)	Average initial setting time (min)	Average final setting time (min)
N4C.51	250	430	238.5	398.5
N4C.52	227	367		

Table A.7: Initial and final setting time of N4CM1

Sample	Initial setting time (min)	Final setting time (min)	Average initial setting time (min)	Average final setting time (min)
N4CM11	248	428	240.5	410.5
N4CM12	233	393		

A.3 Sodium Borate (Borax)

Table A.8: Initial and final setting time of B2A0.75

Sample	Initial setting time (min)	Final setting time (min)	Average initial setting time (min)	Average final setting time (min)
B2A0.751	306	456	305.5	438
B2A0.752	305	420		

Table A.9: Initial and final setting time of B2X0.2

Sample	Initial setting time (min)	Final setting time (min)	Average initial setting time (min)	Average final setting time (min)
B2X0.21	271	401	275.5	390.5
B2X0.22	280	380		

Table A.10: Initial and final setting time of B2C0.5

Sample	Initial setting time (min)	Final setting time (min)	Average initial setting time (min)	Average final setting time (min)
B2C0.51	230	340	224.5	334.5
B2C0.52	219	329		

Table A.11: Initial and final setting time of B2C0.25

Sample	Initial setting time (min)	Final setting time (min)	Average initial setting time (min)	Average final setting time (min)
B2C0.251	277	397	271.5	391.5
B2C0.252	266	386		

Table A.12: Initial and final setting time of B2CM1

Sample	Initial setting time (min)	Final setting time (min)	Average initial setting time (min)	Average final setting time (min)
B2CM11	320	>450	325.5	>450
B2CM12	331	>450		

B

Appendix B: Flowability Test Results

For more exact results, the tables below show all the results of the flowability tests done.

B.1 Reference Sample

Ref [1]			
Begin	**Time**	**Height (mm)**	**Spread (mm)**
9:49	9:59	52	155.9
		52	159.1
		53	159.8
		51	155
AVG		**52**	**157.45**
	10:09	52	156.3
		52	158.6
		53	157.6
		53	153.5
AVG		**52.5**	**156.5**
	10:19	53	146.3
		53	146.1
		52	153.1
		54	145
AVG		**53**	**147.625**
	10:29	55	126.5
		55	125.4
		55	124.1
		57	126.4
AVG		**55.5**	**125.6**

(a) Reference sample slump test (1)

Ref [2]			
Begin	**Time**	**Height (mm)**	**Spread (mm)**
11:49	11:59	50	167.7
		52	164.8
		52	167.4
		51	167.3
AVG		**51.25**	**166.8**
	12:09	52	158.1
		52	163.3
		53	160.9
		51	162.1
AVG		**52**	**161.1**
	12:19	54	148.6
		55	151.4
		53	150.1
		55	153.2
AVG		**54.25**	**150.825**
	12:29	55	138.1
		56	142.6
		56	142.2
		55	141.3
AVG		**55.5**	**141.05**

(b) Reference sample slump test (2)

Ref [Average]			
Begin	**Time (min)**	**Height (mm)**	**Spread (mm)**
0:00	10.00	51.625	162.125
	20.00	52.25	158.8
	30.00	53.625	149.225
	40.00	55.5	133.325

(c) Reference sample slump test [Average]

Figure B.1: Reference Sample Slump Test

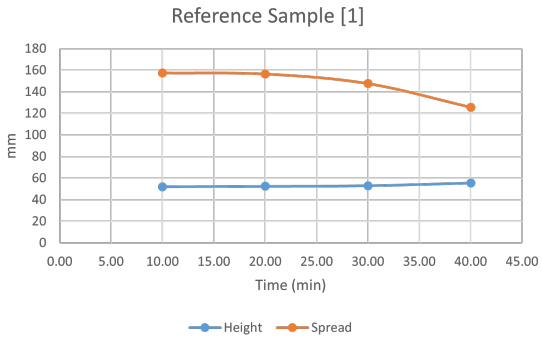

(a) Reference sample slump test (1)

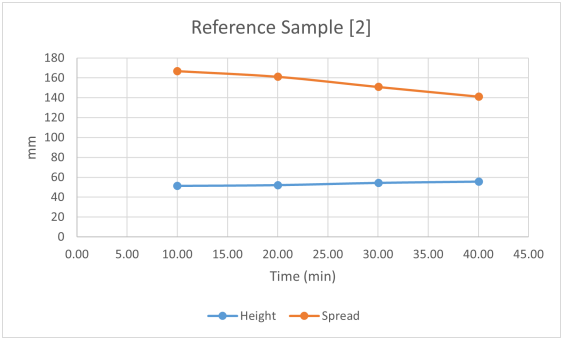

(b) Reference sample slump test (2)

B.2 Sodium Chloride (NaCl)

NaCl 3%			
Begin	**Time**	**Height (mm)**	**Spread (mm)**
10:48	10:59	40	186.4
		38	187.5
		36	186.2
		35	186.4
	AVG	**37.25**	**186.625**
	11:19	40	175.1
		39	176.4
		39	176.5
		38	177.1
	AVG	**39**	**176.275**
	11:39	45	155.2
		46	156.8
		46	158.1
		46	156.5
	AVG	**45.75**	**156.65**
	11:59	53	110.1
		52	111.7
		50	113.4
		52	114.1
	AVG	**51.75**	**112.325**

(a) NaCl 3% slump test (1)

NaCl 3%			
Begin	**Time**	**Height (mm)**	**Spread (mm)**
1:34	1:44	35	190.7
		35	195
		35	198.5
		36	195.3
	AVG	**35.25**	**194.875**
	2:04	44	173.1
		43	172.7
		44	169.9
		42	170.5
	AVG	**43.25**	**171.55**
	2:24	53	118.2
		53	116.4
		55	115.9
		56	116.5
	AVG	**54.25**	**116.75**
	2:44	60	0
		60	0
		60	0
		60	0
	AVG	**60**	**0**

(b) NaCl 3% slump test (2)

NaCl 3%			
Begin	**Time**	**Height (mm)**	**Spread (mm)**
1:35	1:45	32	201.4
		33	202.8
		34	201.9
		33	204.5
	AVG	**33**	**202.65**
	1:55	39	193.6
		39	193.8
		39	192.2
		38	194.2
	AVG	**38.75**	**193.45**
	2:05	43	176.1
		45	178.2
		44	179.5
		42	176.4
	AVG	**43.5**	**177.55**
	2:15	49	158.1
		49	161.2
		48	160.6
		48	158.1
	AVG	**48.5**	**159.5**
	2:25	53	116.2
		54	115.2
		53	115.4
		54	116.7
	AVG	**53.5**	**115.875**
	2:35	59	0
		60	0
		59	0
		59	0
	AVG	**59.25**	**0**

(c) NaCl 3% slump test (3)

NaCl 3%			
Begin	**Time (min)**	**Height (mm)**	**Spread (mm)**
0:00	10.00	35.17	190.75
	30.00	41.92	173.91
	50.00	51.16	136.70
	70.00	59.63	0

(d) NaCl 3% slump test [Average]

Figure B.3: NaCl 3% Slump Test

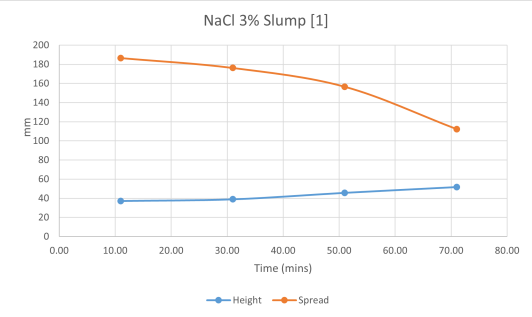

(a) NaCl 3% slump test (1)

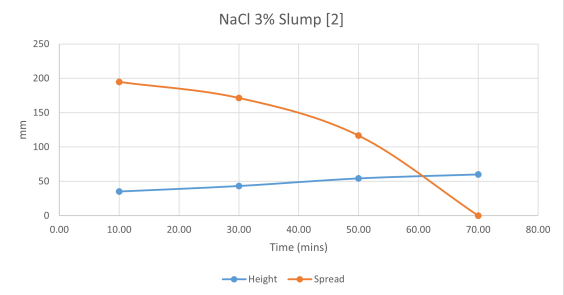

(b) NaCl 3% slump test (2)

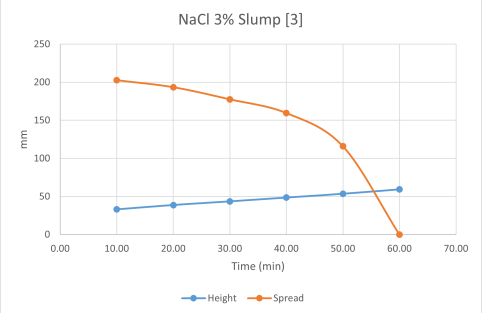

(c) NaCl 3% slump test (3)

NaCl 4%			
Begin	**Time**	**Height (mm)**	**Spread (mm)**
1:30	1:41	34	196.7
		32	198.3
		33	199.5
		33	199.7
	AVG	**33**	**198.55**
	2:01	39	182.2
		39	182.3
		40	185.9
		40	183.2
	AVG	**39.5**	**183.4**
	2:21	50	151.1
		49	154.3
		48	153.6
		48	150.9
	AVG	**48.75**	**152.475**
	2:41	55	118.2
		56	119.3
		56	118.6
		57	117.8
	AVG	**56**	**118.475**

(a) NaCl 4% slump test (1)

NaCl 4%			
Begin	**Time**	**Height (mm)**	**Spread (mm)**
2:13	2:23	33	186.3
		34	186.4
		35	187.5
		34	187.1
	AVG	**34**	**186.825**
	2:33	38	184.8
		39	185.9
		37	185.5
		40	186.5
	AVG	**38.5**	**185.675**
	2:43	40	180
		40	182.5
		37	185.3
		38	182.8
	AVG	**38.75**	**182.65**
	2:53	44	172.6
		44	174.1
		42	175.1
		41	172.1
	AVG	**42.75**	**173.475**
	3:03	49	159.8
		48	158.4
		47	159.9
		47	158.8
	AVG	**47.75**	**159.225**
	3:13	52	141.1
		52	142.5
		52	144.2
		53	145.3
	AVG	**52.25**	**143.275**
	3:23	54	123.2
		53	125.4
		50	125.6
		54	123.1
	AVG	**52.75**	**124.325**
	3:33	58	0
		57	0
		56	0
		58	0
	AVG	**57.25**	**0**

(b) NaCl 4% slump test (2)

NaCl 4%			
Begin	**Time (min)**	**Height (mm)**	**Spread (mm)**
0:00	10.00	33.5	192.69
	30.00	39.13	183.023
	50.00	48.25	155.85
	70.00	55.25	121.4

(c) NaCl 4% slump test [Average]

Figure B.5: NaCl 4% Slump Test

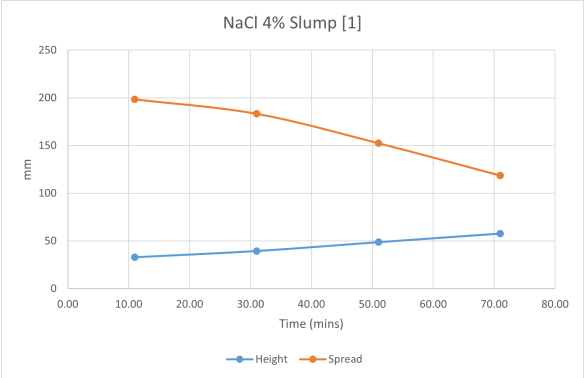

(a) NaCl 4% slump test (1)

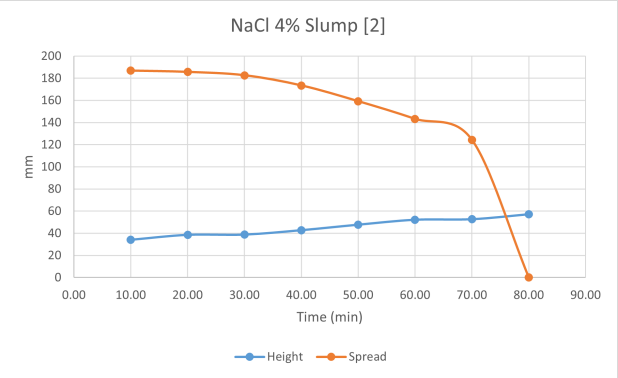

(b) NaCl 4% slump test (2)

NaCl 4% + A0.75% [1]			
Begin	**Time (min)**	**Height (mm)**	**Spread (mm)**
2:06	2:16	50.00	164.30
		50.00	165.40
		50.00	163.50
		49.00	164.10
	AVG	**49.75**	**164.33**
	2:36	50.00	162.40
		50.00	163.40
		51.00	163.10
		51.00	162.50
	AVG	**50.50**	**162.85**
	2:56	50.00	151.30
		50.00	153.40
		51.00	152.50
		50.00	153.70
	AVG	**50.25**	**152.73**
	3:16	55.00	113.50
		56.00	112.30
		57.00	113.40
		56.00	114.20
	AVG	**56.00**	**113.35**

(a) N4A0.75 slump test (1)

NaCl 4% + A 0.75% [2]			
Begin	**Time**	**Height (mm)**	**Spread (mm)**
2:37	2:47	50.00	169.40
		50.00	169.50
		50.00	168.50
		49.00	168.40
	AVG	**49.75**	**168.95**
	2:57	50.00	169.30
		50.00	169.40
		49.00	170.50
		48.00	169.70
	AVG	**49.25**	**169.73**
	3:07	50.00	166.00
		49.00	159.90
		49.00	163.80
		48.00	165.50
	AVG	**49.00**	**163.80**
	3:17	52.00	158.80
		51.00	157.20
		51.00	156.70
		50.00	155.20
	AVG	**51.00**	**156.98**
	3:27	53.00	140.20
		52.00	140.30
		52.00	139.80
		51.00	140.50
	AVG	**52.00**	**140.20**
	3:37	54.00	126.80
		54.00	125.70
		54.00	124.30
		54.00	125.40
	AVG	**54.00**	**125.55**
	3:47	58.00	0.00
		57.00	0.00
		59.00	0.00
		59.00	0.00
	AVG	**58.25**	**0.00**

(b) N4A0.75 slump test (2)

NaCl 4% + A0.75% [Average]			
Begin	**Time (min)**	**Height (mm)**	**Spread (mm)**
0.00	10.00	49.75	166.64
	30.00	49.75	163.33
	50.00	51.13	146.47
	70.00	57.13	113.35

(c) N4A0.75 slump test [Average]

Figure B.7: N4A0.75 Slump Test

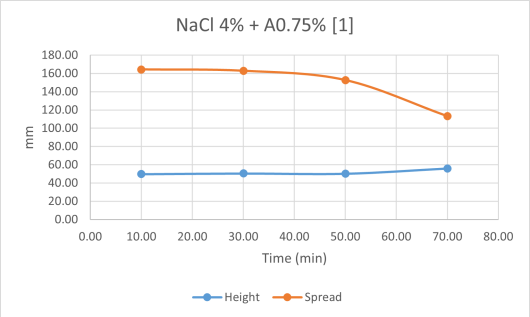

(a) N4A0.75 slump test (1)

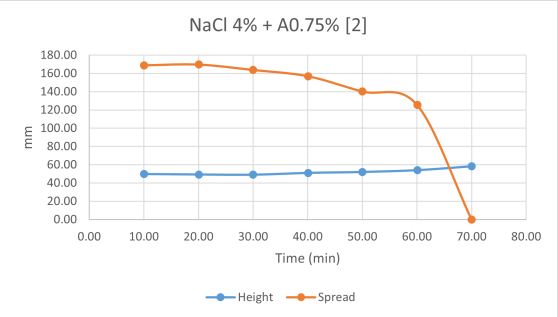

(b) N4A0.75 slump test (2)

NaCl 4% + XG 0.2% [1]			
Begin	**Time**	**Height (mm)**	**Spread (mm)**
2:21	2:31	50.00	139.90
		50.00	138.00
		50.00	139.50
		48.00	138.60
AVG		**49.50**	**139.00**
	2:51	50.00	131.10
		50.00	134.70
		51.00	134.60
		52.00	136.80
AVG		**50.75**	**134.30**
	3:11	55.00	111.10
		56.00	112.40
		57.00	110.60
		57.00	109.70
AVG		**56.25**	**110.95**
	3:31	59.00	0.00
		60.00	0.00
		60.00	0.00
		60.00	0.00
AVG		**59.75**	**0.00**

(a) N4X0.2 slump test (1)

NaCl 4% + XG 0.2% [2]			
Begin	**Time**	**Height (mm)**	**Spread (mm)**
1:58	2:08	48.00	142.60
		48.00	142.30
		46.00	142.50
		46.00	145.30
AVG		**47.00**	**143.18**
	2:18	52.00	138.50
		52.00	140.30
		51.00	136.30
		51.00	139.00
AVG		**51.50**	**138.53**
	2:28	51.00	130.50
		51.00	132.20
		52.00	128.20
		53.00	129.70
AVG		**51.75**	**130.15**
	2:38	52.00	133.20
		53.00	129.30
		53.00	128.40
		53.00	127.60
AVG		**52.75**	**129.63**
	2:48	55.00	122.10
		55.00	120.50
		54.00	120.30
		53.00	120.80
AVG		**54.25**	**120.93**
	2:58	57.00	112.50
		57.00	113.20
		56.00	110.50
		56.00	113.00
AVG		**56.50**	**112.30**
	3:08	59.00	0.00
		59.00	0.00
		60.00	0.00
		60.00	0.00
AVG		**59.50**	**0.00**

(b) N4X0.2 slump test (2)

NaCl 4% + XG 0.2% [Average]			
Begin	**Time (min)**	**Height (mm)**	**Spread (mm)**
0.00	10.00	48.25	141.09
	30.00	51.25	132.23
	50.00	55.25	115.94
	70.00	59.63	0.00

(c) N4X0.2 slump test [Average]

Figure B.9: N4X0.2 Slump Test

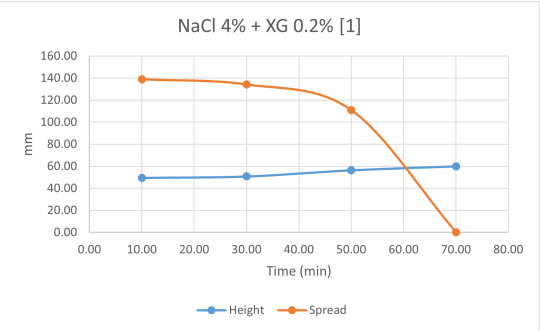

(a) N4X0.2 slump test (1)

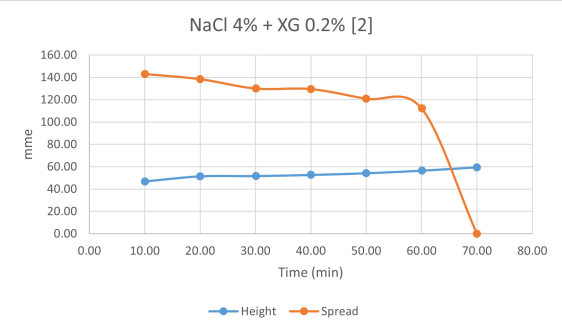

(b) N4X0.2 slump test (2)

NaCl 4% + CMS 0.5% [1]			
Begin	**Time**	**Height (mm)**	**Spread (mm)**
1:51	2:01	47	164.9
		47	161.5
		48	163.7
		46	163.6
AVG		**47**	**163.425**
	2:21	53	143.4
		53	143.2
		52	142.4
		52	140.2
AVG		**52.5**	**142.3**
	2:41	54	120.3
		54	120.2
		54	120.6
		53	126.4
AVG		**53.75**	**121.875**
	3:01	59	0
		59	0
		60	0
		60	0
AVG		**59.5**	**0**

(a) N4C0.5 slump test (1)

NaCl 4% + CMS 0.5% [2]			
Begin	**Time**	**Height (mm)**	**Spread (mm)**
2:59	3:09	48.00	156.10
		49.00	152.90
		50.00	153.40
		50.00	155.30
AVG		**49.25**	**154.43**
	3:19	50.00	148.90
		52.00	146.10
		51.00	146.60
		51.00	145.90
AVG		**51.00**	**146.88**
	3:29	53.00	138.90
		53.00	138.70
		53.00	140.10
		52.00	139.90
AVG		**52.75**	**139.40**
	3:39	55.00	134.70
		54.00	133.00
		55.00	132.60
		54.00	131.50
AVG		**54.50**	**132.95**
	3:49	55.00	129.30
		57.00	127.10
		56.00	127.60
		57.00	128.40
AVG		**56.25**	**128.10**
	3:59	55.00	127.70
		57.00	128.40
		58.00	127.30
		57.00	128.50
AVG		**56.75**	**127.98**
	4:09	58.00	117.50
		57.00	115.10
		57.00	116.30
		58.00	116.90
AVG		**57.50**	**116.45**

(b) N4C0.5 slump test (2)

NaCl 4% + CMS 0.5% [Average]			
Begin	**Time (min)**	**Height (mm)**	**Spread (mm)**
0.00	10.00	48.13	158.91
	30.00	52.63	140.85
	50.00	55.00	125.00
	70.00	58.50	116.45

(c) N4C0.5 slump test [Average]

Figure B.11: N4C0.5 Slump Test

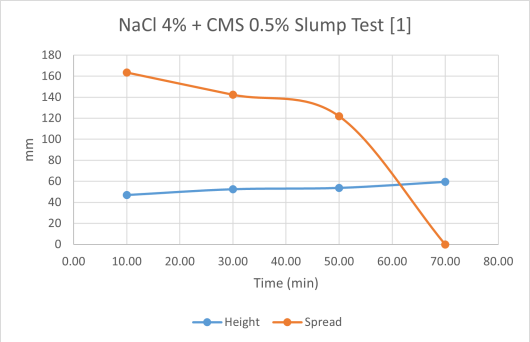

(a) N4C0.5 slump test (1)

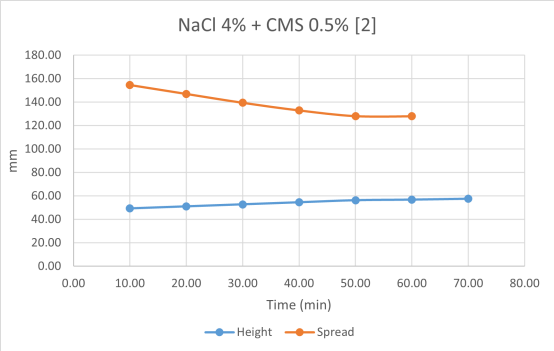

(b) N4C0.5 slump test (2)

NaCl 4% + CM 1% [1]			
Begin	**Time**	**Height (mm)**	**Spread (mm)**
1:14	1:24	40.00	162.30
		42.00	161.10
		38.00	165.90
		39.00	165.20
	AVG	**39.75**	**163.63**
	1:44	50.00	150.90
		48.00	152.60
		51.00	152.70
		51.00	153.40
	AVG	**50.00**	**152.40**
	2:04	53.00	141.30
		52.00	139.50
		52.00	138.70
		52.00	137.30
	AVG	**52.25**	**139.20**
	2:24	59.00	0.00
		59.00	0.00
		58.00	0.00
		57.00	0.00
	AVG	**58.25**	**0.00**

(a) N4CM1 slump test (1)

NaCl 4% + CM 1% [2]			
Begin	**Time**	**Height (mm)**	**Spread (mm)**
2:51	3:01	42.00	165.20
		41.00	163.40
		39.00	164.10
		44.00	161.40
	AVG	**41.50**	**163.53**
	3:11	46.00	154.00
		47.00	155.10
		48.00	152.50
		48.00	156.20
	AVG	**47.25**	**154.45**
	3:21	49.00	150.90
		49.00	147.20
		50.00	149.30
		50.00	149.70
	AVG	**49.50**	**149.28**
	3:31	52.00	150.10
		51.00	149.70
		46.00	148.10
		50.00	148.30
	AVG	**49.75**	**149.05**
	3:41	51.00	146.50
		50.00	146.10
		53.00	145.80
		50.00	145.40
	AVG	**51.00**	**145.95**
	3:51	50.00	136.50
		51.00	135.10
		54.00	133.90
		51.00	137.40
	AVG	**51.50**	**135.73**
	4:01	55.00	125.20
		54.00	122.90
		53.00	123.70
		55.00	122.30
	AVG	**54.25**	**123.53**
	4:11	58.00	0.00
		60.00	0.00
		60.00	0.00
		59.00	0.00
	AVG	**59.25**	**0.00**

(b) N4CM1 slump test (2)

NaCl 4% + A0.75% [Average]			
Begin	**Time (min)**	**Height (mm)**	**Spread (mm)**
0.00	10.00	40.63	163.58
	30.00	49.75	150.84
	50.00	51.63	142.58
	70.00	54.25	123.53
	80.00	59.25	0.00

(c) N4CM1 slump test [Average]

Figure B.13: N4CM1 Slump Test

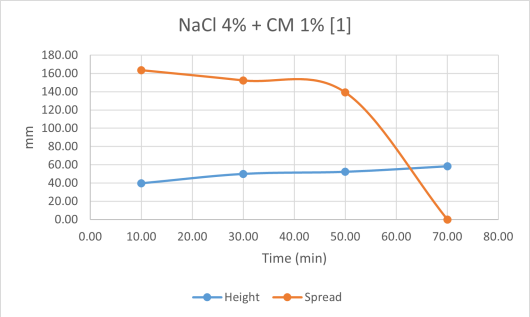

(a) N4CM1 slump test (1)

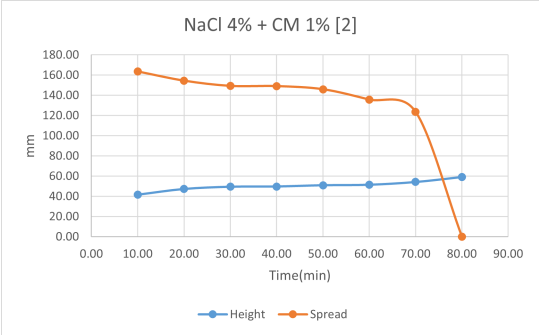

(b) N4CM1 slump test (2)

B.3 Sodium Borate (Borax)

Borax 1.5% [1]			
Begin	**Time**	**Height (mm)**	**Spread (mm)**
2:27	2:37	50	164.8
		49	166.4
		49	168.5
		46	164.9
	AVG	**48.5**	**166.15**
	2:57	50	162.5
		49	160.2
		48	161.4
		47	163.9
	AVG	**48.5**	**162**
	3:17	50	152.2
		50	150.1
		51	150.9
		52	149.6
	AVG	**50.75**	**150.7**
	3:37	55	126.2
		54	124.5
		52	130.3
		52	123.3
	AVG	**53.25**	**126.075**
	3:57	58	0
		59	0
		58	0
		57	0
	AVG	**58**	**0**

(a) Borax 1.5% slump test (1)

Borax 1.5% [2]			
Begin	**Time**	**Height (mm)**	**Spread (mm)**
1:32	1:42	43	172.3
		45	174.1
		46	172.1
		47	173.8
	AVG	**45.25**	**173.075**
	1:52	47	170.5
		46	170.7
		45	168.3
		45	169.6
	AVG	**45.75**	**169.775**
	2:02	47	172.1
		47	171
		45	170.4
		46	171.1
	AVG	**46.25**	**171.15**
	2:12	47	169.5
		47	168.5
		46	165.8
		48	168.4
	AVG	**47**	**168.05**
	2:22	49	162.2
		48	159.1
		47	162.4
		48	162.8
	AVG	**48**	**161.625**
	2:32	50	151.1
		50	148.7
		51	150.1
		49	150.9
	AVG	**50**	**150.2**
	2:42	54	140.3
		54	136.2
		55	138.3
		53	139.4
	AVG	**54**	**138.55**
	2:52	57	118.9
		56	117.3
		56	118.6
		56	116.3
	AVG	**56.25**	**117.775**
	3:02	58	0
		59	0
		60	0
		60	0
	AVG	**59.25**	**0**

(b) Borax 1.5% slump test (2)

Borax 1.5% [Average]			
Begin	**Time (min)**	**Height (mm)**	**Spread (mm)**
0:00	10.00	46.875	169.6125
	30.00	47.375	166.575
	50.00	49.375	156.1625
	70.00	53.625	132.3125
	90.00	58.625	0

(c) Borax 1.5% slump test [Average]

Figure B.15: Borax 1.5% Slump Test

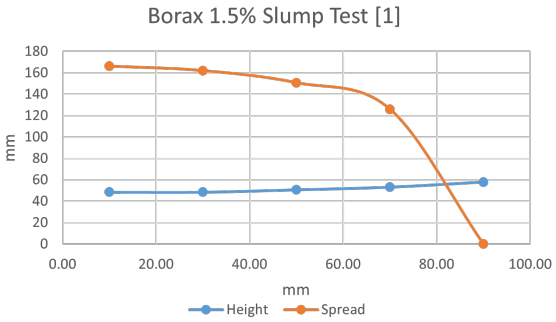

(a) Borax 1.5% slump test (1)

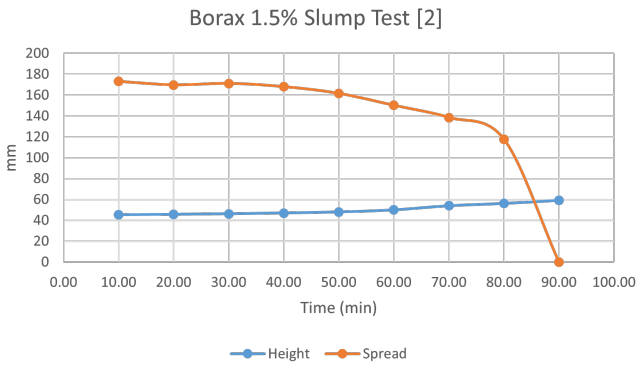

(b) Borax 1.5% slump test (2)

Borax 2% [1]			
Begin	**Time**	**Height (mm)**	**Spread (mm)**
11:44		37	186.8
	11:54	37	187.7
		39	190.1
		40	188.3
AVG		**38.25**	**188.225**
		40	179.2
	12:14	40	182.4
		42	178.2
		43	178.6
49		**41.25**	**179.6**
		45	169.1
	12:34	45	172.7
		45	168.8
		43	169.1
AVG		**44.5**	**169.925**
		50	152.5
	12:54	50	149.1
		50	149.2
		51	148.5
AVG		**50.25**	**149.825**
		55	122.2
	1:14	55	123.6
		55	120.7
		54	121.9
AVG		**54.75**	**122.1**
		58	0
	1:34	59	0
		59	0
		60	0
AVG		**59**	**0**

(a) Borax 2% slump test (1)

Borax 2% [2]			
Begin	**Time**	**Height (mm)**	**Spread (mm)**
10:17		38	190.2
	10:27	38	189.3
		39	188.6
		39	189.9
AVG		**38.5**	**189.5**
		39	189.6
	10:37	38	187.9
		40	188.1
		39	186.8
AVG		**39**	**188.1**
		40	181.8
	10:47	41	183.2
		41	179.8
		43	181.6
AVG		**41.25**	**181.6**
		42	175.9
	10:57	42	174.6
		44	178.6
		43	176.3
AVG		**42.75**	**176.35**
		46	167.8
	11:07	45	168.9
		45	166.2
		44	165.9
AVG		**45**	**167.2**
		47	160.8
	11:17	48	160.1
		48	159.3
		47	161.5
AVG		**47.5**	**160.425**
		52	150.6
	11:27	51	147.8
		51	151.1
		50	149.3
AVG		**51**	**149.7**
		53	131.2
	11:37	54	132.8
		54	130.6
		55	131.5
AVG		**54**	**131.525**
		56	120.3
	11:47	55	124.6
		57	122.7
		56	122.9
AVG		**56**	**122.625**
		59	112.8
	11:57	58	112.4
		58	111.9
		58	113.3
AVG		**58.25**	**112.6**
		60	0
	12:07	60	0
		59	0
		60	0
AVG		**59.75**	**0**

(b) Borax 2% slump test (2)

Borax 2% [Average]			
Begin	**Time (min)**	**Height (mm)**	**Spread (mm)**
0:00	10.00	38.375	188.865
	30.00	41.25	180.6
	50.00	44.75	168.565
	70.00	50.625	149.765
	90.00	55.375	122.365
	110.00	59.375	0

(c) Borax 2% slump test [Average]

Figure B.17: Borax 2% Slump Test

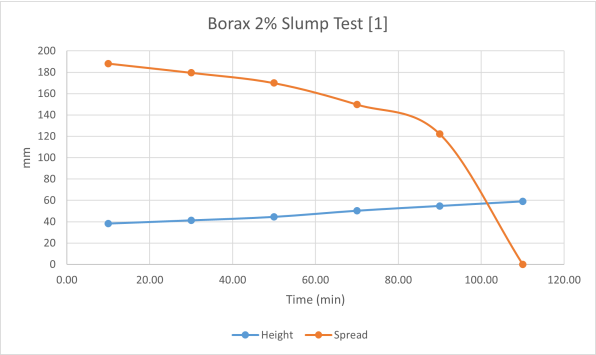

(a) Borax 2% slump test (1)

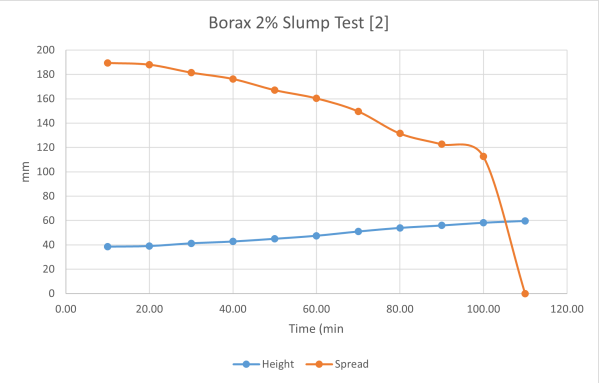

(b) Borax 2% slump test (2)

Borax 3% [1]			
Begin	Time	Height (mm)	Spread (mm)
1:35	1:45	37	185.6
		38	186.1
		35	184.8
		36	185.1
AVG		36.5	185.4
	2:05	40	181.7
		42	180.6
		38	182.3
		39	181.2
49		39.75	181.45
	2:25	41	174.2
		42	171.3
		39	172.8
		40	171.4
AVG		40.5	172.425
	2:45	44	156.3
		46	157.8
		46	156.4
		43	158.1
AVG		44.75	157.15
	3:05	55	146.5
		55	145.8
		55	149.1
		54	147.4
AVG		54.75	147.2
	3:25	55	130.2
		54	129.8
		56	127.6
		55	128.3
AVG		55	128.975
	3:45	59	0
		60	0
		59	0
		59	0
AVG		59.25	0

(a) Borax 3% slump test (1)

Borax 3% [2]			
Begin	Time	Height (mm)	Spread (mm)
1:49	1:59	36	181.8
		35	186.1
		39	183.5
		40	183.6
AVG		37.5	183.75
	2:09	42	181.3
		39	181.8
		38	183.1
		40	182.4
AVG		39.75	182.15
	2:19	41	182.7
		40	182.4
		40	182.2
		39	181.5
AVG		40	182.2
	2:29	40	176.5
		40	176.9
		40	178.1
		43	179.5
AVG		40.75	177.75
	2:39	41	173
		42	172.7
		39	172.8
		38	173.5
AVG		40	173
	2:49	43	166.9
		41	166.66
		40	166.1
		38	167.1
AVG		40.5	166.69
	2:59	45	158.7
		45	160.1
		45	156.5
		45	160.4
AVG		45	158.925
	3:09	50	149.5
		50	151.7
		50	149.6
		50	151.5
AVG		50	150.575
	3:19	54	146.3
		54	143.8
		55	144.4
		53	146.5
AVG		54	145.25
	3:29	54	136.5
		54	138.4
		55	134.7
		53	137.4
AVG		54	136.75
	3:39	55	128.5
		55	128.2
		55	127.1
		55	127.2
AVG		55	127.75
	3:49	56	116.1
		56	118.3
		55	115.9
		55	118.1
AVG		55.5	117.1
	3:59	59	0
		58	0
		59	0
		60	0
AVG		59	0

(b) Borax 3% slump test (2)

Borax 3% (Average)			
Begin	Time	Height	Spread
0:00	10.00	37.00	184.58
	30.00	39.88	181.83
	50.00	40.25	172.72
	70.00	44.88	158.04
	90.00	54.38	146.23
	110	55.00	128.37
	130	59.13	0.00

(c) Borax 3% slump test [Average]

Figure B.19: Borax 3% Slump Test

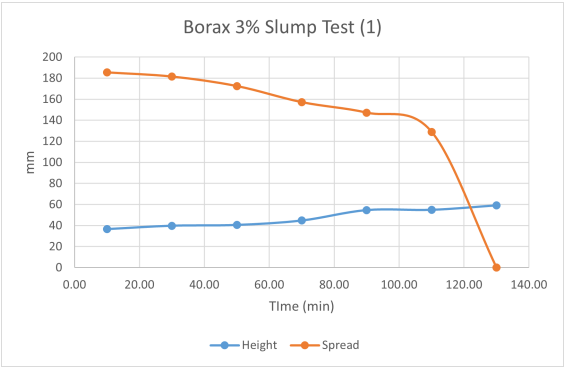

(a) Borax 3% slump test (1)

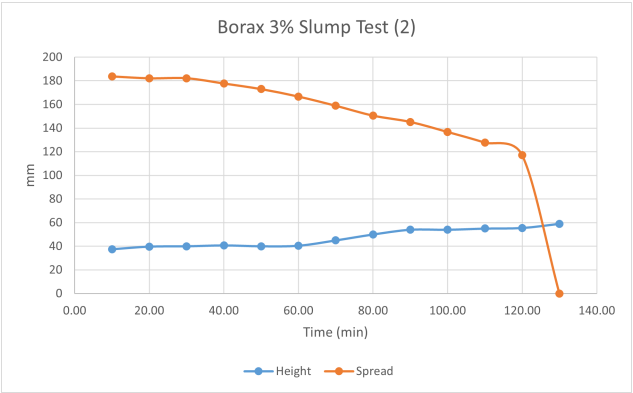

(b) Borax 3% slump test (2)

Borax 3% + A0.75% [1]			
Begin	Time	Height (mm)	Spread (mm)
8:40	8:50	48	163.8
		46	162.7
		47	165.1
		47	162.2
AVG		47	163.45
	9:10	47	159.6
		49	158.4
		49	158.7
		46	157.6
49		47.75	158.575
	9:30	50	154.6
		49	155.8
		49	154.7
		51	152.3
AVG		49.75	154.35
	9:50	50	142.3
		52	140.8
		48	141.6
		50	142.9
AVG		50	141.9
	10:10	55	120.8
		55	122.7
		55	122.4
		54	121.6
AVG		54.75	121.875
	10:30	59	0
		60	0
		58	0
		58	0
AVG		58.75	0

(a) B3A0.75 slump test (1)

Borax 3% + A0.75% [2]			
Begin	Time	Height (mm)	Spread (mm)
11:29	11:39	49	161.1
		48	161.5
		50	160.5
		50	159.1
AVG		49.25	160.55
	11:49	49	158.3
		49	157.9
		50	157.2
		50	156.7
AVG		49.5	157.525
	11:59	46	156.3
		48	157.1
		51	157.2
		50	156.4
AVG		48.75	156.75
	12:09	50	155.2
		50	158.4
		49	156.7
		48	157.1
AVG		49.25	156.85
	12:19	50	152.7
		50	153.1
		52	151.1
		49	152.6
AVG		50.25	152.375
	12:29	51	148.1
		51	145.2
		50	147.3
		50	143.6
AVG		50.5	146.05
	12:39	51	141.5
		51	141.1
		50	140.2
		50	142.5
AVG		50.5	141.325
	12:49	53	131.6
		53	131.2
		52	134.4
		51	131.8
AVG		52.25	132.25
	12:59	56	120.6
		55	120
		55	123.4
		55	123.2
AVG		55.25	121.8
	1:09	56	113.7
		57	115.8
		56	116.7
		56	116.1
AVG		56.25	115.575
	1:19	59	0
		58	0
		59	0
		59	0
AVG		58.75	0

(b) B3A0.75 slump test (2)

Borax 3% + A0.75% (Average)			
Begin	Time	Height (mm)	Spread (mm)
0:00	10.00	48.13	162.00
	30.00	48.25	157.67
	50.00	50.00	153.37
	70.00	50.25	141.62
	90.00	55.00	121.84
	110	58.75	0.00

(c) B3A0.75 slump test [Average]

Figure B.21: B3A0.75 Slump Test

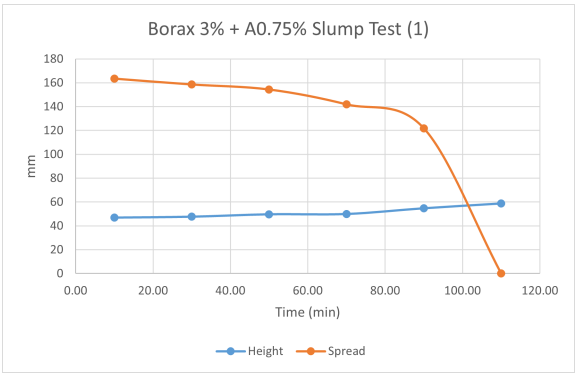

(a) B3A0.75 slump test (1)

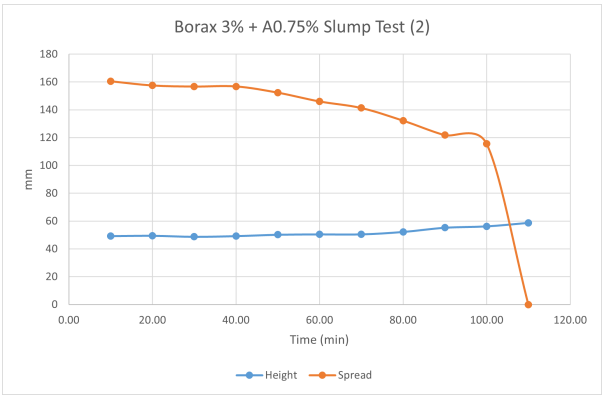

(b) B3A0.75 slump test (2)

B3lbA0.5 Slump			
Begin	**Time**	**Height (mm)**	**Spread (mm)**
2:31	2:41	39	189.2
		39	189.5
		39	188.9
		40	189.1
	AVG	**39.25**	**189.175**
	2:51	39	192.6
		39	188.5
		40	191.2
		40	186.4
	AVG	**39.5**	**189.675**
	3:01	40	186.7
		40	185.6
		39	184.4
		40	188.2
	AVG	**39.75**	**186.225**
	3:11	43	180.4
		42	186.7
		40	184.5
		40	183.2
	AVG	**41.25**	**183.7**
	3:21	43	181.9
		43	182.4
		41	184.3
		41	181.1
	AVG	**42**	**182.425**
	3:31	44	181.1
		45	178.4
		42	179.7
		42	179.5
	AVG	**43.25**	**179.675**
	3:41	44	172.2
		44	171.7
		43	172.3
		45	174.5
	AVG	**44**	**172.675**
	3:51	45	160.4
		45	160.7
		44	162.1
		43	161.6
	AVG	**44.25**	**161.2**
	4:01	48	159.4
		49	160.7
		47	158.9
		49	162.3
	AVG	**48.25**	**160.325**
	4:11	50	154.3
		51	157.6
		50	155.2
		49	155.8
	AVG	**50**	**155.725**
	4:21	51	149.3
		52	152.3
		52	151.2
		52	149.9
	AVG	**51.75**	**150.675**
	4:31	53	143.6
		51	145.3
		53	144.7
		52	146.1
	AVG	**52.25**	**144.925**
	4:41	54	141.1
		52	140.9
		52	139.8
		54	139.5
	AVG	**53**	**140.325**
	4:51	54	132.8
		56	131.7
		55	130.9
		54	133.3
	AVG	**54.75**	**132.175**
	5:01	56	125.6
		54	127.3
		56	124.9
		57	122.5
	AVG	**55.75**	**125.075**
	5:11	58	0
		58	0
		59	0
		60	0
	AVG	**58.75**	**0**

Figure B.23: B3lbA0.5 slump test

Borax 3% + XG 0.2% [1]			
Begin	**Time**	**Height (mm)**	**Spread (mm)**
9:45	9:55	44	176.2
		43	177.6
		44	178.5
		42	176.3
AVG		**43.25**	**177.15**
	10:15	47	167.5
		46	168.4
		46	166.7
		48	169.1
49		**46.75**	**167.925**
	10:35	49	154.6
		49	155.9
		50	153.5
		48	155.8
AVG		**49**	**154.95**
	10:55	55	140.6
		54	138.5
		54	137.9
		53	138.7
AVG		**54**	**138.925**
	11:15	57	111.6
		55	115.8
		56	114.3
		55	114.1
AVG		**55.75**	**113.95**

(a) B3X0.2 slump test (1)

Borax 3% + XG 0.2%[2]			
Begin	**Time**	**Height (mm)**	**Spread (mm)**
1:10	1:20	44	178.5
		42	178.8
		42	178.9
		41	179.5
AVG		**42.25**	**178.925**
	1:30	43	173.5
		43	177.5
		44	177.8
		46	178.1
AVG		**44**	**176.725**
	1:40	47	168.3
		47	172.7
		46	172.1
		45	168.8
AVG		**46.25**	**170.475**
	1:50	47	166.4
		47	164.9
		47	164.5
		48	165.5
AVG		**47.25**	**165.325**
	2:00	48	156.2
		48	159.9
		49	157.7
		49	159.4
AVG		**48.5**	**158.3**
	2:10	51	150.1
		51	149.4
		50	150.5
		50	148.5
AVG		**50.5**	**149.625**
	2:20	54	138.5
		54	137.2
		54	137.8
		53	143.4
AVG		**53.75**	**139.225**
	2:30	55	121.2
		56	122.5
		56	124.2
		56	124.6
AVG		**55.75**	**123.125**
	2:40	56	114.3
		57	116.1
		57	112.2
		55	111.5
AVG		**56.25**	**113.525**
	2:50	58	0
		59	0
		60	0
		60	0
AVG		**59.25**	**0**

(b) B3X0.2 slump test (2)

Borax 3% + XG 0.2% (Average)			
Begin	**Time (min)**	**Height (mm)**	**Spread (mm)**
0:00	10.00	42.875	178.04
	30.00	46.5	169.205
	50.00	48.75	156.625
	70.00	53.875	139.08
	90.00	56	113.74
	100	59.25	0

(c) B3X0.2 slump test [Average]

Figure B.24: B3X0.2 Slump Test

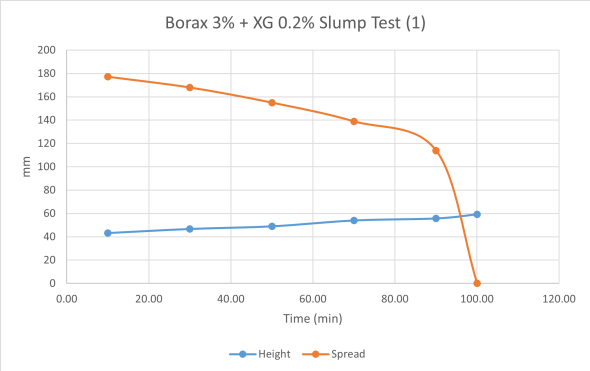

(a) B3X0.2 slump test (1)

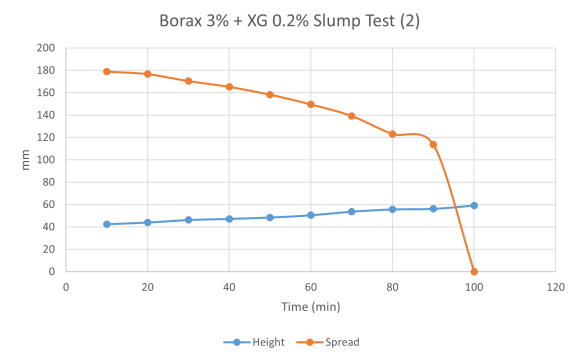

(b) B3X0.2 slump test (2)

Borax 3% + CMS 0.25% [1]			
Begin	Time	Height (mm)	Spread (mm)
10:26		45	167.2
	10:36	43	166.8
		42	166.9
		43	165.3
AVG		43.25	166.55
		42	169.2
	10:56	45	167.3
		43	166.8
		44	166.4
49		43.5	167.425
		48	162.5
	11:16	47	163.9
		47	161.7
		46	161.6
AVG		47	162.425
		55	139.6
	11:36	52	138.7
		52	138.5
		51	140
AVG		52.5	139.2
		55	125.1
	11:56	55	122.9
		55	124.5
		54	124.2
AVG		54.75	124.175
		60	0
	12:16	60	0
		59	0
		59	0
AVG		59.5	0

(a) B3C0.25 slump test (1)

Borax 3% + CMS 0.25%[2]			
Begin	Time	Height (mm)	Spread (mm)
1:22		44	168.3
	1:32	45	168.7
		42	170.1
		41	168.4
AVG		43	168.875
		41	173.4
	1:42	42	177.6
		43	172.7
		42	174.5
AVG		42	174.55
		44	169.2
	1:52	44	169.7
		43	167.8
		42	170.9
AVG		43.25	169.4
		45	163.3
	2:02	45	164
		45	164.6
		42	164.9
AVG		44.25	164.2
		47	157.9
	2:12	47	160.5
		46	158.5
		45	163.9
AVG		46.25	160.2
		50	149.3
	2:22	50	149.6
		50	151.4
		49	150.5
AVG		49.75	150.2
		54	137.7
	2:32	53	140.5
		52	142.2
		52	141.7
AVG		52.75	140.525
		55	129.8
	2:42	55	130.1
		54	129.5
		55	130.2
AVG		54.75	129.9
		55	123.5
	2:52	55	121.1
		55	120.1
		55	125.4
AVG		55	122.525
		57	110.4
	3:02	58	111.6
		57	112.1
		56	113.5
AVG		57	111.9
		59	0
	3:12	60	0
		60	0
		58	0
AVG		59.25	0

(b) B3C0.25 slump test (2)

Borax 3% + CMS 0.25% (Average)			
Begin	Time (min)	Height (mm)	Spread (mm)
0:00	10.00	43	167.715
	30.00	43.375	168.415
	50.00	46.625	161.315
	70.00	52.625	139.865
	90.00	54.875	123.355
	110	59.25	0

(c) B3C0.25 slump test [Average]

Figure B.26: B3C0.25 Slump Test

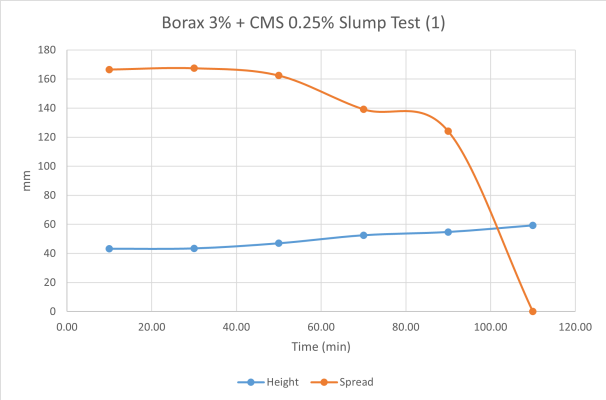

(a) B3C0.25 slump test (1)

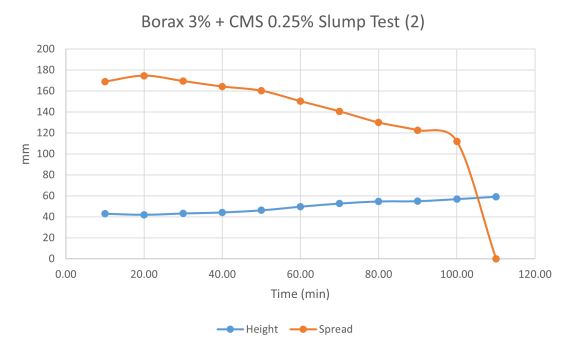

(b) B3C0.25 slump test (2)

Borax 3% + CM1% [1]			
Begin	**Time**	**Height (mm)**	**Spread (mm)**
10:41	10:51	41	174.6
		40	173.2
		42	171.8
		40	173.7
AVG		**40.75**	**173.325**
	11:11	42	168.2
		42	168.9
		43	167.4
		43	166.7
49		**42.5**	**167.8**
	11:31	47	155.2
		46	156.6
		48	155.1
		48	154.5
AVG		**47.25**	**155.35**
	11:51	51	142.3
		51	141.8
		51	145.7
		53	145.1
AVG		**51.5**	**143.725**
	12:11	55	128.2
		55	129.7
		55	127.3
		54	125.9
AVG		**54.75**	**127.775**
	12:31	59	0
		60	0
		59	0
		58	0
AVG		**59**	**0**

(a) B3CM1 slump test (1)

Borax 3% + CM1% [2]			
Begin	**Time**	**Height (mm)**	**Spread (mm)**
11:40	11:50	41	170.9
		42	171.6
		42	172.8
		43	171.2
AVG		**42**	**171.625**
	12:00	42	169.1
		42	168.8
		43	166.9
		43	168.2
AVG		**42.5**	**168.25**
	12:10	43	166.2
		44	167.1
		44	168.5
		44	166.5
AVG		**43.75**	**167.075**
	12:20	45	161.2
		44	160.3
		44	159.7
		46	159.6
AVG		**44.75**	**160.2**
	12:30	49	153.2
		47	152.1
		49	154.5
		48	153.6
AVG		**48.25**	**153.35**
	12:40	51	146.3
		51	145.8
		49	142.3
		49	148.6
AVG		**50**	**145.75**
	12:50	52	139.8
		53	142.2
		53	138.2
		51	137.6
AVG		**52.25**	**139.45**
	1:00	53	130.9
		53	131.8
		54	129.7
		55	129.4
AVG		**53.75**	**130.45**
	1:10	56	125.4
		55	124.6
		55	127.3
		57	126.2
AVG		**55.75**	**125.875**
	1:20	58	114.8
		57	113.6
		56	116.8
		56	114.5
AVG		**56.75**	**114.925**
	1:30	59	0
		60	0
		60	0
		59	0
AVG		**59.5**	**0**

(b) B3CM1 slump test (2)

Borax 3% + CMC 1% (Average)			
Begin	**Time (min)**	**Height (mm)**	**Spread (mm)**
0:00	10.00	41.375	172.48
	30.00	43.125	167.44
	50.00	47.75	154.35
	70.00	51.875	141.59
	90.00	55.25	126.83
	110	59.25	0

(c) B3CM1 slump test [Average]

Figure B.28: B3CM1 Slump Test

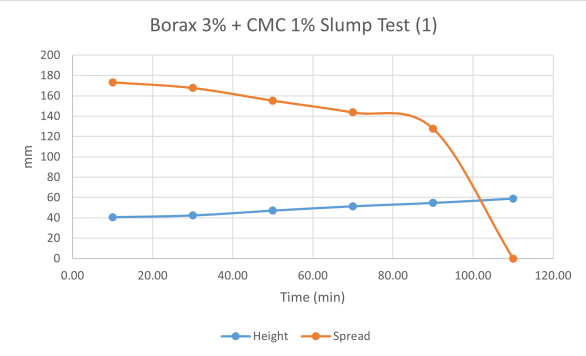

(a) B3CM1 slump test (1)

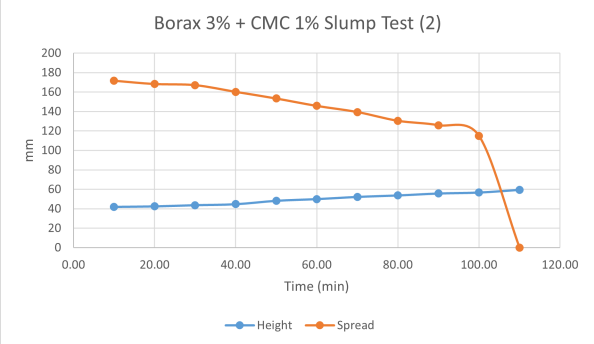

(b) B3CM1 slump test (2)

C

Appendix C: Slug Test Results

For more exact results, the tables below show all the results of the slug tests done.

C.1 Reference Sample

Ref			
Begin	**Time**	**Parameters**	**Value**
11:38	11:48	Slugs	30.00
		Ls	0.05
		V	0.000085
		m	0.180
		S	0.000176
		g	9.81
		Density	2117.65
		Yield Stress (Pa)	587.70
	11:58	Slugs	30.00
		Ls	0.07
		V	0.000095
		m	0.211
		S	0.000176
		g	9.81
		Density	2221.05
		Yield Stress (Pa)	880.57
	12:08	Slugs	25.00
		Ls	0.08
		V	0.00010
		m	0.196
		S	0.000176
		g	9.81
		Density	2063.16
		Yield Stress (Pa)	949.43

(a) Ref slug test

RA0.75 Slug Test			
Begin	**Time**	**Parameters**	**Value**
11:38	11:48	Slugs	23.00
		Ls	0.10
		V	0.000130
		m	0.279
		S	0.000176
		g	9.81
		Density	2143.15
		Yield Stress (Pa)	1213.84
	11:58	Slugs	10.00
		Ls	0.11
		V	0.000055
		m	0.128
		S	0.000176
		g	9.81
		Density	2329.82
		Yield Stress (Pa)	1385.54

(b) RefA0.75 slug test

C.2 Sodium Chloride (NaCl)

N4 Slug Test			
Begin	**Time**	**Parameters**	**Value**
12:13		Slugs	30.00
		Ls	0.08
		V	0.000160
	12:23	m	0.285
		S	0.000176
		g	9.81
		Density	1781.25
		Yield Stress (Pa)	764.72
		Slugs	30.00
		Ls	0.09
		V	0.000150
	12:33	m	0.273
		S	0.000176
		g	9.81
		Density	1822.20
		Yield Stress (Pa)	952.59
		Slugs	30.00
		Ls	0.10
		V	0.00018
	12:43	m	0.335
		S	0.000176
		g	9.81
		Density	1912.51
		Yield Stress (Pa)	1099.46
		Slugs	30.00
		Ls	0.13
		V	0.00018
	12:53	m	0.359
		S	0.000176
		g	9.81
		Density	1993.39
		Yield Stress (Pa)	1411.27

(a) N4 slug test

N4A0.75 Slug Test			
Begin	**Time**	**Parameters**	**Value**
2:30		Slugs	30.00
		Ls	0.10
		V	0.000110
	2:40	m	0.303
		S	0.000176
		g	9.81
		Density	2750.36
		Yield Stress (Pa)	1588.91
		Slugs	30.00
		Ls	0.11
		V	0.000130
	2:50	m	0.327
		S	0.000176
		g	9.81
		Density	2513.85
		Yield Stress (Pa)	1580.41
		Slugs	30.00
		Ls	0.12
		V	0.00017
	3:00	m	0.369
		S	0.000176
		g	9.81
		Density	2234.73
		Yield Stress (Pa)	1544.16
		Slugs	24.00
		Ls	0.13
		V	0.00019
	3:10	m	0.393
		S	0.000176
		g	9.81
		Density	2126.11
		Yield Stress (Pa)	1597.96

(b) N4A0.75 slug test

N4X0.2 Slug Test			
Begin	**Time**	**Parameters**	**Value**
2:07		Slugs	30.00
		Ls	0.12
		V	0.000150
	2:17	m	0.322
		S	0.000176
		g	9.81
		Density	2149.20
		Yield Stress (Pa)	1460.72
		Slugs	30.00
		Ls	0.12
		V	0.000180
	2:27	m	0.403
		S	0.000176
		g	9.81
		Density	2236.78
		Yield Stress (Pa)	1482.24
		Slugs	30.00
		Ls	0.13
		V	0.00019
	2:37	m	0.420
		S	0.000176
		g	9.81
		Density	2210.53
		Yield Stress (Pa)	1565.00

(c) N4X0.2 slug test

N4C0.5 Slug Test			
Begin	**Time**	**Parameters**	**Value**
11:48		Slugs	30.00
		Ls	0.11
		V	0.000165
	11:58	m	0.355
		S	0.000176
		g	9.81
		Density	2152.48
		Yield Stress (Pa)	1292.27
		Slugs	30.00
		Ls	0.12
		V	0.000185
	12:08	m	0.388
		S	0.000176
		g	9.81
		Density	2095.19
		Yield Stress (Pa)	1392.36
		Slugs	30.00
		Ls	0.12
		V	0.00020
	12:18	m	0.412
		S	0.000176
		g	9.81
		Density	2112.51
		Yield Stress (Pa)	1475.67
		Slugs	30.00
		Ls	0.13
		V	0.00021
	12:28	m	0.420
		S	0.000176
		g	9.81
		Density	2050.15
		Yield Stress (Pa)	1532.74
		Slugs	27.00
		Ls	0.14
		V	0.00022
	12:38	m	0.446
		S	0.000176
		g	9.81
		Density	2073.81
		Yield Stress (Pa)	1585.67

(d) N4C0.5 slug test

N4CM1 Slug Test			
Begin	**Time**	**Parameters**	**Value**
11:43		Slugs	30.00
		Ls	0.11
		V	0.000200
	11:53	m	0.366
		S	0.000176
		g	9.81
		Density	1832.10
		Yield Stress (Pa)	1110.30
		Slugs	30.00
		Ls	0.12
		V	0.000175
	12:03	m	0.357
		S	0.000176
		g	9.81
		Density	2042.74
		Yield Stress (Pa)	1384.51
		Slugs	28.00
		Ls	0.13
		V	0.00020
	12:13	m	0.394
		S	0.000176
		g	9.81
		Density	1970.75
		Yield Stress (Pa)	1432.45
		Slugs	30.00
		Ls	0.14
		V	0.00022
	12:23	m	0.441
		S	0.000176
		g	9.81
		Density	2002.45
		Yield Stress (Pa)	1553.79
		Slugs	28.00
		Ls	0.14
		V	0.00024
	12:33	m	0.475
		S	0.000176
		g	9.81
		Density	1977.17
		Yield Stress (Pa)	1590.16

(e) N4CM1 slug test

C.3 Sodium Borate (Borax)

B3 Slug Test			
Begin	**Time**	**Parameters**	**Value**
2:05		Slugs	30.00
		Ls	0.09
		V	0.000140
	2:15	m	0.277
		S	0.000176
		g	9.81
		Density	1975.57
		Yield Stress (Pa)	1044.33
		Slugs	30.00
		Ls	0.10
		V	0.000155
	2:25	m	0.312
		S	0.000176
		g	9.81
		Density	2014.45
		Yield Stress (Pa)	1137.18
		Slugs	30.00
		Ls	0.10
		V	0.00015
	2:35	m	0.298
		S	0.000176
		g	9.81
		Density	2058.00
		Yield Stress (Pa)	1220.05
		Slugs	30.00
		Ls	0.11
		V	0.00014
	2:45	m	0.292
		S	0.000176
		g	9.81
		Density	2085.36
		Yield Stress (Pa)	1290.95
		Slugs	30.00
		Ls	0.12
		V	0.00014
	2:55	m	0.284
		S	0.000176
		g	9.81
		Density	2026.14
		Yield Stress (Pa)	1319.70
		Slugs	25.00
		Ls	0.11
		V	0.00011
	3:05	m	0.235
		S	0.000176
		g	9.81
		Density	2237.90
		Yield Stress (Pa)	1377.02

(a) B3 slug test

B3lb Slug Test			
Begin	**Time**	**Parameters**	**Value**
12:40		Slugs	30.00
		Ls	0.10
		V	0.000130
	12:58	m	0.266
		S	0.000176
		g	9.81
		Density	2047.08
		Yield Stress (Pa)	1179.13
		Slugs	30.00
		Ls	0.13
		V	0.000155
	1:10	m	0.341
		S	0.000176
		g	9.81
		Density	2200.06
		Yield Stress (Pa)	1566.31
		Slugs	30.00
		Ls	0.13
		V	0.00017
	1:20	m	0.367
		S	0.000176
		g	9.81
		Density	2157.12
		Yield Stress (Pa)	1620.85
		Slugs	30.00
		Ls	0.14
		V	0.00020
	1:30	m	0.433
		S	0.000176
		g	9.81
		Density	2165.75
		Yield Stress (Pa)	1733.65
		Slugs	23.00
		Ls	0.16
		V	0.00019
	1:40	m	0.403
		S	0.000176
		g	9.81
		Density	2177.14
		Yield Stress (Pa)	1916.03
		Slugs	21.00
		Ls	0.16
		V	0.00019
	1:50	m	0.404
		S	0.000176
		g	9.81
		Density	2184.00
		Yield Stress (Pa)	1979.16

(b) B3lb slug test

B3A0.5 Slug Test			
Begin	**Time**	**Parameters**	**Value**
12:00		Slugs	30.00
		Ls	0.09
		V	0.000130
		m	0.274
	12:10	S	0.000176
		g	9.81
		Density	2107.00
		Yield Stress (Pa)	1103.86
		Slugs	30.00
		Ls	0.09
		V	0.000140
		m	0.286
	12:20	S	0.000176
		g	9.81
		Density	2041.29
		Yield Stress (Pa)	1087.50
		Slugs	21.00
		Ls	0.09
		V	0.00011
		m	0.238
	12:30	S	0.000176
		g	9.81
		Density	2264.57
		Yield Stress (Pa)	1170.38
		Slugs	29.00
		Ls	0.09
		V	0.00012
		m	0.236
	12:40	S	0.000176
		g	9.81
		Density	2052.61
		Yield Stress (Pa)	1024.50
		Slugs	25.00
		Ls	0.09
		V	0.00012
		m	0.234
	12:50	S	0.000176
		g	9.81
		Density	2032.52
		Yield Stress (Pa)	996.49
		Slugs	20.00
		Ls	0.09
		V	0.00009
		m	0.181
	1:00	S	0.000176
		g	9.81
		Density	2123.88
		Yield Stress (Pa)	1037.52
		Slugs	18.00
		Ls	0.08
		V	0.00008
		m	0.170
	1:10	S	0.000176
		g	9.81
		Density	2266.67
		Yield Stress (Pa)	1078.39

(a) B3A0.5 slug test

B3lbA0.5 Slug Test			
Begin	**Time**	**Parameters**	**Value**
2:28		Slugs	30.00
		Ls	0.11
		V	0.000170
		m	0.357
	2:38	S	0.000176
		g	9.81
		Density	2101.53
		Yield Stress (Pa)	1360.87
		Slugs	30.00
		Ls	0.12
		V	0.000175
		m	0.363
	2:48	S	0.000176
		g	9.81
		Density	2073.14
		Yield Stress (Pa)	1362.06
		Slugs	30.00
		Ls	0.13
		V	0.00019
		m	0.377
	2:58	S	0.000176
		g	9.81
		Density	2037.35
		Yield Stress (Pa)	1469.32
		Slugs	30.00
		Ls	0.14
		V	0.00020
		m	0.396
	3:08	S	0.000176
		g	9.81
		Density	2028.26
		Yield Stress (Pa)	1558.49
		Slugs	30.00
		Ls	0.14
		V	0.00020
		m	0.411
	3:18	S	0.000176
		g	9.81
		Density	2056.25
		Yield Stress (Pa)	1622.70
		Slugs	30.00
		Ls	0.14
		V	0.00023
		m	0.458
	3:28	S	0.000176
		g	9.81
		Density	2036.09
		Yield Stress (Pa)	1664.45
		Slugs	30.00
		Ls	0.15
		V	0.00023
		m	0.466
	3:38	S	0.000176
		g	9.81
		Density	2027.30
		Yield Stress (Pa)	1737.65
		Slugs	30.00
		Ls	0.16
		V	0.00025
		m	0.517
	3:48	S	0.000176
		g	9.81
		Density	2067.96
		Yield Stress (Pa)	1874.00
		Slugs	30.00
		Ls	0.17
		V	0.00024
		m	0.493
	3:58	S	0.000176
		g	9.81
		Density	2053.67
		Yield Stress (Pa)	1942.47
		Slugs	27.00
		Ls	0.17
		V	0.00024
		m	0.496
	4:28	S	0.000176
		g	9.81
		Density	2066.25
		Yield Stress (Pa)	1977.78

(b) B3lbA0.5 slug test

B3C0.25 Slug Test			
Begin	**Time**	**Parameters**	**Value**
12:08		Slugs	30.00
		Ls	0.11
		V	0.000170
	12:18	m	0.361
		S	0.000176
		g	9.81
		Density	2121.88
		Yield Stress (Pa)	1271.90
		Slugs	30.00
		Ls	0.12
		V	0.000165
	12:28	m	0.338
		S	0.000176
		g	9.81
		Density	2046.79
		Yield Stress (Pa)	1337.29
		Slugs	30.00
		Ls	0.13
		V	0.00019
	12:38	m	0.381
		S	0.000176
		g	9.81
		Density	2004.05
		Yield Stress (Pa)	1443.14
		Slugs	30.00
		Ls	0.13
		V	0.00018
	12:48	m	0.356
		S	0.000176
		g	9.81
		Density	2032.46
		Yield Stress (Pa)	1484.98

(a) B3C0.25 slug test

B3lbC0.25 Slug Test			
Begin	**Time**	**Parameters**	**Value**
12:21		Slugs	30.00
		Ls	0.11
		V	0.000150
	12:31	m	0.304
		S	0.000176
		g	9.81
		Density	2024.73
		Yield Stress (Pa)	1242.33
		Slugs	30.00
		Ls	0.12
		V	0.000160
	12:41	m	0.346
		S	0.000176
		g	9.81
		Density	2163.63
		Yield Stress (Pa)	1466.44
		Slugs	30.00
		Ls	0.12
		V	0.00018
	12:51	m	0.388
		S	0.000176
		g	9.81
		Density	2158.17
		Yield Stress (Pa)	1507.56
		Slugs	30.00
		Ls	0.13
		V	0.00019
	1:01	m	0.400
		S	0.000176
		g	9.81
		Density	2103.42
		Yield Stress (Pa)	1568.59
		Slugs	30.00
		Ls	0.14
		V	0.00022
	1:11	m	0.467
		S	0.000176
		g	9.81
		Density	2170.60
		Yield Stress (Pa)	1741.63
		Slugs	30.00
		Ls	0.15
		V	0.00024
	1:21	m	0.519
		S	0.000176
		g	9.81
		Density	2208.60
		Yield Stress (Pa)	1888.87

(b) B3lbC0.25 slug test

B3CM0.75 Slug Test			
Begin	**Time**	**Parameters**	**Value**
2:42	2:52	Slugs	30.00
		Ls	0.11
		V	0.000090
		m	0.190
		S	0.000176
		g	9.81
		Density	2111.11
		Yield Stress (Pa)	1365.08
	3:02	Slugs	30.00
		Ls	0.11
		V	0.000095
		m	0.202
		S	0.000176
		g	9.81
		Density	2126.53
		Yield Stress (Pa)	1375.05
	3:12	Slugs	30.00
		Ls	0.12
		V	0.00010
		m	0.201
		S	0.000176
		g	9.81
		Density	2115.79
		Yield Stress (Pa)	1378.09

(a) B3CM0.75 slug test

B3lbCM0.75 Slug Test			
Begin	**Time**	**Parameters**	**Value**
11:40	11:50	Slugs	30.00
		Ls	0.12
		V	0.000155
		m	0.330
		S	0.000176
		g	9.81
		Density	2127.16
		Yield Stress (Pa)	1417.63
	12:00	Slugs	30.00
		Ls	0.13
		V	0.000170
		m	0.365
		S	0.000176
		g	9.81
		Density	2145.47
		Yield Stress (Pa)	1531.09
	12:10	Slugs	30.00
		Ls	0.13
		V	0.00019
		m	0.391
		S	0.000176
		g	9.81
		Density	2111.08
		Yield Stress (Pa)	1548.40
	12:20	Slugs	30.00
		Ls	0.14
		V	0.000190
		m	0.408
		S	0.000176
		g	9.81
		Density	2145.26
		Yield Stress (Pa)	1660.55
	12:30	Slugs	30.00
		Ls	0.14
		V	0.000210
		m	0.456
		S	0.000176
		g	9.81
		Density	2171.14
		Yield Stress (Pa)	1733.87
	12:40	Slugs	28.00
		Ls	0.15
		V	0.00021
		m	0.446
		S	0.000176
		g	9.81
		Density	2125.86
		Yield Stress (Pa)	1781.99
	12:50	Slugs	29.00
		Ls	0.16
		V	0.000245
		m	0.518
		S	0.000176
		g	9.81
		Density	2113.43
		Yield Stress (Pa)	1951.12
	1:00	Slugs	30.00
		Ls	0.17
		V	0.000280
		m	0.585
		S	0.000176
		g	9.81
		Density	2089.46
		Yield Stress (Pa)	1982.25
	1:10	Slugs	30.00
		Ls	0.14
		V	0.00023
		m	0.480
		S	0.000176
		g	9.81
		Density	2133.11
		Yield Stress (Pa)	1667.25

(b) B3lbCM0.75 slug test

D

Appendix D: Flexural and Compressive Strength Test Results

Table D.1: Flexural and Compressive Strength of Reference Sample

Ref Sample				
Day	**1**	**7**	**14**	**28**
Flexural Strength 1	2.04	4.42	5.64	6.94
Flexural Strength 2	1.92	3.79	5.57	6.84
Flexural Strength 3	1.87	4.32	5.18	6.65
Average Flexural Strength (MPa)	1.94	4.18	5.46	6.81
Compressive Strength 1	7.24	26.02	32.11	43.91
Compressive Strength 2	7.17	26.40	38.21	38.75
Compressive Strength 3	7.48	25.89	36.08	44.21
Compressive Strength 4	7.70	26.11	34.83	41.07
Compressive Strength 5	8.17	26.71	38.93	40.07
Compressive Strength 6	7.73	25.76	33.87	41.74
Average Compressive Strength (MPa)	7.58	26.15	35.67	41.62

Table D.2: Flexural and Compressive Strength of B3lb Sample

B3lb Sample				
Day	**1**	**7**	**14**	**28**
Flexural Strength 1	1.20	2.78	3.71	5.36
Flexural Strength 2	1.36	2.67	3.98	5.23
Flexural Strength 3	1.50	2.86	3.67	5.09
Average Flexural Strength (MPa)	1.35	2.77	3.79	5.23
Compressive Strength 1	4.39	15.16	21.03	32.29
Compressive Strength 2	3.86	14.85	23.82	31.13
Compressive Strength 3	4.25	14.25	20.45	30.68
Compressive Strength 4	4.37	15.05	23.17	30.42
Compressive Strength 5	4.22	16.95	21.00	29.21
Compressive Strength 6	4.34	14.80	20.87	30.69
Average Compressive Strength (MPa)	4.24	15.18	21.72	30.74

Table D.3: Flexural and Compressive Strength of B3lbA0.5 Sample

B3lbA0.5 Sample				
Day	**1**	**7**	**14**	**28**
Flexural Strength 1	1.31	2.69	3.98	5.64
Flexural Strength 2	1.19	2.56	3.90	5.78
Flexural Strength 3	1.35	2.57	3.68	5.73
Average Flexural Strength (MPa)	1.28	2.61	3.85	5.72
Compressive Strength 1	3.98	14.01	22.10	29.72
Compressive Strength 2	3.93	13.72	20.37	30.60
Compressive Strength 3	4.12	13.89	20.94	32.48
Compressive Strength 4	4.02	13.60	20.24	28.90
Compressive Strength 5	4.09	13.38	21.87	-
Compressive Strength 6	3.76	13.97	21.30	-
Average Compressive Strength (MPa)	3.98	13.76	21.14	30.42

Table D.4: Flexural and Compressive Strength in Vertical Direction of Printed B3lbA0.5 Sample

B3lbA.5 Printed Prism (Vertical Direction)	
Day	**7**
Flexural Strength 1	3.93
Flexural Strength 2	4.07
Flexural Strength 3	3.05
Average Flexural Strength (MPa)	3.68
Compressive Strength 1	12.82
Compressive Strength 2	10.44
Compressive Strength 3	13.58
Average Compressive Strength (MPa)	12.28

Table D.5: Flexural and Compressive Strength in Horizontal Direction of Printed B3lbA0.5 Sample

B3lbA.5 Printed Prism (Horizontal Direction)	
Day	**7**
Flexural Strength 1	2.53
Flexural Strength 2	1.69
Flexural Strength 3	2.01
Average Flexural Strength (MPa)	2.08
Compressive Strength 1	19.33
Compressive Strength 2	19.54
Compressive Strength 3	15.52
Average Compressive Strength (MPa)	18.13